

AD-A145 078

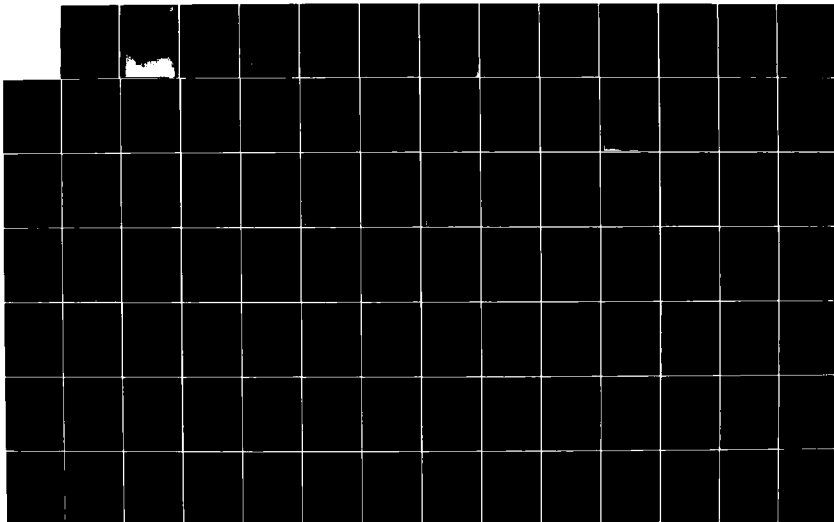
NUCLEAR MAGNETIC RESONANCE OF POLYMERIC MATERIALS:
PROCEEDINGS OF THE AUT..(U) TRINITY COLL DUBLIN
(IRELAND) 1983

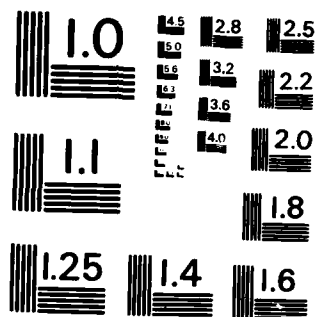
1/2

UNCLASSIFIED

F/G 20/8

NL





MICROCOPY RESOLUTION TEST CHART
NATIONAL BUREAU OF STANDARDS-1963-A

PROCEEDINGS

BRITISH RADIOFREQUENCY SPECTROSCOPY GROUP

AUTUMN MEETING, 1983

TRINITY COLLEGE, DUBLIN 2, IRELAND

NUCLEAR MAGNETIC RESONANCE OF POLYMERIC MATERIALS

ACKNOWLEDGEMENTS

The Conference Committee wishes to thank the following sponsor organizations for their support.

Allied Irish Banks

Bank of Ireland

Bord Failte

Bruker Spectrospin

U.S. Army, European Research Office

A Guinness, Son & Co (Dublin) Ltd

Industrial Development Authority of Ireland

Loctite (Ireland) Ltd

National Board for Science and Technology

Trinity College, Dublin.

Accession For	
NTIS GRA&I	<input checked="" type="checkbox"/>
DTIC TAB	<input type="checkbox"/>
Unannounced	<input type="checkbox"/>
Justification	<input type="checkbox"/>
<i>form 50 per</i>	
By	
Distribution/	
Availability Codes	
Dist	Avail and/or Special
<i>A-1</i>	



This document has been approved
for public release and subject
distribution.

CONTENTS:

COMPONENT PART NOTICE

THIS PAPER IS A COMPONENT PART OF THE FOLLOWING COMPILATION REPORT:

(TITLE): Nuclear Magnetic Resonance of Polymeric Materials:

Proceedings of the Autumn Meeting of the British Radiofrequency Group

Held at Dublin (Ireland).

(SOURCE): Trinity College, Dublin (Ireland).

TO ORDER THE COMPLETE COMPILATION REPORT USE AD-A145 078.

THE COMPONENT PART IS PROVIDED HERE TO ALLOW USERS ACCESS TO INDIVIDUALLY AUTHORED SECTIONS OF PROCEEDINGS, ANNALS, SYMPOSIA, ETC. HOWEVER, THE COMPONENT SHOULD BE CONSIDERED WITHIN THE CONTEXT OF THE OVERALL COMPILATION REPORT AND NOT AS A STAND-ALONE TECHNICAL REPORT.

THE FOLLOWING COMPONENT PART NUMBERS COMPRISE THE COMPILATION REPORT:

AD#: P003 907 TITLE: Dynamics of Polymers in Solution and Melts.

AD-P003 908 > NMR (Nuclear Magnetic Resonance) and Macromolecular Migration in a Melt or in Concentrated Solutions.

AD-P003 909 > ¹³C and ¹H NMR (Nuclear Magnetic Resonance) Studies of Solid Polyolefines.

AD-P003 910 > Deuteron NMR (Nuclear Magnetic Resonance) in Relation to the Glass Transition in Polymers.

AD-P003 911 > Theory of Nuclear Magnetic Relaxation. and

AD-POC3 912 > NMR (Nuclear Magnetic Resonance) of Solid Biopolymers.

DTIC
ELECTRONIC
S SEP 11 1984
A

This document has been approved for public release and sale; its distribution is unlimited.

Distribution/	
Availability Codes	
Dist	Avail and/or Special
A-1	

Dynamics of Polymers in Solution and melts




S.F. Edwards

Cavendish Laboratory
Cambridge.

Abstract

➤ Simple models of polymer dynamics are available in dilute solution, moderate concentrations and melts, since it is possible to make models of the motion in these cases. A series of power laws result which fit well with computer simulation. It is more difficult to derive these models directly from sensible equations of motion, but progress in this direction is reported in the paper.



September 1983



§1 Introduction

Polymer dynamics involve different time scales according to the part of the polymer involved and the environment that it finds itself in. In smaller molecule dynamics one can identify three obvious regimes, the molecule alone, usually meaning in the gaseous phase where one has an n body problem if there are n atoms, an n body problem with external noise and friction which, roughly speaking, is what one expects in a liquid, and to some extent a glass, and finally part of an Nn body problem in a crystal. Notoriously the middle problem is the worse since the first has non stochastic equations, and the crystal is at least quite explicit, and there is a well defined band theory. The liquid case is the most difficult since the molecule has a structure comparable to its surroundings, it could for example be in the liquid phase of its own species, and there is no easy way to simplify the environment as there is with a large Brownian particle in a small molecule fluid.

If one studies a polymer which is a string of smaller monomers then only those aspects of its behaviour which have to do with the polymerized nature have any hope of being easier to understand than the corresponding monomeric liquid, and the solid state of polymers will always be more difficult than the crystalline phase of the monomer, although again they may have some features which are simpler than the monomeric glass.

One can consider the behaviour of polymers characterized by relaxation times or typical frequencies, and the discussion above amounts to saying that when one studies high frequencies, a polymer melt is only marginally different from a monomeric melt, and indeed this is borne out experimentally. But the polymerized nature of the material totally alters melt and solution behaviour at low frequencies, the long chain nature being reflected in the spectacular increases in viscosity which are so characteristic of polymers. There will of

course be effects in the solid state also, but they are not so spectacular since the fall of temperature means that Van der Waals or hydrogen bonds are now real bonds and all glasses are polymer networks in some sense; a glass made of polymer is much the same as any other glass once one is well past the glass temperature.

So if one wants to study stimulating theoretical ideas it is natural to aim at effects which are characterized by long time scales, and an obvious pitfall ensues. To graft that kind of theory onto monomeric structure is a hard problem, but one inescapable if that is what one really wants to do; it is no good solving by methods which are fine on long time scales and extrapolating to short time scales. This is a general caution to be noted. Current polymer dynamics initiated in the famous Rouse paper is at the level of elastic wave theory of solids, the Born Von-Karman theory, or equivalently it is equivalent to the Rayleigh, Jeans and Wien formulae of black body theory. The Born Von-Karman theory does not produce that multiplicity of branches in the vibrational spectrum, and in the way that faults affect it. But there is an enormous richness in polymer theory at the Rouse level since a whole host of new problems, still entirely confined to long time scales, appear in polymer problems, and they pose problems which are very deep mathematically but intuitively obvious, for example: how long will it take for a knot to untie if the string is subjected to Brownian motion? (If the string is in a melt, the melt encloses it like a tube, and one question is asking how long it takes for the chain to wriggle out of this knotted configuration into a new configuration. This is clearly a shorter time than wriggling right out of the initial tube into an entirely new tube, and that time can be calculated by reptation theory and is proportional to L^{-2} . So unless the new tube is the same class of knot one has the solution to the query at a crude level).

I shall put forward a chain of developments of dynamics in recent years which amount to a reasonable intuitive solution for long time scales, and point out the basic problem of improving these theories to the level of mathematical proof.

§2. The single chain

Forces between monomers, and also forces between the polymer and its surroundings have the effect of expanding or contracting the chains. This paper is concerned with dynamics, so it will omit all discussions of swelling or precipitation. This is a topic 'under control' and can be built into the analysis without too much difficulty; it is not worth while muddying the equation with complexity which will not be used. There is a dynamical equivalent to this simplification in that every motion involves crossing potential barriers in quite complex ways, and these ways are affected by the environment just as a single particle can have complex jump behaviour but still in the end will have its long time motion governed by a simple diffusion equation:

$$\left(\frac{\partial}{\partial t} - D \frac{\partial^2}{\partial x^2} \right) P(x, t) = 0 \quad (2.1)$$

one can hope for a similar equation for the polymer.

In the presence of a potential $V(x)$ a particle in equilibrium will have

$$P_0 = \left(e^{(F - V(x))/kT} \right)$$

where $e^{F/kT}$ is the normalisation. This modifies (2.1) to

$$\left(\frac{\partial}{\partial t} - D \frac{\partial}{\partial x} \left(\frac{\partial}{\partial x} + \frac{1}{kT} \frac{\partial V}{\partial x} \right) \right) P = 0 \quad (2.2)$$

a simple but rather unfamiliar form since one generally does not find Brownian particles in central fields of force. The mathematical form is familiar in the Fokker-Planck equation for the case of particles with inertia and soft forces which has the form:

$$\left(\frac{\partial}{\partial t} + v \cdot \frac{\partial}{\partial \mathbf{r}} - \frac{\partial}{\partial v_\mu} D_{\mu\nu} \left(\frac{\partial}{\partial v_\nu} + \frac{m v_\nu}{kT} \right) \right) \rho = 0$$

$D_{\mu\nu}(\mathbf{v})$ being the velocity dependent (2.3)

tensor diffusivity required in say plasma physics.

What is P_0 for a polymer? In equilibrium it is a random walk. Suppose it were freely hinged rods whose ends were at $\mathbf{r}_1, \mathbf{r}_2, \dots, \mathbf{r}_N$ and each rod is of length l :

$$P_0 = \prod_i \delta(|\mathbf{r}_i - \mathbf{r}_{i+1}| - l) \quad (2.4)$$

It is well known that the end to end statistics or indeed the statistics of any points distant from one another along the chain is independent of the precise neighbour configuration, and the analogue of the variable ~~which~~ which describes elastic waves in a solid, or the macroscopic density or velocity in a liquid, are the fourier components

$$R_q = \sum r_n e^{2\pi i n q / L} \quad (2.5)$$

which gives (by a well known straightforward derivation not reproduced here)

$$P_0 = N \exp \left(- \frac{3}{2l} \frac{1}{2\pi} \sum_q q^2 / |R_q|^2 \right)$$

(N the normalization) (2.6)

(I have used the complex form for simplicity, but it contains the real form if required by relations between the real and imaginary parts of \tilde{R}_q). The q in the sum cannot exceed the number of links (recall the Born theory) but in fact if ever we need to restrict the sum the theory will be wrong since high q brings us into a region outside the present validity. Note that there is no κT in P_0 , the random walk has entropy but not ~~some~~ internal energy. The analogue of (2.2) is now

$$\left(\frac{\partial}{\partial t} - \sum_q \frac{\partial}{\partial \tilde{R}_q} D \left(\frac{\partial}{\partial \tilde{R}_q} + \frac{3q^2}{2\pi l} \tilde{R}_q \right) \right) P = 0 \quad (2.7)$$

Provided one realises that only the q variables have meaning, one can also back Fourier transform

$$P_0 = N e^{-\frac{3}{2l} \int_0^L \left(\frac{\partial B}{\partial s} \right)^2 ds}$$

$$\left(\frac{\partial}{\partial t} - \int ds \frac{\partial}{\partial R(s)} D \left(\frac{\partial}{\partial R(s)} - \frac{3R''(s)}{l} \right) \right) P = 0 \quad (2.8)$$

where the continuous arc lengths have replaced the discrete nl , but for those who find functional differential equations hard to swallow one may emphasize that (2.7) is exactly the same as a equation for highly damped phonons in a solid, or radiation in a highly emitting and absorbing material.

Equation (2.7) is the Rouse equation and the q 's label Rouse modes. It can be solved exactly, for if one writes

$$P = \tilde{P} e^{-\frac{1}{2} \left(\frac{3}{2l} \frac{1}{2\pi} \sum_q q^2 |\tilde{R}_q|^2 \right)} \quad (2.9)$$

one has

$$\left(\frac{\partial}{\partial t} - \sum_q \left(\frac{\partial^2}{\partial \tilde{R}_q \partial \tilde{R}_q} + \frac{D}{4} q^4 |\tilde{R}_q|^2 \left(\frac{3}{4\pi l} \right)^2 - \frac{3}{2l} \frac{1}{2\pi} q^2 \right) \right) \tilde{P} = 0 \quad (2.10)$$

which is Hermite's equation and is in all the books under the quantum theory of the harmonic oscillator, give or take a few constants and i.

From this equation one can work out the probability of the polymer getting from any given shape to any other. By taking the first moment of (2.7) we see that it is derivable from a Langevin equation:

$$\gamma \dot{\underline{R}}_q + \frac{3\kappa T}{2\pi l} q^2 \underline{R}_q = \underline{f}_q \quad (2.11)$$

where γ is a friction $\frac{\kappa T}{\gamma} = D$ (2.12)

and $\frac{3\kappa T}{4\pi l} q^2 |\underline{R}_q|^2$ (2.13)

is the free energy per mode,

\underline{f}_q being a random force. This friction $\gamma \dot{\underline{R}}$ is just like the $(6\pi a\eta)$ of a Brownian sphere in Stokes formula, which amounts to saying that the chain suffers a Stokes drag along its length and this drag shows no coupling along the chain.

In fact it must show coupling since the flow around any point will affect neighbouring parts of the chain, unlike Stokes' problem where each Brownian sphere is considered remote from each other one. The hydrodynamic effects have been put in by Zimm and modify the diffusion equation in a way most easily written in the form (2.8).

$$\left(\frac{\partial}{\partial t} - \sum_{\mu, \nu} \int \int \frac{\partial}{\partial R_{\mu}^{(1)}(s_{\mu})} D_{\mu\nu}(R_{(s_{\mu})}^{(1)}, R_{(s_{\nu})}^{(1)}) \left(\frac{\partial}{\partial R_{\nu}^{(3)}(s_{\nu})} - \frac{3R_{\nu}^{(3)}(s_{\nu})}{l} \right) \right) P = 0 \quad (2.14)$$

\uparrow
 $ds_{\mu} ds_{\nu}$

where α, β label a pair of polymers, μ, ν are Cartesian indices and $D_{\mu\nu}$ is known in the hydrodynamical literature as the Oseen tensor. It is most easily written in fourier transform

$$D_{\mu\nu}(k) = \left(\frac{\delta_{\mu\nu} - k_\mu k_\nu / k^2}{\eta k^2} \right) \kappa T \quad (2.15)$$

(The speed of propagation of the signal through the liquid is here ignored).

Equation (2.10) is frequently simplified by replacing D by its average for a random walk:

$$\begin{aligned} \langle e^{i \underline{k} \cdot (R^{(\alpha)}(s) - R^{(\beta)}(s'))} \rangle \\ = \delta^{\alpha\beta} e^{-k^2 \lambda |s - s'|/6} \end{aligned} \quad (2.16)$$

so that

$$\begin{aligned} & \sum_{\alpha\beta} \iint ds_\alpha ds_\beta \frac{\partial}{\partial R_\mu^{(\alpha)}(s_\alpha)} D_{\mu\nu}(R^{(\alpha)}(s_\alpha) R^{(\beta)}(s_\beta)) \frac{\partial}{\partial R^{(\beta)}(s_\beta)} \\ & \text{becomes} \quad \sum_\alpha \frac{\partial}{\partial R_q^{(\alpha)}} \frac{\kappa T}{\eta q^{1/2}} \left(\frac{\partial}{\partial R_{-q}^{(\alpha)}} + \frac{3q^2 R_q^{(\alpha)}}{2\pi\lambda} \right) \end{aligned} \quad (2.17)$$

From these forms, or directly from the Langevin equation one can derive the correlation functions

$$\begin{aligned} & \langle e^{ik(R^{(\alpha)}(s_\alpha, t) - R^{(\beta)}(s_\beta, 0))} \rangle \\ &= e^{-\frac{k^2}{3} \langle (R^{(\alpha)}(s_\alpha, t) - R^{(\beta)}(s_\beta, 0))^2 \rangle} \end{aligned} \quad (2.18)$$

$$\begin{aligned} & \langle (R^{(\alpha)}(s_\alpha, t) - R^{(\beta)}(s_\beta, 0))^2 \rangle \\ &= \delta^{\alpha\beta} \int dq dw \frac{(1 - e^{i\omega t + iqs}) DkT}{\omega^2 + (Dq^2kT)^2} \end{aligned} \quad (2.19)$$

for the Rouse case and

$$\int \frac{dq dw (1 - e^{i\omega t + iqs})}{\omega^2 + \left(\frac{3kT}{\eta} q^{3/2}\right)^2} - \left(\frac{3kT}{\eta} q^{1/2}\right)^2 \quad (2.20)$$

for the Zimm case. The Zimm result is more realistic since it is derived from possibly realistic model, that of a polymer embedded in a fluid with normal hydrodynamics. The weakness of the model lies in the neglect of the entanglements. The Rouse model on the other hand is not realistic as it stands since there is no justification for assuming a drag coefficient in the form of a simple constant, which certainly will not result from the equations of hydrodynamics. Experimentally the viscosity of a dilute polymer solution verifies the Zimm result, for the viscosity in this case is proportional to $L^{1/2}$

(i.e. $M^{1/2}$ where M is the molecular weight).

screened once the density of polymer is such that the chains overlap. If one takes equation (2.14) and averages away all polymers except one, one finds that simple screening does obtain, and just using mean densities the equation governing the effective hydrodynamics equation.

$$\frac{\partial u}{\partial t} + \eta(k) u_k + \frac{\nabla p}{\rho_{\text{fluid}}} = f_{\text{external}} \quad (2.21)$$

and the effective polymer dynamics

$$\dot{R}_q + \kappa T q^2 R_q J(q) = \int u(R(s)) e^{iqs} ds \quad (2.22)$$

where

$$\eta(k) = \eta_0 k^2 + c \sum \frac{k^2 l/3}{k^4 l^2/36 + q^2} \frac{3\kappa T q^2/l}{i\omega + 3\kappa T q^2 J(q)/l} \quad (2.23)$$

where c is the polymer concentration, and

$$J(q) = \frac{1}{3\pi^2 \eta_0} \int_0^\infty dj \frac{j^2}{\eta(j^2)} \frac{j^2 l/3}{(j^4 l^2/36) + q^2} \quad (2.24)$$

(If an arbitrary friction term is still left in, it will appear as

$$(1 + \nu J(q)) \dot{R}_q + \kappa T q^2 J(q) R_q = u \quad (2.25)$$

At high enough densities one can expect a solution

$$\begin{aligned} \eta(k) &= (\eta_0 + \delta\eta)k^2 & k^2 L < 1 \\ &= \eta_0(k^2 + \xi^{-2}) & k^2 L > 1 \end{aligned} \quad (2.26)$$

where, by studying (2.23, 2.24) one finds that

$$\xi^{-2} = \frac{\pi}{2} \zeta^{-1} \quad (2.27)$$

This is of course an asymptotic solution to have so simple a form and the full equations are quite complicated. A particular problem is that the entanglements must dominate at high enough density, and it is not clear if this screened regime is ever realistic; but experimentally one certainly has a regime of viscosity M before the melt behaviour characterized by M^{3+} sets in.

This region will be considered below.

The conclusion of this section is then that the diffusion of a single point on a polymer in solution, or the two body correlation function, can be obtained provided that entanglements are ignored, from the formula

$$\begin{aligned} &\langle e^{ik R(st)} - R(s', 0) \rangle \\ &= \exp\left(-\frac{k^2}{3} \iint \frac{(1 - e^{i\omega t + iq(s-s')}) \kappa J J(q)}{(\omega^2 + (\kappa T q^2 J(q))^2)} d\omega dq\right) \end{aligned} \quad (2.28)$$

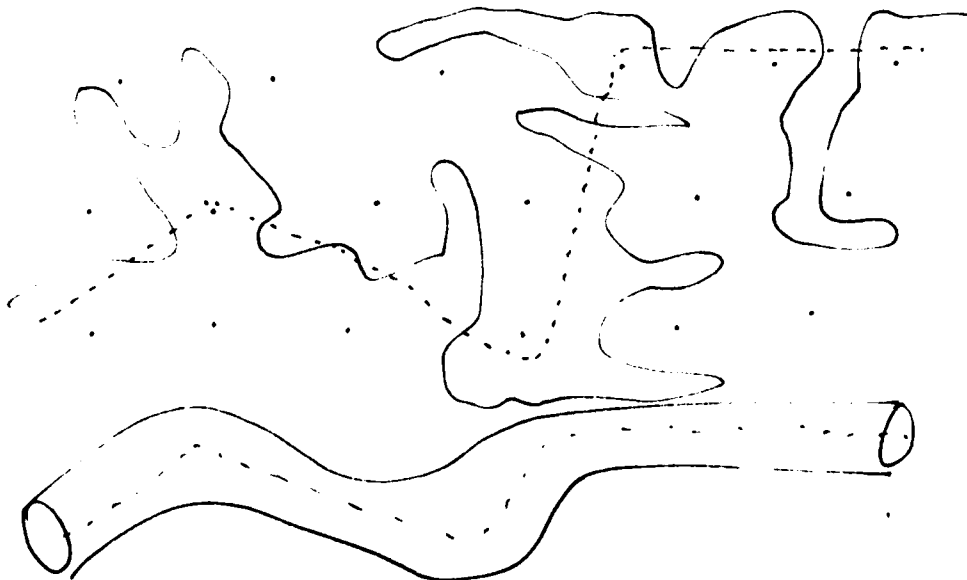
(one point function has $S = S'$, 2 two body correlation integrates over $S-S'$)

where J is given by (2.24) coupled with (2.23).

§3. Entanglements

We have seen in the last section that the dynamics of chains which are transparent to themselves can be resolved which they are in Brownian motion with a simple drag friction, or surrounded by a viscous fluid, and when many chains are present some screening phenomenon intervenes. But in fact all chains are non transparent, and this fact dominates motion in melts or concentrated solutions since almost all motions are blocked. A surviving motion will be the wriggling of the chain up and down the statistical tube which one can imagine surrounding it on average, and a plausible visco elastic theory can be developed from the reptative motion. It is also possible that some kind of collective motion could exist, but no convincing theory of this exists at present. To illustrate the concept of reptation there is a simple computer experiment.

Suppose a lattice is made up in two or three dimensions which we illustrate by a two dimensional array of dots. The polymer is moved by Monte Carlo moves. It is well known that without the lattice this gives the Rouse equation. If one regards the lattice as defining a tube one can characterize this by pulling the polymer taut one generates another walk with a larger steplength, called the primitive path. The steplength of this primitive path, a say, is also the thickness of the tube.



Suppose the distance along the tube is S and the absolute coordinate R

$$\langle (R(S_1) - R(S_2))^2 \rangle = a|S_1 - S_2|. \quad (3.1)$$

Now consider a point on the polymer initially labelled S_2 and after a time labelled S_1 . Then

$\langle (S_1 - S_2)^2 \rangle$ is given by the Rouse equation in one dimension and this as was shown above gives

$$\int \frac{dq \sin^2 qL/2}{\omega^2 + q^4} \sim \sqrt{t} \quad (3.2)$$

(Note the distinction between this and a Brownian point particle which gives t).

Hence $\langle (S(t) - S(0))^2 \rangle \propto \sqrt{t}$ (3.3)

$$\langle (R(S, t) - R(S, 0))^2 \rangle \propto t^{1/4}. \quad (3.4)$$

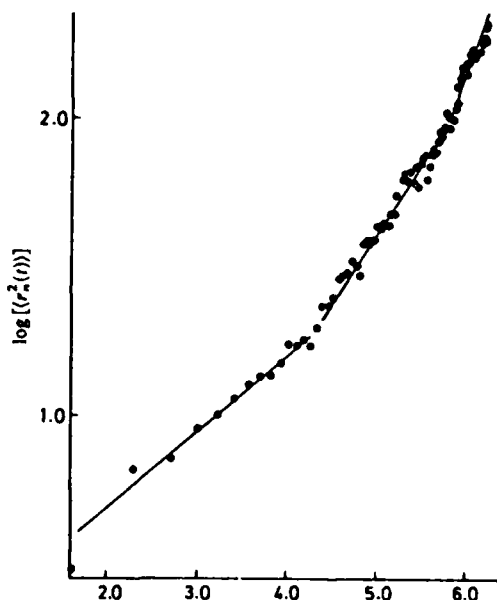
Thus one might expect a time scale initially of $t^{1/4}$ for the polymer has yet to notice the tube. Then $t^{1/4}$, it is diffusing up and down the tube. The centre of mass of the time is the special component $q = 0$ and will have the usual t for S and hence $t^{1/4}$ for R , so after a longer time again the c.m. will diffuse and take any point with it, giving $t^{1/2}$.

Finally the polymer gets right out of the tube and creates a new tube

and the final t law must result. Thus one expects the hierarchy

$$t^{-1/2}, t^{-1/4}, t^{-1/2}, t \quad (3.5)$$

The initial $t^{1/2}$ is a bit difficult to find with a computer which is moving the system very quickly indeed to get into the other ranges, but with the eye of faith one can see the other three ranges.



This is for a fixed lattice and a free polymer. When all the polymers move the time taken over the computation has to be immense both because one has to move many more polymers and the checking of the topological integrity is much more difficult and no longer can be incorporated into the program without the use of memory and because the system becomes 'soggy' and collective modes are clearly possible, but not easy to incorporate in a one point Monte Carlo system. Various authors give various results, but my belief is that the

reptation picture has to be the starting point of any theory. The authors' papers with K E Evans illustrate a whole range of dynamical effects of the fixed lattice models, and these results have been extended by R J Needs to star molecules, verifying the results of the theories of de Gennes and of Doi, and the experimental diffusion results of J Klein.

Thus we can now argue that the diffusion law as a function of concentration will go like

Low concentration (hydrodynamics) Zimm) $t^{2/3}$ finally t

Higher concentration (Screened) $t^{1/2}$ finally t 3.6
(to Rouse)

Melt (Reptation: de Gennes) $t^{1/2}$, $t^{1/4}$, finally $t^{1/2}$ then t .

The intermediate regions are difficult and a principal difficulty is that the fundamental problem of how to describe the motion of entanglements has to be resolved in the region between higher concentration and very high concentration. In the former (and in the Zimm regime) one just ignores it. In the very high density regime it becomes straightforward once it can be represented by a tube.

How can one give a representation of the tube in mathematics? One way is to consider the polymer at two times. Since this paper is being read at an NMR conference I will not worry about very long time scales; alternatively we can consider rubbers where the tubes are permanent. Suppose the polymer is initially $R_2(S)$ or $R_2(q)$ and later at $R_1(q)$. Then over the time scale over which the polymer moves a tube step length it will not encounter the walls.

(This whole argument is going to be 'average'). Let this time be called $(Dq_0^2)^{-1}$

where q_0 has the dimension of q and is related to a , $q_0 \sim la^{-2}$: (3.7)

The Rouse equation is a version of Hermite's equation and the joint probability of finding $\underline{R}_1(q)$ at $t=0$ and $\underline{R}_2(q)$ at $t = t$ is given by

$$P([\underline{R}_1][\underline{R}_2]) = \prod_q \exp \left\{ -\frac{3}{2} \frac{q^2}{2\pi} (|\underline{R}_{1q}|^2 + |\underline{R}_{2q}|^2) - q^2 (|\underline{R}_{1q}|^2 + |\underline{R}_{2q}|^2) \coth Dq^2 t + q^2 (\underline{R}_{1q} \underline{R}_{2q} + \underline{R}_{1-q} \underline{R}_{2-q}) \csc h Dq^2 t \right\} \times \left[(\sinh Dq^2 t) / Dq^2 t \right]^{-3/2} \quad (3.8)$$

Note that

$$\int P([\underline{R}_1], [\underline{R}_2], t) \prod_q d\underline{R}_{1q} = P_0([\underline{R}_2])$$

and

$$\int P([\underline{R}_1], [\underline{R}_2], t) \prod_q d\underline{R}_{2q} = P_q([\underline{R}_{1q}]) \quad (3.9)$$

where

$$P_0 = \mathcal{N} \exp \left(-\frac{3}{2L} \frac{1}{2\pi} \sum_q |\underline{R}_q|^2 \right) \quad (3.10)$$

This is for a free polymer.

We now argue that for a polymer in a pipe the joint probability is the expression above with $Dq^2 t = q^2/q_0^2$, giving

$$P_{00} = P([\underline{R}_1], [\underline{R}_2], \frac{1}{Dq_0^2})$$

Note the complexity of the joint form. It would have been quite wrong to solve the problem of a single polymer constrained to one dimension. The dynamics of a polymer R tied by a tube constraint represented by a locus R_2 can be developed by noting that $P_{00}([\underline{R}], [\underline{R}_2])$ is the equilibrium distribution of R hence the equation:

$$\left(\frac{\partial}{\partial t} - \iint D \frac{\partial}{\partial \underline{R}} \left(\frac{\partial}{\partial \underline{R}} - \frac{1}{P_{00}} \frac{\partial P_{00}}{\partial \underline{R}} \right) \right) P_{\text{tube}}([\underline{R}], t) = 0 \quad (3.11)$$

It will be seen from the structure of P_{00} that R and R_2 are strongly correlated over $q < q_0$ i.e. $S > a$

but weakly correlated for $q > q_0$ i.e. $S < a$,

which is precisely the primitive path picture.

It will be seen that $\frac{1}{P_{00}} \frac{\partial P_{00}}{\partial R}$ is a linear expression in

R and R_2 , so that (3.11) is still a version of Hermite's equation and can still be written down in closed solution so that one can now derive a form

$$P([R], [\tilde{R}], [[R_2]] t)$$

for the probability that a chain constrained by a tube to R_2 starts at \tilde{R}

and is at R at t .

But the answer is sufficiently algebraically tedious that I will not write it down (it possesses the property of being tedious even though trivial!)

A phenomenology is now complete, but what of the mathematics of entanglement.

4. Arigorous theory

This can be ^{derived} ~~derived~~ from the full hydrodynamic form (2.14),

because this equation comes from the Stokes boundary condition

$$\dot{\underline{R}} = \underline{u}(\underline{R})$$

where \underline{u} is the fluid velocity. Hence if $\underline{R}_1 = \underline{R}_2$

$$\dot{\underline{R}}_1 = \dot{\underline{R}}_2$$

It is now possible to argue that this condition is sufficient to stop the polymers crossing. Hence the entanglements are already in (2.14). A particularly simple version of this is to freeze all the polymers except one. Then one can show that the last polymer $R^{(1)}$, satisfies

$$\left(\frac{\partial}{\partial t} - \iint ds ds' \frac{\partial}{\partial R^{(1)}(s)} D(R^{(1)}(s) [R^{(2)}][R^{(3)}] \dots) \left(\frac{\partial}{\partial R^{(1)}(s')} - \frac{\partial}{\partial t} R^{(1)}(s') \right) \right) = 0 \quad (4.1)$$

where D vanishes if any point of $R^{(1)}$ touches any point of $R^{(2)}$, $R^{(3)}$ (4.1)

So at a rigorous level we have (4.1) or (3.11) which ~~must~~ ^{3.11} be equivalent to (3.11) which expresses the primitive path structure explicitly, i.e. if one could average away $R^{(2)}$ $R^{(3)}$ it would have to be in terms of one of the primitive paths defined by these loci. The point is that the solutions of (4.1) (as shown in ref()) break up into a set of probabilities each associated with one of the primitive paths of the network.

This is all quite straightforward for melts for in spite of the apparent complexity it is merely showing a pathway from basic equations to the results of § 3, and to a much more accurate form of correlation functions. I have hope that having got these basic equations one can explore the transition region, but have a horrible suspicion that computer simulation will get there first.

References

The results of the first sections are spread through the literature.
A crisp derivation of all of them are given in de Gennes' book (which is not confined to its title!)

- | | |
|--------------------------------|--|
| de Gennes P.G. | Scaling concepts in polymer physics
Cornell U.P. |
| Evans K.E. and
Edwards S.F. | (1981) J.Chem.Soc.Farad.Trans 2 <u>77</u> , 1891, 1913, 1929 |
| Edwards S.F. | (1982) Proc.Roy.Soc. A <u>381</u> , 17 |



ABSTRACT

A procedure of analysis of NMR measurements is proposed as an approach to the observation of a single chain diffusion process in a melt. The dynamic screening effect is applied to the definition of a temporary submolecule ; this is used as a semi-local probe to investigate collective motions of all parts of a polymer chain. Measurements performed on ^{13}C nuclei or protons lead to similar conclusions. The best agreement with experimental results is obtained by combining a M^3 dependence of the terminal relaxation time (M is the chain molecular weight) with a multiple-mode relaxation spectrum ; all modes have the same statistical weight.

AD-P003 908



NMR AND MACROMOLECULAR MIGRATION IN A MELT OR IN CONCENTRATED SOLUTIONS

J.P. COHEN ADDAD

Laboratoire de Spectrométrie Physique (associé au C.N.R.S.)

Université Scientifique et Médicale de Grenoble

B.P. 68 - 38402 SAINT MARTIN D'HERES CEDEX (France)

I - INTRODUCTION

→ The purpose of this paper is to analyse the migration process of long polymer molecules in a melt or in concentrated solutions as it may be observed from the dynamics of the transverse magnetization of nuclear spins linked to these chains.

→ The low frequency viscoelastic relaxation of polymer systems is known to be mainly controlled by the mechanism of dissociation of topological constraints excited on chains and which are called entanglements^{1,2}. This mechanism exhibits a strong dependence upon the chain molecular weight.

→ These topological constraints also govern the diffusion process of polymer chains²⁽³⁾. So, the accurate description of the diffusion motion of a chain may be a convenient way to characterize disentanglement processes necessarily involved in any model proposed to explain viscoelastic effects.

Therefore, it is worth trying to define an experimental procedure giving a direct observation of the diffusion of a single chain at a molecular scale although it is in dynamical interactions with all surrounding chains.

Two problems are encountered in attempting to observe the diffusion of a chain at a molecular scale.

Space-scale of measurements

One of these is a problem of space-scale of measurement. It is due to a dynamic screening effect induced by topological constraints and characterized by a correlation length $\sigma_e \approx 20 \text{ \AA}$. Within a space domain defined by σ_e^3 , dynamical fluctuations concern short chain segments, only (the number of skeletal bonds N_e is about 2×10^2); they correspond to high relaxation frequencies ($\approx 10^8 \text{ Hz}$)⁴. These motions do not depend upon the molecular weight of polymer chains. There are no correlations of fluctuations of these short segments from one screening domain to another one. Therefore, to observe a significant displacement of a long chain, it is necessary to have a space-scale of measurement longer than σ_e ; otherwise, only local motions will be perceived. This difficulty could be overcome by performing light scattering or neutron scattering experiments. But there is also a problem about the time-scale of measurement.

The time scale of measurement

The time interval T_{Rep} requires to observe the diffusion of a chain over its own dimension, R_G , is about 1 sec for a chain molecular weight $M \sim 10^6$ and $R_G \sim 2 \times 10^2 \text{ \AA}$; this corresponds to a diffusion coefficient $D_{\text{self}} \sim 10^{-10} \text{ cm}^2 \text{ sec}^{-1}$. The time interval is about equal to .1 msec for a displacement over a distance smaller than $\sigma_e \approx 20 \text{ \AA}$. These time scales are not appropriate to light scattering or neutron scattering experiments.

Diffusion coefficient measurements

The difficulties about time scales and space scales have been overcome in two ways. The first one was to observe the diffusion of a chain at a macroscopic scale and not at a molecular one. Early measurements were made using chains labeled with radio-tracers⁵. Deuterated chains moving through a protonated matrix were observed from infrared spectroscopy⁶; the diffusion coefficient of polyethylene chains measured according to this experimental procedure was found to vary as the square of the chain molecular weight within a reasonable accuracy.

Another way was to shorten the time scale of chain diffusion by considering short chains in concentrated solutions or long chains in semi-dilute solutions. The diffusion coefficient of polystyrene chains labeled with a photochromic probe and moving through a pulsed pattern of interference fringes was shown to well obey the predicted formula ³ :

$$D_{\text{self}} \propto M^{-2} C^{-1.75} \quad (1)$$

C is the polymer concentration ⁷. A pulsed field gradient NMR technique ⁸ was recently used to measure the diffusion coefficient in the concentration range $0.04 < C < 0.16$ (W/W) for chain molecular weights lower than 3×10^5 .

It will be shown from this paper that quantum coherence properties of nuclear spins may be used to investigate a chain diffusion process not by measuring any diffusion coefficient D_{self} but by adjusting and comparing the chain relaxation spectrum characterized by :

$$T_{\text{Rep}}^{-1} \propto D_{\text{self}} / \langle R_G^2 \rangle \quad (2)$$

to an internal NMR reference frequency much lower than the Larmor frequency.

The adiabatic relaxation of the transverse nuclear magnetization $M_x(t)$:

$$M_x(t) = \langle M_x(0) M_x(t) \rangle \quad (3)$$

is known not to depend upon any exchange of energy between the spin-system and the thermal bath ; therefore there is no resonance condition to be fulfilled with the Larmor frequency ; it is the reason why slow diffusional processes can be observed.

II - TWO BASIC NMR RESULTS

Two basic NMR results are used to investigate the diffusion process of a chain in a melt.

The solid-like spin-system response

1) When the temperature of a polymer system is raised starting from its glassy state, the resonance line-width of nuclear spins is found to rapidly decrease through the glass transition temperature ; then two cases must be considered. For a polymer system made of short chains, the spin-system made of short chains, the spin-system has a liquid-like response (narrow line analogous to that observed on conventional liquids). Whereas for a polymer system made of long chains the spin-system exhibits a solid-like response ; the resonance line ($\sim 5 \times 10^2$ Hz) is of course much narrower than that observed in the glassy state. This is the first basic NMR result. The solid-like response is easily controlled from a spectrum narrowing effect induced by a sample rotation around an axis perpendicular to the direction of the steady magnetic field⁹.

The disentanglement NMR transition curve

11) At a given temperature, a transition of NMR properties from a solid-like spin-system response to a liquid-like one is induced by decreasing the chain molecular weight ; correspondingly, the resonance line-width is found to decrease from about 5×10^2 Hz to about 10 Hz according to a reasonably sharp curve which we called a disentanglement NMR transition curve because the strong chain length dependence of the resonance line-width is necessarily associated with an increase of the rate of dissociation of entanglements¹⁰. This is the second basic NMR result (Fig 1.)

III - RESIDUAL DIPOLE-DIPOLE INTERACTIONS

Before explaining how the chain migration process may be involved in these basic NMR properties, it is worth emphasizing that magnetic relaxation processes observed on most polymer systems are induced by dipole-dipole interactions of nuclei ; they are tensorial functions of nucleus coordinates ; they strongly depend upon the distance $|\vec{r}|$ between two nuclei and also upon the orientation of the vector joining two nuclei with respect to the steady magnetic field direction. For the sake of simplicity, the energy of dipole-dipole interaction is written as :

$$W = (3 \cos^2 \theta - 1)/r^3 \quad (4)$$

(θ is one of the angular coordinates of \vec{r}).

Most polymer chains are made of proton pairs and methyl groups. Within a proton pair or a $\{CH_3\}$ group, the distance between nuclei is a constant and only angular properties are observed, translational diffusion effects between different solvents are eliminated.

We consider that the solid-like response reflects a residual energy of dipole-dipole interactions because a partial spectrum narrowing effect, only, is induced by macromolecular motions. Although the chain diffusional motion is isotropic, it is like observing an apparent non-isotropic motion because the diffusion of a chain over its own dimension is achieved within a time interval longer than the NMR time scale of measurements.

IV - A BASIC ASSUMPTION : A TWO-STEP MOTIONAL AVERAGING Two dispersions

The only basic assumption necessary to account for the solid-like response and the disentanglement NMR transition curve is to consider that there is a two-step motional averaging of spin-spin interactions ; this is supposed to result from a wide chain relaxation spectrum consisting of two well separated parts ¹¹ : two dispersions Ω_1 and Ω_2 . This hypothesis is in agreement with general viscoelastic properties and with the dynamic screening effect : to the cut in space correlations also corresponds a cut in time correlations.

Ω_1 is called the transition spectrum ; it is associated with local motions of short segments ; it may be studied from the nuclear magnetic spin-lattice relaxation. While $\Omega_2(n)$ is called the terminal spectrum ; it is associated with the collective diffusion of all parts of a chain ; it strongly depends upon the chain molecular weight.

Loss of memory of orientations

The memory of orientations of a given monomeric unit observed through dipole-dipole interactions, \mathcal{H}_D , is lost in two steps ; the memory function :

$$\phi(t) = \langle \mathcal{P}_D(t) \mathcal{H}_D(0) \rangle \quad (5)$$

is splitted in two parts, with :

$$\phi(0) = \langle \mathcal{H}_D(t) - \mathcal{H}_{D\Omega_1} \rangle_{\Omega_1}^2 + (\mathcal{H}_{D\Omega_1})^2 \quad (6)$$

1) There is a fast decay of the memory function associated with the Ω_1 spectrum ; this leads to a residual energy $\langle \mathcal{H}_{D\Omega_1} \rangle$ calculated within a dynamic screening domain, i.e. over short segment motions corresponding to the Ω_1 spectrum (Fig. 2).

ii) There is a long decay of $\phi(t)$ associated with the $\Omega_2(M)$ spectrum.

Spectrum narrowing conditions

Two conditions must be fulfilled to observe a complete spectrum narrowing effect :

$$1) \langle \mathcal{H}_D - \mathcal{H}_{D\Omega_1} \rangle \tau_c \lesssim 1. \text{ for the } \Omega_1 \text{ spectrum} \quad (7)$$

and

$$ii) \langle \mathcal{H}_{D\Omega_1} \rangle T_{\text{rep}} \lesssim 1. \text{ for the } \Omega_2(M) \text{ spectrum} \quad (8) ;$$

τ_c is the longest relaxation time of Ω_1 ; and $|\langle \mathcal{H}_{D\Omega_1} \rangle|$ plays the role of an internal NMR reference frequency which can be used to monitor the terminal relaxation spectrum $\Omega_2(M)$.

A temporary network structure

Finally, all these properties may be pictured by considering there exists a temporary network structure made of temporary submolecules. A submolecule is a temporary object characterized by :

1) its size defined from the dynamic screening length $\sigma_e \propto Ne^{.5}$,
with :

$$Ne \propto C^{-1} M^0 \quad (9)$$

11) its life-time identified with the relaxation time of disentanglement :

$$T_{\text{Rep}} \propto CM^3 \quad (10)$$

For polymer systems made of long chains, we only observe NMR properties of the temporary network structure, while for polymer systems made of short chains we observe the dynamical dissociation of the network structure.

Characteristic NMR properties of this network structure must be now determined.

V - RESIDUAL DIPOLE-DIPOLE ENERGY WITHIN A SUBMOLECULE

Temporary average orientational order

Whatever the complex nature of all topological constraints exerted on a submolecule, we suppose that it is fully characterized at any time, t , by its temporary end-to-end vector $\vec{r}_e(t)$; it is supposed to be the only relevant thermodynamic variable describing a submolecule. The residual energy of dipole-dipole interaction corresponding to a given end-to-end vector, $\vec{r}_e(t)$, can be calculated for a proton pair or a methyl group^{12,13} :

$$E(\vec{r}_e) = \left| \frac{\mu_0}{4\pi} \frac{q^2}{r_e^3} \right| \propto \langle 3 \cos^2\theta - 1 \rangle_{\vec{r}_e} \quad (11)$$

$$E(\vec{r}_e) \propto \vec{r}_e^{-1} \cdot \vec{r}_e^{-1} = 2\vec{r}_e^2 / N_e^2 \quad (12)$$

The non-zero end-to-end vector $\vec{r}_e(t)$, induces a reduction of the chain entropy; it is like considering that every monomeric unit experiences an additional potential energy hindering its isomerisation process. This entropy reduction effect can be observed on polymeric gels^{14,15} and on polymer systems with surface interactions, too.

Formula (12) actually describes a transfer of localisation of NMR properties from a local space scale to a semi-local one defined by $\vec{r}_e(t)$: there is a temporary average orientational order of monomeric units. This order is a small effect since it reflects a strength of correlation equal to about 10^2 Hz while the strongest correlation or orientation (in a glass) is about 10^5 Hz. We are not interested anymore in the memory of orientation of a monomeric unit but in the loss of memory of orientation of $\vec{r}_e(t)$ vectors.

Calibrated gels : superposition NMR property

NMR properties may be shown to obey the key formula (12) by observing the progressive swelling process of elementary chains in calibrated covalent gels. End-to-end vectors are identified with vectors joining two consecutive cross-link points ; they hardly vary with time in a covalent gel corresponding to a permanent network structure. The characteristic dependance of $E(\vec{r}_g)$ with respect to the submolecule (elementary chain) end-to-end vector \vec{r}_g is observed by swelling the covalent gel. Applying a packing condition to partly swollen elementary chains, $|\vec{r}_g|$ may be expressed as a function of the swelling ratio, q , according to the formula :

$$|\vec{r}_g| \propto q^{2/3} \quad (13)$$

q is defined as the ratio of the volume V of the swollen gel over the volume V_0 of the dry gel ($q = V/V_0$) (Fig. 3).

To observe the characteristic dependance of E with respect to the number of bonds of a submolecule (elementary chain), N_g is varied by changing the concentration of synthesis, v_c , of covalent gels¹⁵ :

$$N_g \propto v_c^{-5/4} \quad (14)$$

Combining (13) and (14), the residual energy of dipole-dipole interaction should vary as

$$E \propto q^{2/3} v_c^{5/3} \quad (15)$$

Using the reduced variable $q^{2/3} v_c^{5/3}$, transverse relaxation rates measured on calibrated polydimethylsiloxane gels have been shown to obey a superposition property¹⁵. Several concentrations of synthesis $v_c = .84, .74$ and $.46 \text{ g/cm}^3$ and two swelling agents (toluene and chloroform) were used. The methyl group is well appropriate to the study of submolecule properties because the fast rotation around its C-axis eliminate most of the dipole-dipole interaction. The remaining part only depends upon the orientation of the \vec{C} -axis i.e. of skeletal bonds.

Entangled chains : a superposition property

NMR properties may also be shown to obey formula (12) by increasing the mesh size of the temporary network structure. The number of bonds, N_e , in a submolecule is increased by slightly diluting concentrated solutions of long polymer chains according to formula (9) ; while the rate of dissociation of entanglements is not high enough to induce the second step of motional averaging process. Therefore, by increasing the mesh size we expect to only observe a reduction of the residual energy of spin-spin interactions, reflecting more freedom given to isomerisation processes of monomeric units. The relaxation function of the transverse magnetization is expected to keep its mathematical structure (Fig. 4).

Relaxation functions of protons recorded on five concentrated solutions ($.45 < C < .9 \text{ g/cm}^3$) of long polyisobutylene chains ($M \sim 10^6$) in carbon disulfide, have been recently shown to obey a superposition property, by applying a suitable shift factor to the time scale ¹⁶. All relaxation functions correspond to a solid-like response ; the superposition property reflects less average order of monomeric units ; the chain entropy is increased within sub-molecules.

VI - CHAIN DYNAMICS

Internal reference frequency

We now have a quantitative way to characterize NMR properties of the temporary network structure, from the residual energy of dipole-dipole interactions :

$$(\overline{\mathcal{H}_{DD}}_{\Omega_1})^2 = \overline{E^2(r_a)} = T_V^{-2} \quad (16)$$

T_V^{-1} will serve as an internal reference frequency.

A submolecule is then considered as an ephemeral element which will be used as a probe to analyse long range fluctuations in a chain. We suppose that the two-step motional averaging process still applies when the network structure dissociates quickly enough to induce a complete spectrum narrowing effect. The second step of this effect is closely related to the loss of memory of orientation not of a monomeric unit but of a end-to-end vector of a sub-molecule.

When the chain molecular weight is decreased, the mesh size is kept constant but the rate of dissociation of the network structure is increased. The residual energy of dipole-dipole interactions is now considered as a time function, $E(\vec{r}_e(t))$, obeying the obvious condition :

$$\overline{E^2(\vec{r}_e(t))} = T_v^{-2} \quad (17)$$

at any time t . The description of the network at any time, t . The description of dynamical fluctuations of the network structure is a complex many body problem which has been solved until now within a mean field approximation. The dissociation process of the network structure is supposed to be closely reflected by the diffusion motion of a single chain in dynamical interactions with all surrounding chains. Therefore, it is considered that the loss of memory of orientation of a submolecule end-to-end vector may be associated with the $\Omega_2(M)$ terminal spectrum of a chain. Two main models have been proposed until now to describe diffusional motions of a chain in a melt.

Rouse model

According to the Rouse model, the memory of position of a polymer molecule is lost in each of its points, at any time. This model is built from linear thermodynamic fluctuations governed by a free energy :

$$F_{e,j} \propto 3 kT \vec{r}_{e,j}^2 / N_e \quad (18)$$

associated with the end-to-end vector $\vec{r}_{e,j}$ of the whole chain is a sum of all elementary free energies $F_{e,j}$. Collective motions of submolecule end-to-vectors $\vec{r}_{e,j}(t)$ are described from normal modes determining the $\Omega_2(M)$ spectrum. Any relaxation time τ_p^R is defined from

$$\tau_p^R = \tau_1^R p^{-2}, \quad p = 1, 2 \quad (19)$$

τ_1^R is the terminal relaxation time ; normal modes have an uniform statistical weight ; τ_1^R is predicted to vary as the square of the chain molecular weight. It is currently considered that this model well applies to short chains in a melt, without any entanglements ¹(fig. 5).

Reptation model

The other model proposed to describe the diffusional motion of a chain in a melt is founded on the tube concept and the reptation motion. The tube concept was first introduced by Edwards to describe statistical fluctuations of chains, at equilibrium. The reptation motion of a chain in its surrounding tube was proposed by De Gennes. According to the reptation model, the memory of orientation of submolecules is lost at tube ends only. The memory of orientation is kept in central parts of the tube until these are reached by one of the ends of the chain moving backwards and forwards in a random way, along the tube. The $\Omega_2(M)$ terminal spectrum consists of a series of modes characterized by relaxation times :

$$\tau_p^{\text{Re}} \propto T_{\text{Rep}}/p^2 \quad p = 1, 3, 5 \dots$$

The terminal relaxation time T_{Rep} was predicted to vary as M^3 instead of M^2 . The statistical weight of each mode is proportional to p^{-2} ; this gives a negligible weight to all modes, except for the first one. The reptation model is in reasonable agreement with viscoelastic properties (Fig. 6).

Comparison with NMR results

The principle of the NMR observation of the diffusion process of a single chain in a melt is to shift the $\Omega_2(M)$ spectrum through the internal reference frequency τ_v^{-1} . Starting from very long chains Ω_2 is shifted towards short values of chain relaxation times by decreasing the chain molecular weight¹⁷. Then, the relaxation rate of the transverse component of the nuclear magnetization is decreased according to the disentanglement NMR transition curve discussed in section I.

The relaxation function of the transverse magnetization has been calculated according to the formula :

$$M_x(t) = \exp\{-\alpha \tau_v^{-2} (\sum_{p,q} \tau_{p,q}^2 [\exp(-t \tau_{p,q}^{-1}) + t \tau_{p,q}^{-1} - 1])\} \quad (20)$$

with
$$\tau_{p,q}^{-1} = \tau_p^{-1} + \tau_q^{-1} \quad (21)$$

α is a constant depending upon the chain diffusion model chosen to describe NMR properties ^{13,17}. The best agreement with experimental NMR results is obtained by combining the chain molecular weight dependance of the terminal relaxation time T_{Rep} given by the reptation model, with the $\Omega_2(M)$ relaxation spectrum given by the Rouse model ^{10,16,18}. Values of the terminal relaxation times obtained from previously reported NMR measurements were 5×10^{-2} , 2×10^{-2} and 8×10^{-2} sec polydimethylsiloxane (PDMS), polystyrene (PS) and polyisobutylene (PIB) chains, respectively ; the concentrations were 1., .53 and .47 g/cm³, respectively ; while the molecular weights were 2.2×10^5 , 2.5×10^5 and 2.25×10^5 , respectively. These relaxation times are about ten times longer than those usually estimated from viscoelastic measurements and defined by the ratio η_0/G_N^0 ; η_0 is the zero shear rate viscosity and G_N^0 is the plateau modulus. Results observed on protons were found to be similar to those observed on ¹³C nuclei in natural abundance. Such a property clearly shows that magnetic interactions between nuclei located on different chain segments have negligible effects. These interactions are averaged to zero by local motions of short segments in dynamic screening domains. Therefore, a linear distribution nuclear magnetization is defined along polymer chains in a melt. Consequently, it is possible to observe dynamical properties of a single chain although it is in dynamical interactions with all other surrounding chains.

CONCLUSION

Long range fluctuations of polymer chains in a melt observed from NMR correspond to the loss of memory of orientation of temporary submolecules associated with dynamic screening domains. The criterion of isotropy is defined from the residual energy of tensorial interactions of nuclear spins within screening domains. More details about the reptation model would be probably necessary to actually account for all NMR results. Also, a more tedious characterization of the spin-system response would probably lead to a better accuracy in the determination of the chain molecular weight dependance of terminal relaxation times.

Finally, it is worth emphasizing that the NMR approach to the observation of a chain diffusion process necessarily leads to the analysis of the whole terminal relaxation spectrum whereas measurements of a diffusion constant do not give any detailed information about this spectrum.

R E F E R E N C E S

- (1) Ferry, J.D., in "Viscoelastic Properties of Polymers"
3rd Edition, J. Wiley, New York (1983)
- (2) Graessley, W.W., in "Advances in Polymer Science", Vol. 16, Springer-
Verlag, New York (1974)
- (3) De Gennes, P.G., in "Scaling Concepts in Polymer Physics", Cornell
University Press, Ithaca (1979)
- (4) Muthukumar, M. and Edwards, S.F., Polymer (1982) 23, 345
- (5) Bueche, F., Cashin, W., and Debye, P., J. Chem. Phys. (1952) 20, 1156
- (6) Klein, J., Macromolecules (1981) 14, 460
Leger, L., Hervet, H., and Rondelez, F., Macromolecules (1981) 14, 1732
- (8) Callaghan, P.T. and Pinder, D.N., Macromolecules (1981) 14, 1334
- (9) Cohen Addad, J.P. and Faure, J.P., J. Chem. Physics (1974) 61, 1571
- (10) Cohen Addad, J.P., Domard, M. and Boileau, S., J. Chem. Phys. (1981) 75, 4107
- (11) Graessley, W.W. and Edwards, S.F., Polymer (1981) 22, 1329
- (12) Cohen Addad, J.P., J. Chem. Phys. (1976) 64, 3438
- (13) Cohen Addad, J.P., J. Physique (1982) 43, 1509
- (14) Cohen Addad, J.P., Domard, M. and Herz, J., J. Chem. Phys. (1982) 76, 2744
- (15) Cohen Addad, J.P., Domard, M., Lorentz, G. and Herz, J., J. Physique,
in press
- (16) Cohen Addad, J.P. and Guillermo, A., J. Polym. Sci. Polym. Phys. Ed.
in press
- (17) Cohen Addad, J.P., Polymer (1983) 24, 1128
- (18) Cohen Addad, J.P. and Feio, G., J. Polym. Sci. Polym. Phys. Ed., in press.

FIGURE CAPTIONS

- Fig. 1 - A schematic disentanglement NMR transition curve
- Fig. 2 - The two-part correlation function of dipole-dipole interactions, associated with the two-dispersion chain relaxation spectrum
- Fig. 3 - A schematic progressive swelling of elementary chains in a covalent gel
- Fig. 4 - The mesh size of the temporary network structure is increased by slightly diluting the polymer system; the number of bonds N_e in a submolecule is increased
- Fig. 5 - According to the Rouse model, the memory of position of a chain is lost in each of its points at any time
- Fig. 6 - According to the reptation model the memory orientation is lost at tube ends.
- Fig. 7 - The $\Omega_2(M)$ terminal spectrum is shifted through the internal reference frequency τ_v^{-1} by decreasing the chain molecular weight.

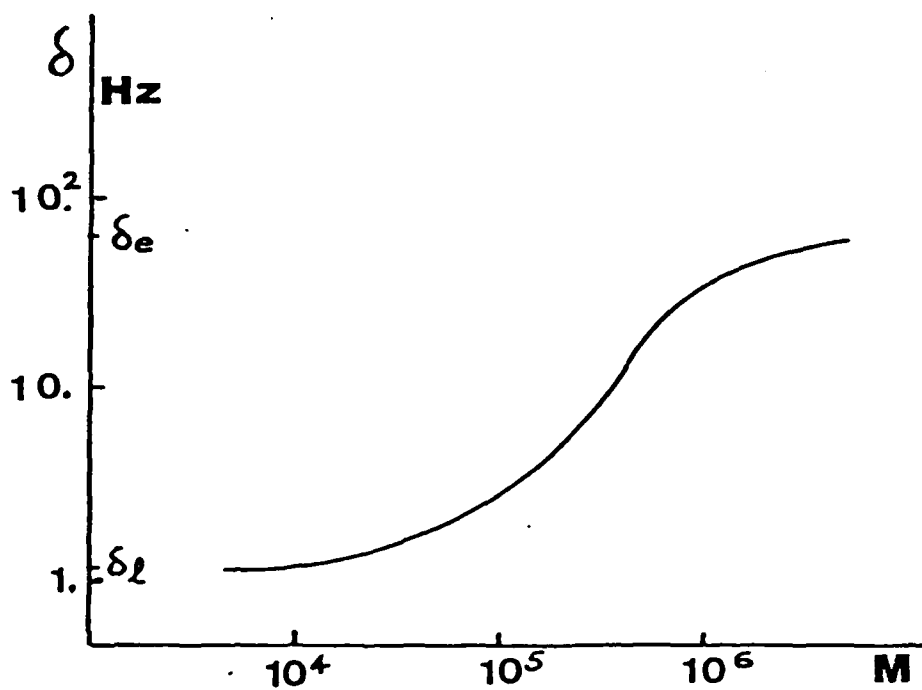


Fig 1

St. John's and St. John's

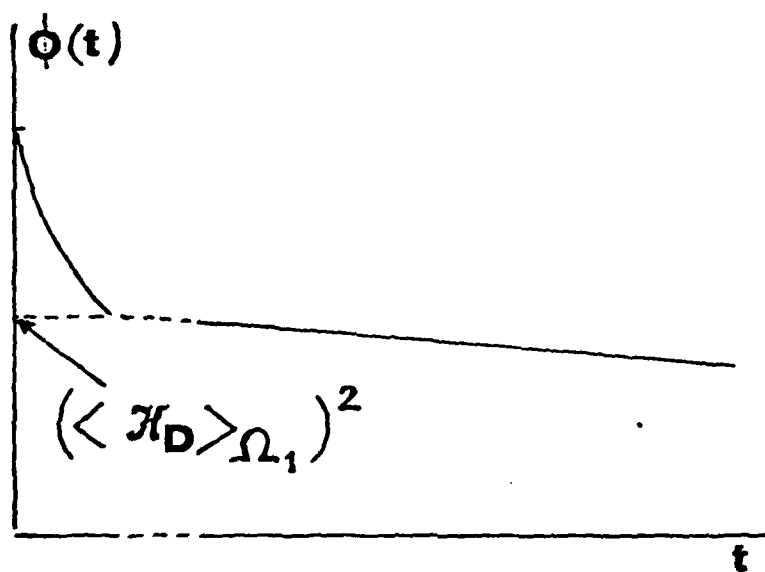
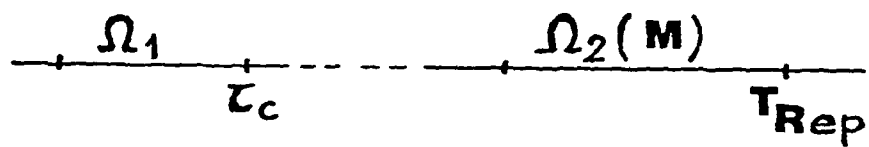
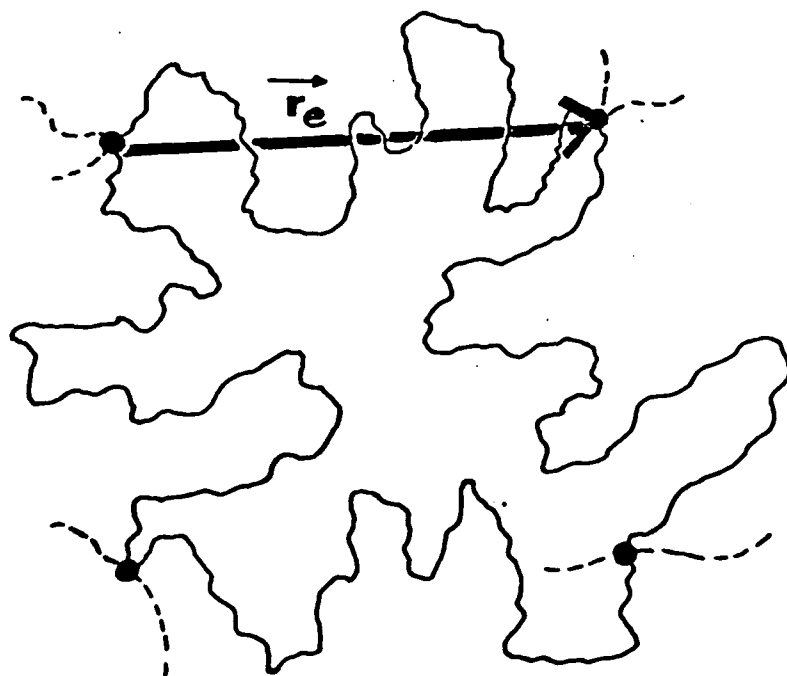
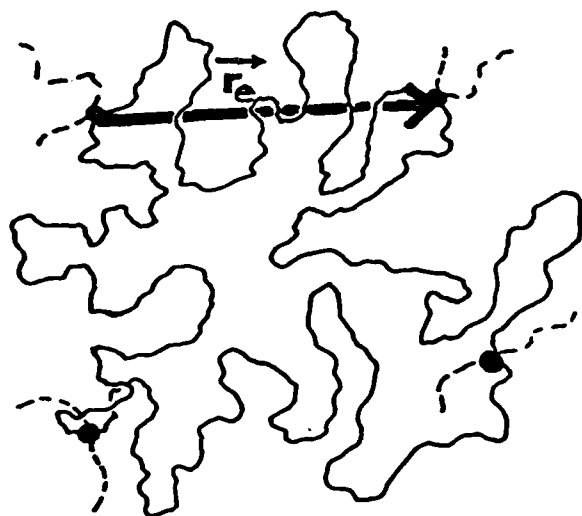


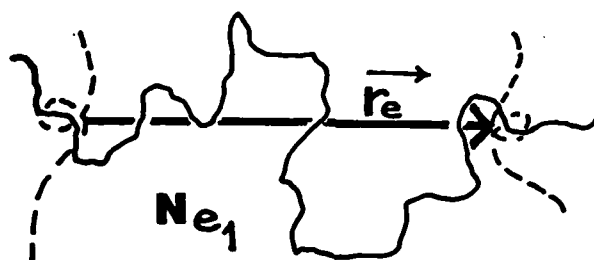
Fig 2

of the A-2-1

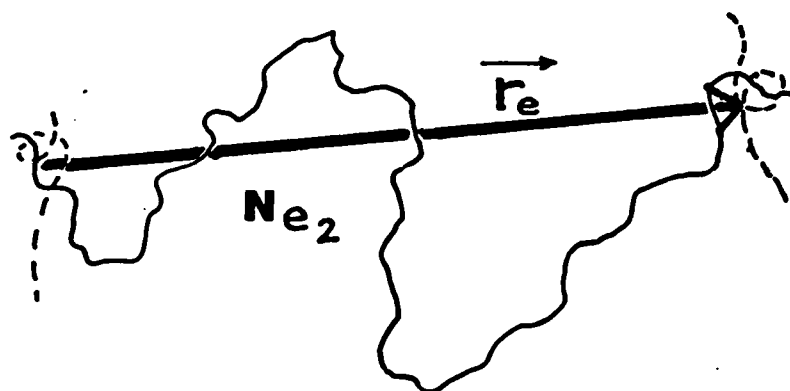


386

T193

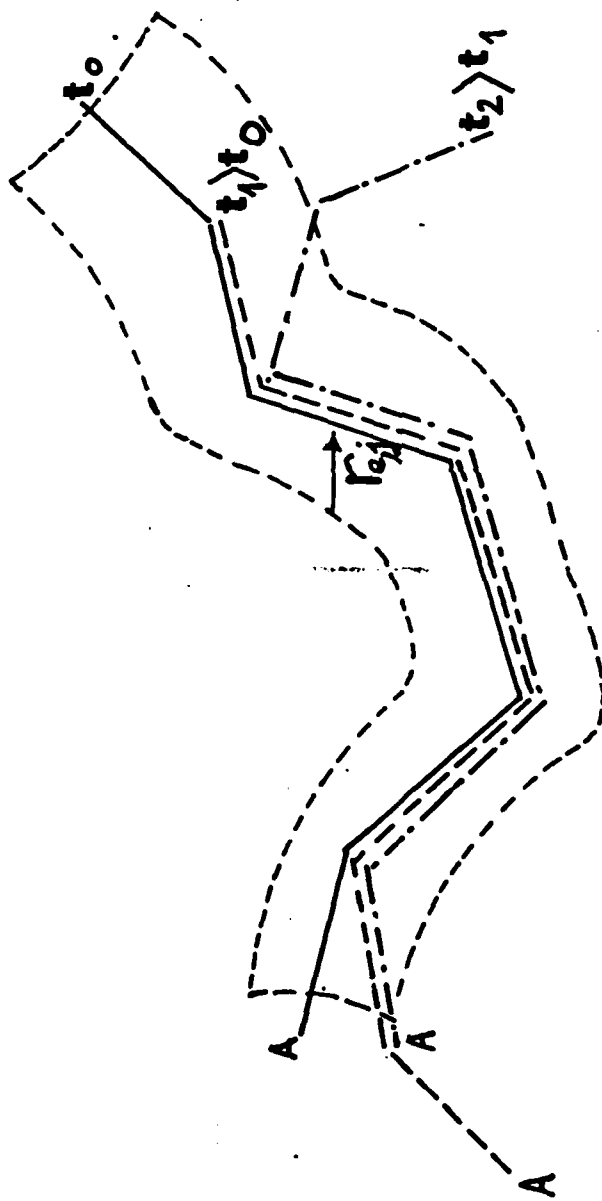


Ne_1



Ne_2

$Ne_2 > Ne_1$

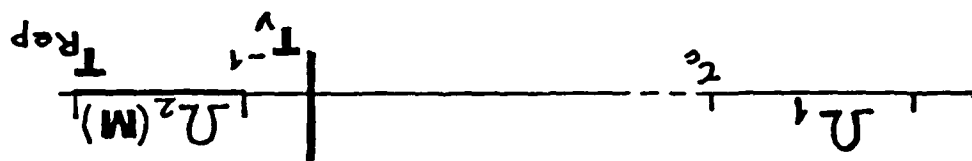
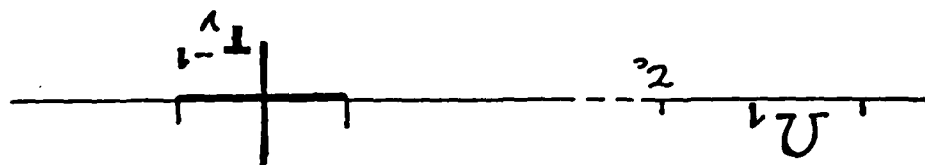
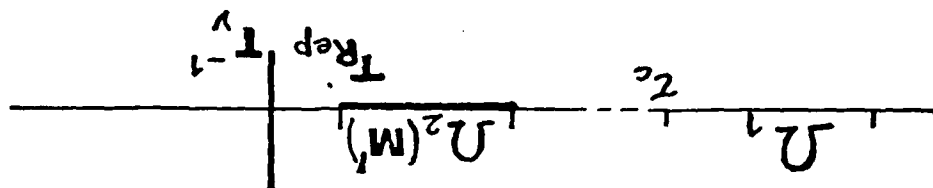


JP 6844 Added Fig. 6,

$\pm \frac{1}{2}$

2121-11212

$M > M'$



AD-P003 909

^{13}C AND ^1H NMR STUDIES OF SOLID POLYOLEFINES

by

M.E.A. Cudby, R.K. Harris, K. Metcalfe, K.J. Packer*

and P.W.R. Smith

(School of Chemical Sciences, University of East Anglia,
Norwich, NR4 7TJ, Norfolk, U.K.)

and

A. Bunn

(ICI plc, Plastics and Petrochemicals Division, P.O. Box 90,
Wilton, Middlesbrough, Cleveland, TS6 8JE, U.K.)

Manuscript pages: 19

Figures: 6

*Correspondence to: Professor K.J. Packer

School of Chemical Sciences

University of East Anglia

Norwich NR4 7TJ

Norfolk, U.K.

Abstract

The basis of ^1H and ^{13}C high-resolution NMR investigations of solid polymers is outlined. The ^{13}C NMR spectra of solid syndiotactic and isotactic polypropene are discussed and their interpretation in terms of conformation and chain-packing effects are reviewed. The effects of decreasing temperature on the ^{13}C high-resolution spectrum of an annealed sample of isotactic polypropene is described and interpreted in terms of the crystal structure. The question of the proportion of the sample giving rise to ^{13}C signals is addressed and some results reported. The main cause for observing only part of the total sample is shown to be the ^1H rotating frame spin-lattice relaxation behaviour. The ^1H spin-lattice relaxation and spectral characteristics of a number of polyolefine samples are summarised and the role of spin-diffusion discussed. The heterogeneity revealed by the multicomponent $T_{1\rho}^0$ behaviour has been modeled numerically using a computer and the conclusions are outlined. The recovery behaviour of poly-1-butene, following conversion to a meta-stable form by heating, is observed using both cross-polarization and single-pulse excitation techniques. In addition, an example of the investigation of a propene/ethylene copolymer by both ^{13}C and ^1H methods is described to illustrate the interdependence of the techniques.

- 1 -

1. Introduction

NMR studies of solid polymers have a long history and a considerable volume of literature. In the main, until about a decade ago, these investigations relied on the use of ^1H broadline spectra and associated measurements of spectral moments and spin-lattice relaxation behaviour. More recently, other nuclei have become important, largely because of advances in technology and developments in NMR techniques. In particular the use of ^2H and ^{13}C has become widespread. In this paper we describe some work carried out in our laboratory which involves investigations of solid polyolefines. It is presented as illustrative of some of the possibilities of both ^{13}C high-resolution NMR spectroscopy and ^1H broad-line investigations. No attempt is made at a review of other work in the literature and the interested reader is referred to articles elsewhere for such reviews [1-4].

2. Experimental

2.1 Samples

- (a) Polyethylene: Two samples of high-density PE will be mentioned. PEI is a single-crystal mat obtained by slow crystallisation of an 0.1% w/w solution in xylene at 70°C followed by washing with methanol and drying under vacuum at ambient temperature. The second sample, PEII, is a melt-crystallised sample, annealed at 403K for 30 minutes.
- (b) Polypropene: The isotactic polypropene used was a commercially available grade, manufactured by ICI plc, having a melt flow index of 20 and an isotactic content in excess of 97% as determined by proton NMR in solution via the racemic diad concentration (5). PPI was fabricated as a thin film and was annealed at 433K for 60 minutes.

PPII was also a thin film obtained by rapid quenching from the melt to 273K followed by brief heating to 373K to remove any of the smectic form.

(c) Polybut-1-ene: This was a commercially produced sample with an X-ray determined crystallinity of ~30%. PBI was used as obtained whilst PBII was made by heating a sample of PBI to just above the melting temperature (~380K) followed by rapid cooling to room temperature.

(d) A propene/ethylene copolymer: a block copolymer comprising 85% propene as a main block and an end block made with a 50-50 mixture of ethylene and propene. The polymer was examined as made (PECI) but was also subjected to extraction with boiling heptane giving two further samples, the heptane soluble (PECII) and insoluble (PECIII) fractions.

2.2 NMR measurements

^1H NMR measurements were made at two operating frequencies of 60MHz and 200MHz using two separate spectrometers. The measurements at 60MHz were made with a conventional high-power pulse spectrometer operating with a low-resolution magnet. Provision was available for adjustment of the r.f. field amplitude which, for spin-locking measurements, was generally 40 or 60kHz ($= \gamma_{1\text{H}} B_1/2\pi$). Data acquisition was by means of a digital signal averager. Samples were contained in 10mm o.d. flat-bottomed glass tubes with the temperature controlled by a conventional gas-flow system, settable to $+5^\circ\text{C}$.

The 200MHz ^1H measurements were made on a computer-controlled double-resonance spectrometer, utilising the high-frequency channel. The spectrometer is based around an Oxford Instruments wide-bore 4.7T high-resolution magnet and is operated by a Nicolet 1180 computer system and peripherals. The two frequency channels each allow for four pulses of

separately adjustable r.f. phase at up to 1KW output power, the latter being under computer control. Each channel has a broadband quadrature receiver followed by a dual-channel, 4-pole Bessel-function filter of variable bandwidth. The ^1H spectra were recorded using a digital fast transient recorder operating at up to 20MHz with 8-bit resolution. Normally a sweep width of 312.5 kHz was used (3.2 μs dwell). Samples were contained in 5mm tubes placed in the horizontal solenoid coil of a Bruker Z 32HP probe. Generally, 90 $^\circ$ pulse lengths of the order of 1 μs were employed with lower r.f. fields being used for long spin-locking pulses (40-60kHz).

^{13}C high-resolution spectra were measured using dipolar-decoupling (60kHz decoupling fields) and magic-angle sample rotation (MAR) (6). The ^{13}C signal was either obtained via cross-polarization from protons (7,8) or by normal spin-lattice polarization. Some of the ^{13}C spectra were measured on the double-resonance system described above, (i.e. $\nu_0^{13}\text{C} = 50\text{MHz}$) using Andrew-Beams style of rotors fabricated from Macor and Delrin (polyoxymethylene). The latter formed the rotor base and, if sufficiently far removed from the coil, gives little or no signal. Sample volumes were approximately 0.3cm 3 . The probe is a Bruker CPMAR probe.

Other ^{13}C spectra were obtained on a spectrometer operating at 90MHz/22.63 MHz based on an electromagnet. The probe system is a new design based on the spinning system described elsewhere (9,10). It employed cylindrical sample containers made of glass or Macor of 8mm o.d. Only the sample plus coil is in the magnet and the probe is remotely tuned and matched for both frequencies. Once the magic-angle is set it remains constant even on changing samples, unlike the Andrew-Beams system used in our Bruker probe where it is necessary to include some solid KBr in the sample and observe the ^{79}Br resonance to allow adjustment of the angle on each sample (11).

The remotely-tuned probe on the 90/22.63 MHz spectrometer allows for variation of the sample temperature whilst performing CPMAR experiments and some results are given later using this facility.

3. General Considerations

Most solid polymers are structurally heterogeneous and the semi-crystalline polyolefins are no exception to this. This heterogeneity reveals itself in ^1H NMR studies of these materials in a number of ways. Spectra may comprise a number of superimposed lines of differing width and shape (12-15) and spin-lattice relaxation may be more complex than a simple single exponential process. These ^1H NMR properties are usually dominated by the magnetic dipolar couplings between the protons which produce spectral lineshapes and relaxation behaviour characteristic of the spatial distributions of the protons and their relative movements due to thermal motions. Thus at a given temperature, crystalline and disordered regions of a polymer will tend to give rise to broader and narrower resonances respectively whilst spin lattice relaxation (T_1 and $T_{1\rho}$), which depends on motional frequencies of the order of the proton precession frequency in B_0 (typically of order 10^7 - 10^8 Hz) and B_1 (typically 10^4 - 10^5 Hz) respectively for T_1 and $T_{1\rho}$, can vary over a considerable range of values. Generally, the rotating frame relaxation is much more efficient than the T_1 process in solids. All the above is complicated by the fact that the proton dipolar coupling produces a spatial transport of nuclear magnetization, called spin-diffusion, which couples together the relaxation behaviour of different regions. Thus, as is shown below, a single uniform T_1 behaviour may be observed when $T_{1\rho}^0$ and spectra indicate heterogeneity.

Apart from the intrinsic value of these effects in the study of solid polymers, which we shall give examples of below, they are important in

the use of ^{13}C high-resolution NMR since, often, the work done with this nucleus involves cross-polarization, (CP), in which the ^{13}C signal is generated from the ^1H spin system. Two typical double-resonance pulse sequences used for ^{13}C high-resolution NMR in solids are shown in Figure 1. The cross-polarization sequence (figure 1a) has the following features. A 90_x^0 pulse is applied on the ^1H channel and the magnetization is spin-locked with a field B_{1y} . The delay τ_1 is usually zero but is indicated here to suggest the possibility of using T_2 as a means of selectively retaining only part of the proton magnetization for subsequent use. A further delay, τ_2 , allows discrimination or selection by means of differing ^1H $T_{1\rho}$ values before a contact pulse on the ^{13}C channel produces a ^{13}C signal by polarization transfer from the protons. It is clear that ^{13}C signal can only be derived from the proton magnetization remaining after both the T_2 and $T_{1\rho}$ effects in times τ_1 and τ_2 have acted. A further delay, τ_3 , allows for discrimination based on ^{13}C - ^1H dipolar coupling strengths (16). Following CP the ^{13}C signal is recorded in the presence of the strong dipolar decoupling field. Following this, when $\tau_3 = 0$, a 90_{-x} pulse flips any remaining ^1H magnetization back along B_0 (17). The time T_R is a period during which the ^1H system undergoes spin-lattice relaxation following which the procedure is repeated, the ^{13}C signals being accumulated in the spectrometer computer. Figure 1b illustrates an alternative experiment in which the ^{13}C signal is generated via its own spin-lattice processes. In this case the time T_R is crucial in determining which ^{13}C spins give signals. Only those for which $T_1(^{13}\text{C}) \leq T_R$ will be detected. These sequences are usually combined with magic angle sample rotation to yield "liquid-like" spectra (6).

With these general comments in mind we now discuss a number of investigations of polyolefines using these techniques.

4. ^{13}C spectra of polypropenes

4.1 Effects of conformation

The ^{13}C spectrum of solid syndiotactic polypropene has been described elsewhere (18). The interesting feature of this spectrum is a 1:1 splitting of the methylene carbon resonance of 8.7ppm. This was interpreted in terms of the conformation of this molecule in the solid, which X-ray diffraction had suggested to be a $4_2/1$ helix in which there are two distinct and equally probable sites for methylene groups: one on the helix axis, the other on either side of this axis. Consideration of shielding effects of γ -substituents suggest a shift difference of $\sim 8\text{ppm}$ between the two sites which is close to the observed value. In addition the higher frequency peak, assigned to the site on the outside of the chain, shows additional broadening/splitting consistent with interchain effects (see below).

4.2 Effects of crystal packing

The ^{13}C spectra of samples PPI and PPII have been presented elsewhere (19). The essential features of the spectra of these isotactic polypropene samples are that PPI, the highly annealed material, shows splittings of the methyl and methylene resonances in approximately a 2:1 ratio, the more intense peak being to high-frequency in each case. Close examination of the methine resonance shows a shoulder in the same sense. The quenched sample does not show these splittings, of order of 0.5-1.0ppm, and the spectra indicate a shift of resonance intensity in the PPII methylene and methyl regions to the frequencies characteristic of the lower intensity signals in these regions in PPI. The interpretation given to these observations was that the unit cell of α isotactic polypropene contains paired left and right-handed 3:1 helices and that this generates distinguishable sites for methyl, methine and methylene carbons in a

2:1 ratio by virtue of inter-chain interactions. The effect of quenching, on this basis, would seem to be an increase in resonance intensity at frequencies characteristic of the more open environment associated with interactions between chains in different pairs and hence the suggestion that quenching traps a significant fraction of the chains in a non-paired arrangement. X-ray diffraction still indicates the same basic structure so these effects are on a very local scale.

4.3 Effects of decreasing temperature

Lyerla et al have reported that on decreasing the temperature of solid isotactic polypropene the ^{13}C NMR signal from the methyl group broadens due to interference of the modulation of the ^{13}C - ^1H dipolar coupling due to the thermal motion of the methyl group with that due to the strong proton decoupling (20). Figure 2 shows the temperature variation of the ^{13}C spectrum of the annealed sample, PPI, obtained using the VT probe system mentioned in the experimental section. The spectra show similar behaviour to that reported by Lyerla et al but, owing to the resolution of different peaks in this sample, various other features are apparent. Firstly, the methylene signal shows little change over the range of temperatures covered, showing the maintenance of resolution with temperature variations.

Indeed, the Hartmann-Hahn matching and the general electronic properties of the probe also remained unchanged. Secondly, it is clear that, as the temperature is lowered from 300K, the larger of the two methyl resonances is the first to broaden. This can be taken as supporting the assignment of this splitting, given elsewhere (19) and mentioned above, to the existence of paired helices of opposite handedness. The methyls within the close-meshed pair of helices would be likely to experience more hinderance to their motion than those on the outside, this leading to the observed behaviour with temperature.

4.4 Quantitative considerations

Observations of the ^{13}C spectra of polybut-1-ene led us to determine the proportion of the total carbon in the polypropene samples that was being detected by the usual cross-polarization experiment. The probe system 90° pulse length was calibrated using adamantane and the efficiency of the cross-polarization process checked using hexamethylbenzene. The proportion of carbon was then determined by comparing known masses of PPI and PPII with calibration samples of hexamethylbenzene. The results obtained indicated that for PPI and PPII approximately 80% and 70% respectively was being observed (21). The reason for this is apparent when the ^1H relaxation properties are considered. For the CP process the ^{13}C signal produced depends on both the ^1H $T_{1\rho}$ behaviour and the ^{13}C - ^1H cross-relaxation time (22). If the former is short then it may not be possible to obtain thermal equilibrium between the two spin systems before the proton bath is significantly heated by the spin-lattice process ($T_{1\rho}$). In the case of many polymer samples ^1H $T_{1\rho}$ behaviour is multiexponential in character and, for PPI and PPII has a short-time component which is of the order of 600-800 μs which, in turn, is associated with a narrow (long T_2) component in the ^1H spectrum. These two factors make it extremely unlikely that any significant cross-polarization arises from that part of the proton magnetization. This largely accounts for the deficit in the CP experiments mentioned above.

5. ^1H relaxation and spectra

In this section we present a summary of results which have been described in detail elsewhere (23). The proton spin-lattice relaxation in each of PPI, PEII, PPI, PPII and PBI at room temperature is described by a

single characteristic relaxation time. The on-resonance rotating-frame spin-lattice relaxation ($T_{1\rho}^{90}$), on the other hand, requires a minimum of three exponential processes for its description in each case. Of particular note is the fact that the long time behaviour of the $T_{1\rho}^{90}$ process is strongly dependent on the physical history of the samples. Thus for PEI and PEII the long-time component relaxation times are 60 and 190ms respectively, whilst for PPI and PPII they are 109 and 30ms respectively.

Further measurements of the spin-lattice relaxation behaviour in the off-resonance rotating frame, with the magnetization spin-locked at the "magic angle" of 54.7° with respect to the B_0 (Z) axis, showed that the relaxation became a lot slower, whilst remaining three-component.

A number of possible explanations are possible for this overall relaxation behaviour but the most likely is that the three relaxation components relate to three physically distinct regions in the polymers in which the protons have different NMR properties. This heterogeneity of structure in semi-crystalline polymers is well-known (2,3) and the number of spectral components used to fit experimental data has varied. For example, Bergmann (13) and Smith et al (15) have used three components to fit spectral lineshapes but Bergmann has more recently chosen to describe the data in terms of a crystalline component plus an amorphous component describable by a lineshape involving a distribution of correlation times (24). Analysis of spectra in this way to yield information on crystallinities etc. is quite successful but subject to a degree of arbitrariness in choice of lineshape functions.

Spin-lattice relaxation, on the other hand, is subject to the complication of spin-diffusion (23). This, as stated above, is a spatial transport of magnetization via homonuclear dipolar couplings and leads to a coupling of the spin-lattice relaxation of spatially separated regions.

This can be invoked to explain why single T_1 's are observed and multiple $T_{1\rho}^{90}$'s. In the first place, T_1 , being dependent on fluctuations at ω_0 and $2\omega_0$ ($\omega_0 = \gamma B_0$) is often considerably longer than $T_{1\rho}^{90}$, which depends on low-frequency fluctuations, of order ω_1 ($=\gamma B_1$). In addition the spin-diffusion coefficient, D_s , is proportional to the secular dipolar interaction strength which, under on-resonance spin-locking is scaled by 0.5. Thus T_1 gives a longer timescale for a faster diffusion process to take effect.

The observations that $T_{1\rho}^{54.7^\circ}$ was on a considerably longer timescale than $T_{1\rho}^{90}$ indicated that even for $T_{1\rho}^{90}$, spin-diffusion is causing a partial mixing of the intrinsic relaxation properties. To illustrate this, as reported elsewhere (23), we have simulated the relaxation behaviour for a three region system allowing for spin-diffusion in one dimension. The equation governing this behaviour is

$$\dot{M}_\alpha(x) = D_s^q \{ \partial^2 M_\alpha(x) / \partial x^2 \} + R_j^q \{ M_\alpha^{eq} - M_\alpha(x) \}$$

where α labels the magnetization component (e.g. z for T_1 , etc.), q the region ($q = 1, 2$ and 3) and j the relaxation process ($1, 1\rho$, etc.).

$M_z^{eq} = M_0$ otherwise $M^{eq} = 0$. The spin-diffusion coefficients and relaxation rates are different in each region (hence the label q) but constant within each region (not a function of x). Numerical solutions of this equation using values for the sizes of crystalline lamellae etc. taken from other sources demonstrated that the observed behaviour of $T_{1\rho}^{90}$ could be explained on the basis of the model. In particular, it demonstrated that the long-time $T_{1\rho}^{90}$ components largely reflect the time for magnetization to diffuse out of the crystalline regions into the less ordered regions which, for these materials at the temperature used, act as relaxation sinks.

Other experiments involving partially relaxed proton spectra have been carried out and, in particular, experiments using $T_{1\rho}$ behaviour to spatially label the sample have been reported (23). These involve, inter alia, a preparation period in which the system is allowed to relax ($T_{1\rho}^{90}$) until only the long-time component remains. This magnetization is then placed along B_0 (z) to allow maximum spin-diffusion and the progress of this mixing is examined via the spectrum obtained with a 90° pulse. These experiments again confirm the overall behaviour and heterogeneity discussed above.

6. Isotactic Polybut-1-ene

The ^{13}C spectrum of PBI obtained using CPMAR is shown in Figure 3. This spectrum shows splittings of the methylene resonances, probably arising from the details of the crystal structure as with the isotactic polypropene. The ^1H $T_{1\rho}$ behaviour of this material (23) is again three component with the longest component being of the order of 243ms and the short-time component ($T_{1\rho} \sim 500\mu\text{s}$) being a much larger proportion of the total signal than for the PE or PP samples. After heating to the melt and cooling, the sample was examined by both the CP and SPE experiments to record ^{13}C spectra at various times after the transformation to the 11:3 helix structure which this treatment brings about. Figure 4 illustrates the results. It should also be noted that the ^1H $T_{1\rho}$ immediately after the transformation is close to being a single exponential with $T_{1\rho} \sim 400\mu\text{s}$. This fact clearly explains why the CP experiment fails to give a good spectrum immediately following the transformation. On the other hand, the SPE experiment also fails to give a well-resolved spectrum and, since the ^1H , T_1 is 250ms the ^{13}C T_1 's are unlikely to be very long so this is perhaps unexpected. The likely explanation is that

the chains are executing substantial motions which give rise to large linewidth contributions arising possibly from the decoupler/thermal motion interference effect described earlier.

As the recovery of the material towards the 3:1 helix form proceeds the CP and SPE experiments increasingly give improved quality spectra both in terms of signal-to-noise and resolution. It is interesting that the best spectra are obtained after some two weeks of annealing but that the final spectra, taken after two months, seem to have lost resolution. This is possibly because the material which recrystallises first gives better crystals and that the eventual apparent decrease in resolution arises from the slower conversion and crystallisation of less perfect chains.

7. Propene-ethylene co-polymers

We have undertaken studies of a number of propene-ethylene co-polymers and the results of one such investigation are given here. The samples were as described in the experimental section. Figure 5 shows the ^1H spectra (normal and partially $T_{1\rho}^{90}$ relaxed) for PECII and III, the heptane soluble and insoluble fractions respectively. These show that PECIII behaves rather similarly to PPI and II as described elsewhere (23). PECII, however, shows the presence of a very sharp spectrum with a small underlying broad component which is revealed in the partially relaxed spectrum. Figure 6 illustrates the ^{13}C spectra for all three samples under different conditions. Figure 6(a) shows the standard CPMAR experiment for PEI. It is essentially the spectrum of isotactic polypropene (19) although the methylene and methyl peaks seem more symmetric. Use of the delayed contact experiment produces changes in this spectrum which are not presented here but which indicate a composite nature of the spectrum. Figure 6(b) shows the spectra obtained by means

of the CPMAR and SPE experiments on PECIII, the heptane insolubles. These exhibit some distinctive features. The methylene resonance in the CP spectrum shows some signs of resolved splitting although the methyl still does not. The SPE experiment, with a recycle time of 1sec, gives a dominant, unsplit methyl resonance and smaller methine and methylenes. This arises because the methyl groups in the crystalline portions of the main polypropene block have sufficient motions to give ^{13}C T_1 values short enough to contribute significantly to the SPE experiment with this recycle time. The smaller methine and methylene signals are probably associated with more mobile fractions of the main polypropene block.

Figure 6(c) shows the CPMAR and SPE spectra for PECII, the heptane solubles. The CPMAR spectrum is essentially that of isotactic polypropene although there are no obvious resolved splittings and there may be additional resonances in the methylene region. The SPE spectrum with a recycle time of 1sec however shows quite a different pattern of lines. The relative intensities of the lines are varied by changing the recycle period. For example the peak at the frequency corresponding to the methine resonance in isotactic polypropene is lost when the recycle time is reduced to 0.3sec. The detailed interpretation of these observations will be dealt with elsewhere.

Acknowledgements

We wish to thank the Science and Engineering Research Council for grants supporting this work and ICI plc for their continuing interest, assistance and financial support.

18. Bunn, A., Cudby, M..E.A., Harris, R.K., Packer, K.J. and Say, B.J., J. Chem. Soc. Chem. Comm. 1981, 15
19. Bunn, A., Cudby, M.E.A., Harris, R.K., Packer, K.J. and Say, B.J., Polymer, 1982, 23, 694
20. Fleming, W.W., Fyfe, C.A., Kendrick, R.D., Lyerla, J.R., Vanni, H. and Yannoni, C.S., 1980, ACS Symp. Ser., 142, 193
21. Nadarajah, M., MSc thesis, University of East Anglia, 1981
22. Stejskal, E.O., Schaefer, J. and Steger, T.R., 1978, Faraday Symp. Roy. Soc. Chem., No. 13, 56
23. Packer, K.J., Pope, J.M. and Yeung, R.R., J. Polym. Sci. Polym. Phys.. Ed., 1983/4, in press
24. Bergmann, K., Polymer Bull., 1981, 5, 355

18. Bunn, A., Cudby, M..E.A., Harris, R.K., Packer, K.J. and Say, B.J., J. Chem. Soc. Chem. Comm. 1981, 15
19. Bunn, A., Cudby, M.E.A., Harris, R.K., Packer, K.J. and Say, B.J., Polymer, 1982, 23, 694
20. Fleming, W.W., Fyfe, C.A., Kendrick, R.D., Lyerla, J.R., Vanni, H. and Yannoni, C.S., 1980, ACS Symp. Ser., 142, 193
21. Nadarajah, M., MSc thesis, University of East Anglia, 1981
22. Stejskal, E.O., Schaefer, J. and Steger, T.R., 1978, Faraday Symp. Roy. Soc. Chem., No. 13, 56
23. Packer, K.J., Pope, J.M. and Yeung, R.R., J. Polym. Sci. Polym. Phys.. Ed., 1983/4, in press
24. Bergmann, K., Polymer Bull., 1981, 5, 355

References

1. McBrierty, V.J. and Douglass, D.C., Physics Reports, 1980, 63
2. McBrierty, V.J. and Douglass, D.C., J. Polym. Sci., Macromol. Revs., 1981, 16, 295
3. Schaefer, J. and Stejskal, E.O., Topics in Carbon-13 NMR Spectroscopy, 1979, (Ed. G.C. Levy), 3, 284
4. Lyster, J.R., Contemp. Top. Polym. Sci., 1979, 3, 143
5. Heatley, F., Salovey, R. and Bovey, F.A., Macromolecules, 1969, 2, 619
6. Schaefer J. and Stejskal, E.O., J. Amer. Chem. Soc., 1976, 98, 1031
7. Pines, A., Gibby, M.G. and Waugh, J.S., J. Chem. Phys., 1973, 59, 569
8. Hartmann, S.R. and Hahn, E.L., Phys. Rev., 1962, 128, 2042
9. Balimann, G., Burgess, M.J.S., Harris, R.K., Oliver, A.G., Packer, K.J., Say, B.J., Tanner, S.F., Blackwell, R.W., Brown, L.W., Bunn, A., Cudby, M.E.A. and Eldridge, J.W., Chem. Phys. 1980, 46, 469
10. Blackwell, R.W., Burgess, M.J.S., Harris, R.K., Packer, K.J. and Say, B.J., unpublished work
11. Frye, J.S. and Maciel, G.E., J. Mag. Res., 1982, 48, 125
12. Phaorubul, O., Loboda-Cackovic, J., Cackovic, H., and Hosemann, R., Die Makromol. Chem., 1974, 175, 2991
13. Bergmann, K., J. Polym. Sci. Polym. Phys. Ed., 1978, 16, 1611
14. Zachmann, H.G., J. Polym. Sci. Symp., 1973, 43, 111
15. Smith, J.B., Manuel, A.J., and Ward, I.M., Polymer, 1975, 16, 57
16. Opella, S.J. and Frey, M.H., J. Amer. Chem. Soc., 1979, 101, 5854
17. Tegenfeldt, J. and Haeberlen, U., J. Mag. Res., 1979, 36, 453

Figure Captions

- Figure 1 Typical pulse sequences used in obtaining ^{13}C NMR spectra of solids. (a) A general double-resonance, cross-polarization sequence; (b) the single-pulse excitation sequence. The details of each sequence are discussed in the text.
- Figure 2 The variation with temperature of the ^{13}C high-resolution NMR spectrum of annealed isotactic polypropene (PPI). Each spectrum is the result of 2000 FID's acquired with a 60kHz decoupling field, 5ms contact time and 2s recycle time. The spectrometer frequencies were 90MHz for ^1H and 22.633MHz for ^{13}C . *For clarity, the methine peak has been omitted except from the spectrum at 290K*
- Figure 3 The ^{13}C high-resolution NMR spectrum of solid polybut-1-ene (PBI) at 300K. 2000 FID's were added and were obtained with a 60kHz decoupling field strength, 1ms contact and 1s recycle time. The spectrometer frequencies were as for Figure 2. *The peak assignments are: $\delta = 12.0$ ppm, CH_3 ; $\delta = 26.8$ (doublet), CH_2 (sidechain); $\delta = 31.3$, CH ; $\delta = 38.3$ (doublet), CH_2 (backbone).*
- Figure 4 The ^{13}C NMR spectra of solid polybut-1-ene (PBII) as a function of time following conversion from PBI by heating/cooling as described in the text. Single pulse excitation (SPE) experiments utilised a $6.25\mu\text{s}$ ^{13}C 90° pulse length and recycle time of 2s. All experiments employed a proton decoupling field strength of 60kHz and the CP experiments used a recycle time of 1.2s. The spectra are identified as (a) SPE, immediately after conversion; (b) CP, $T_c = 0.6\text{ms}$, $t = 4$ hrs; (c) CP, $T_c = 0.6\text{ms}$, $t = 8$ hrs; (d) SPE, $t = 12$ hrs; (e) CP, $T_c = 0.6\text{ms}$, $t = 16$ hrs; (f) SPE, $t = 17$ days;

(g) CP, $T_c = 3.5$ ms, $t = 17$ days; (h) CP, $T_c = 3.5$ ms, $t = 50$ days; (i) SPE, $t = 50$ days.

Figure 5 ^1H NMR spectra of (a) PECII and (b) PECIII, the heptane soluble and insoluble fractions of the propene/ethylene copolymer PECI. The spectra were recorded at $\nu_0^{^1\text{H}} = 200\text{MHz}$ following spin-locking $\{(\omega_1/2\pi) = 40\text{kHz}\}$ for a time T as indicated. Typically, 400 FID's were accumulated with a recycle time of 3s and a solid echo was used to measure the signal after the end of the spin-lock.

Figure 6 (a) The CPMAR ^{13}C high-resolution NMR spectrum of PECI. 4000 FID's were accumulated using a contact time of 1ms, a recycle time of 1s and a 60kHz decoupling field strength. (b) The ^{13}C spectra of PECIII obtained using SPE (lower trace) and CP (upper trace). The recycle time for both experiments was 1s with other conditions as for (a). (c) As for (b) except the sample is PECII, the heptane soluble fraction of PECI.

Figure 1. Two pulse sequences for the study of the 13C NMR spectra.

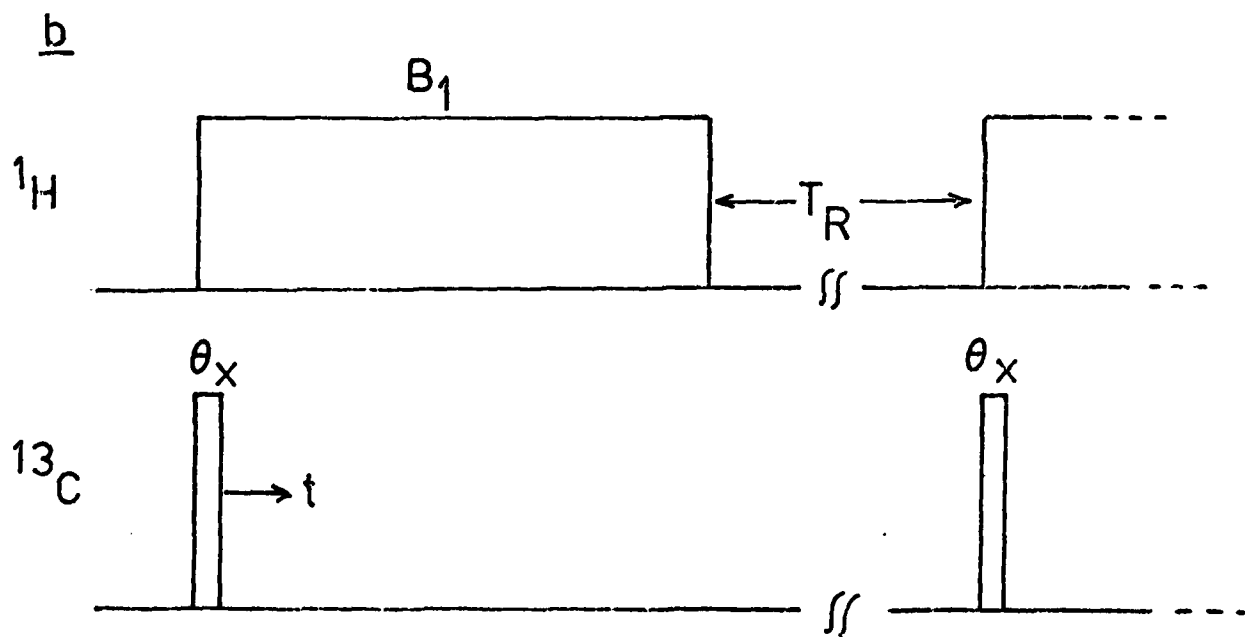
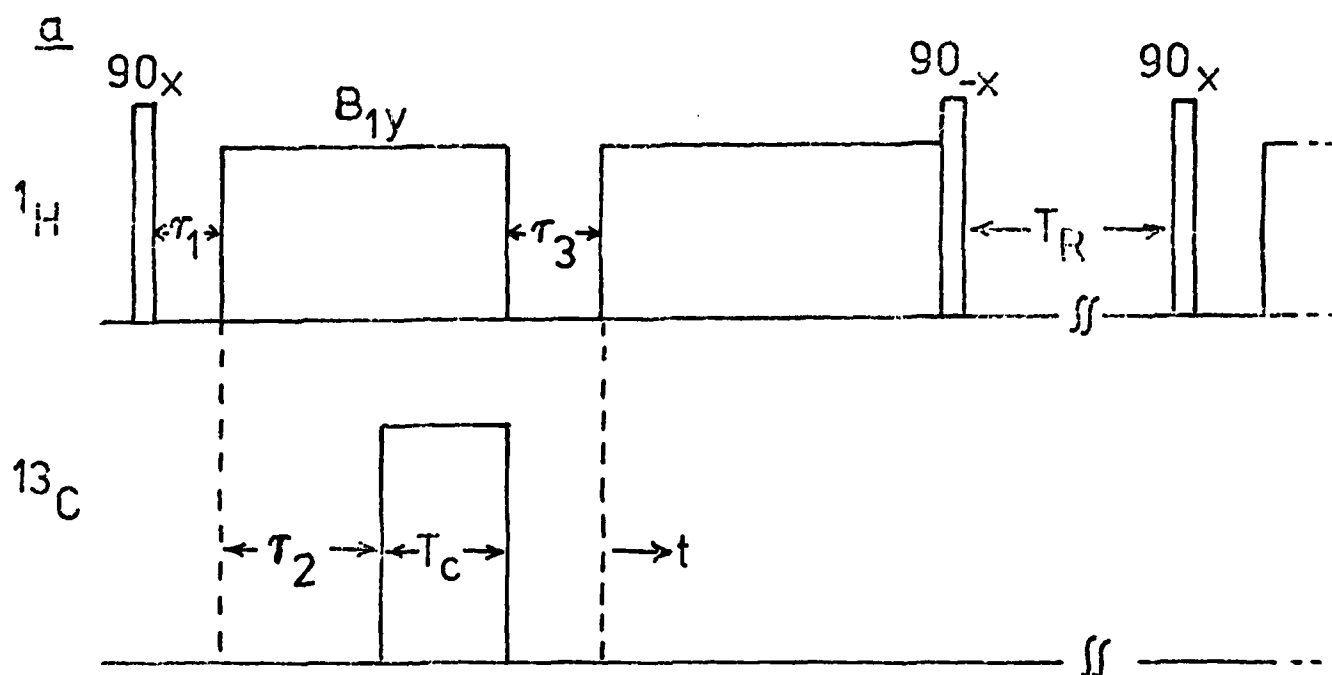


Fig 1.

Figure 2. ^{13}C NMR spectra of poly(2-vinylpyridine) at different temperatures.

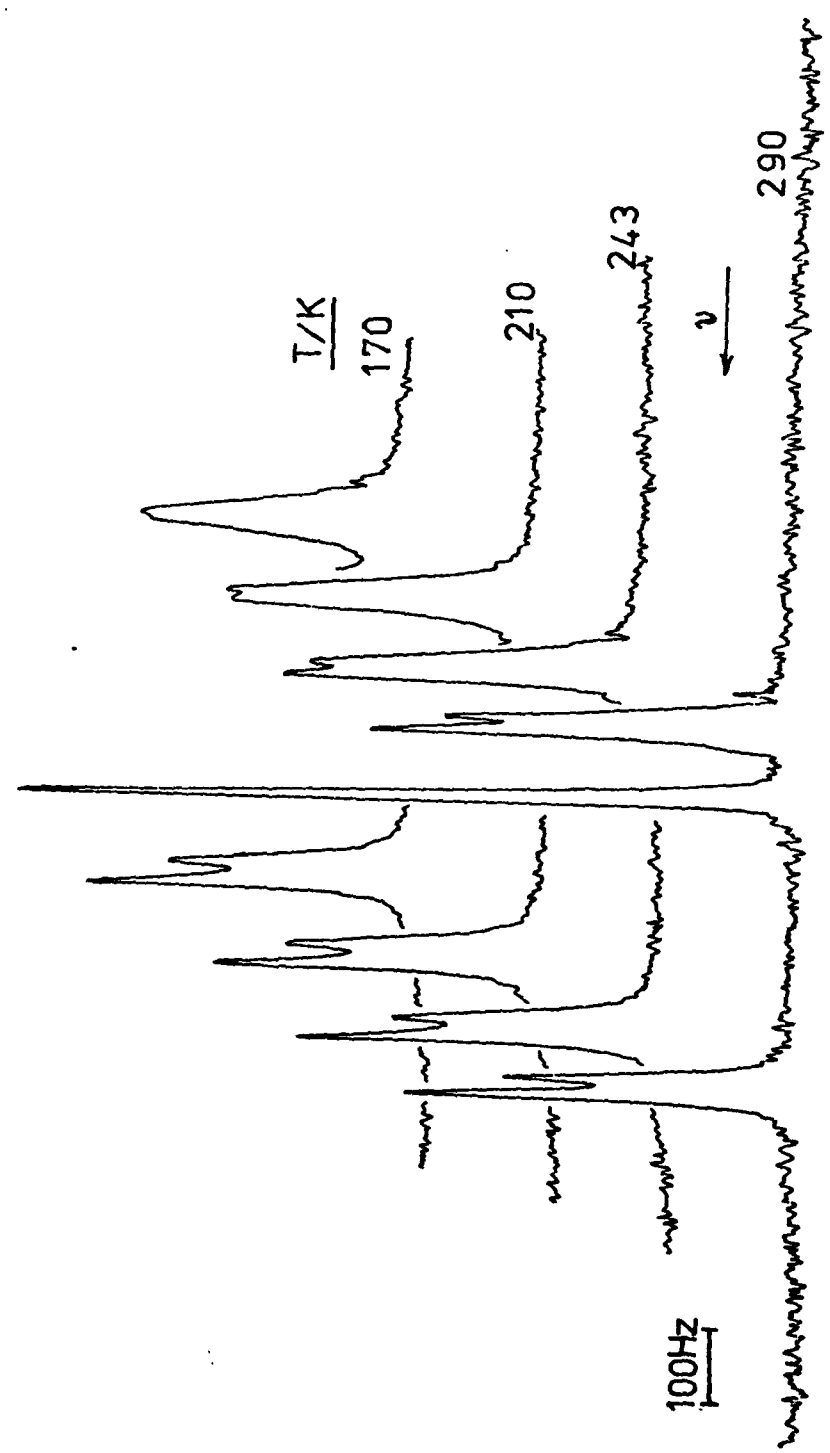


Figure 3. *Chetty, Harris, Metcalfe, Parker, Smith & Brown*

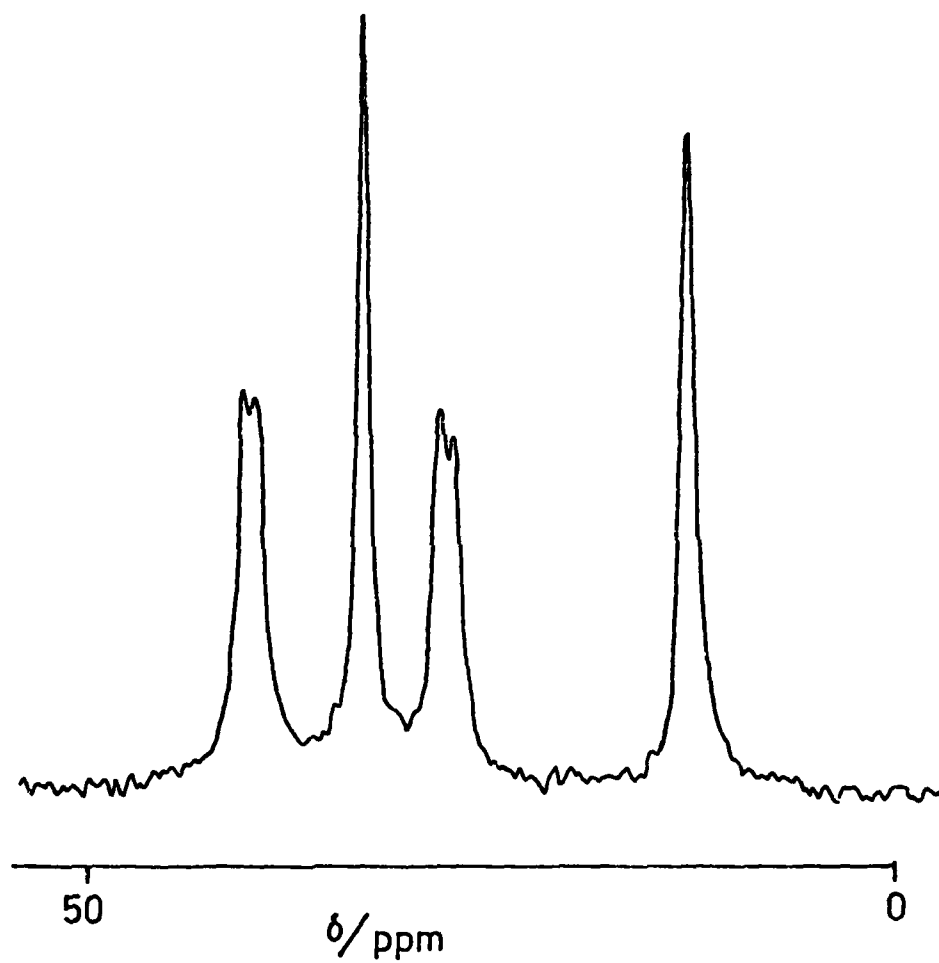


FIG-3

Fig-3

a

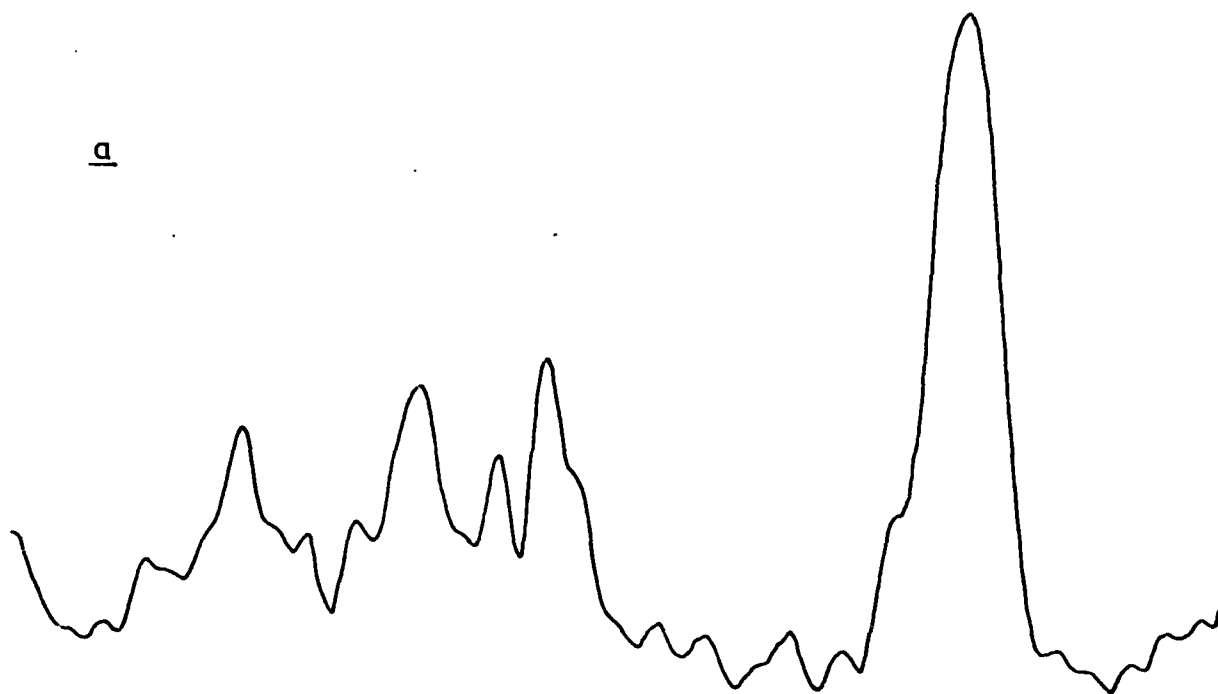


Figure 4b Cerdby, Harris, McAuliffe, Paekun, Smith & Brown

b

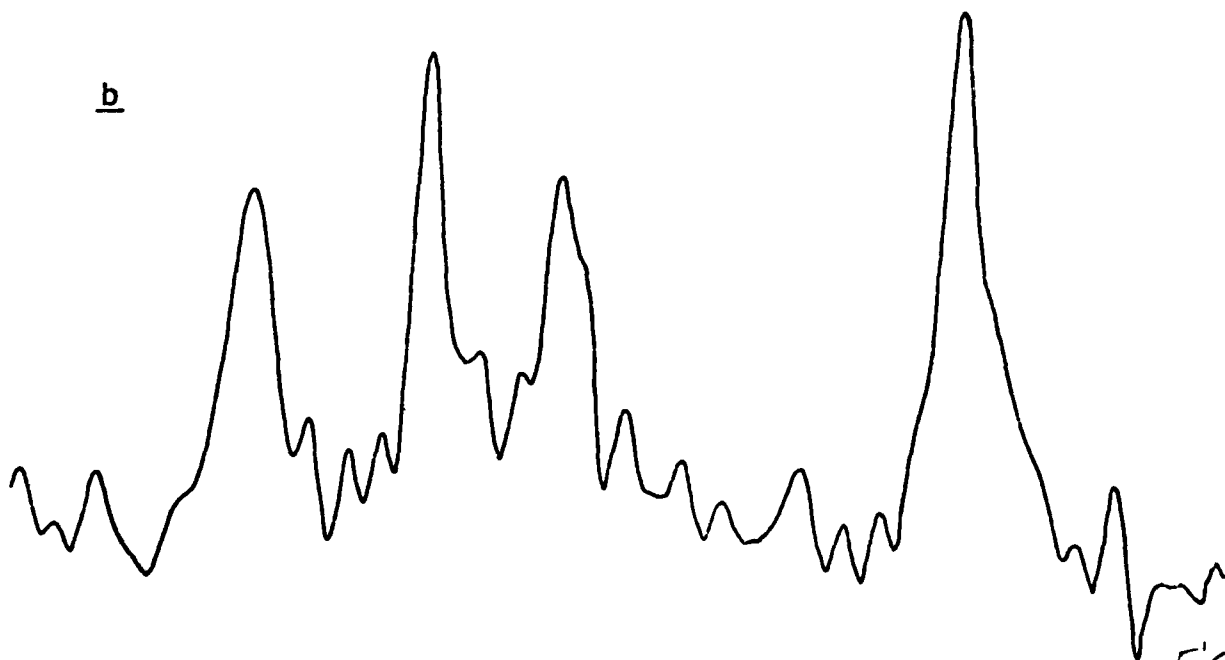


Fig 4a & b

Fig 4a & b

Figure 4c Cardiac trace, 1000 Hz, 2000 Hz, 4000 Hz, 8000 Hz

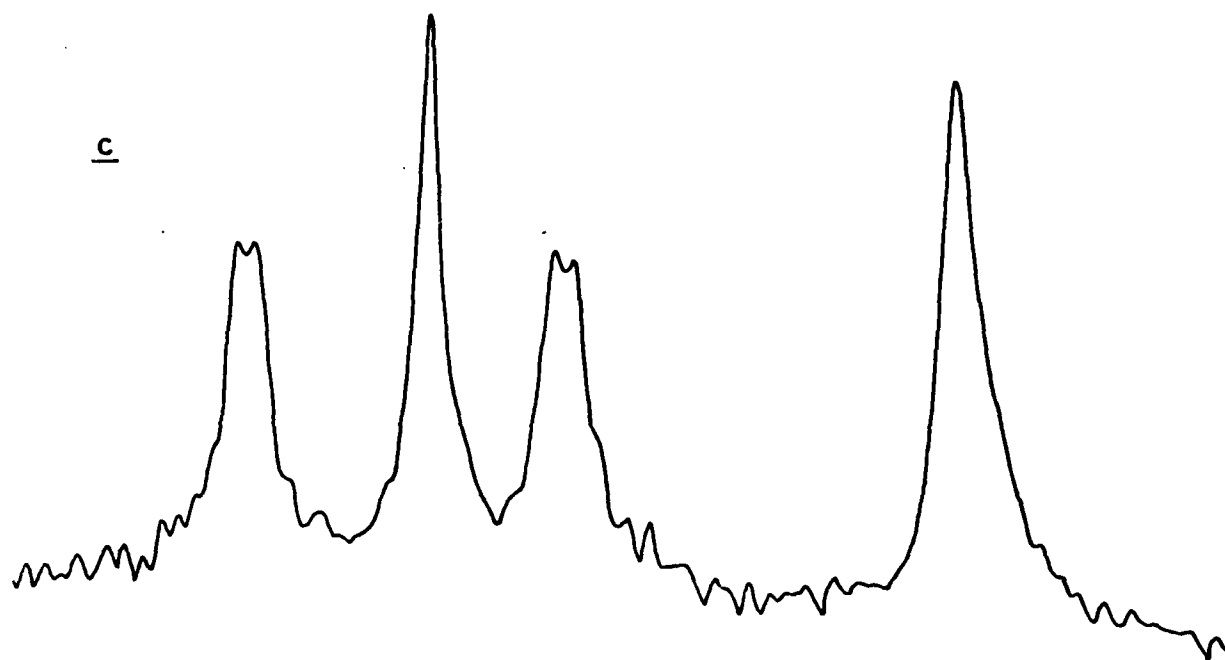


Figure 4d Cardiac trace, 1000 Hz, 2000 Hz, 4000 Hz, 8000 Hz

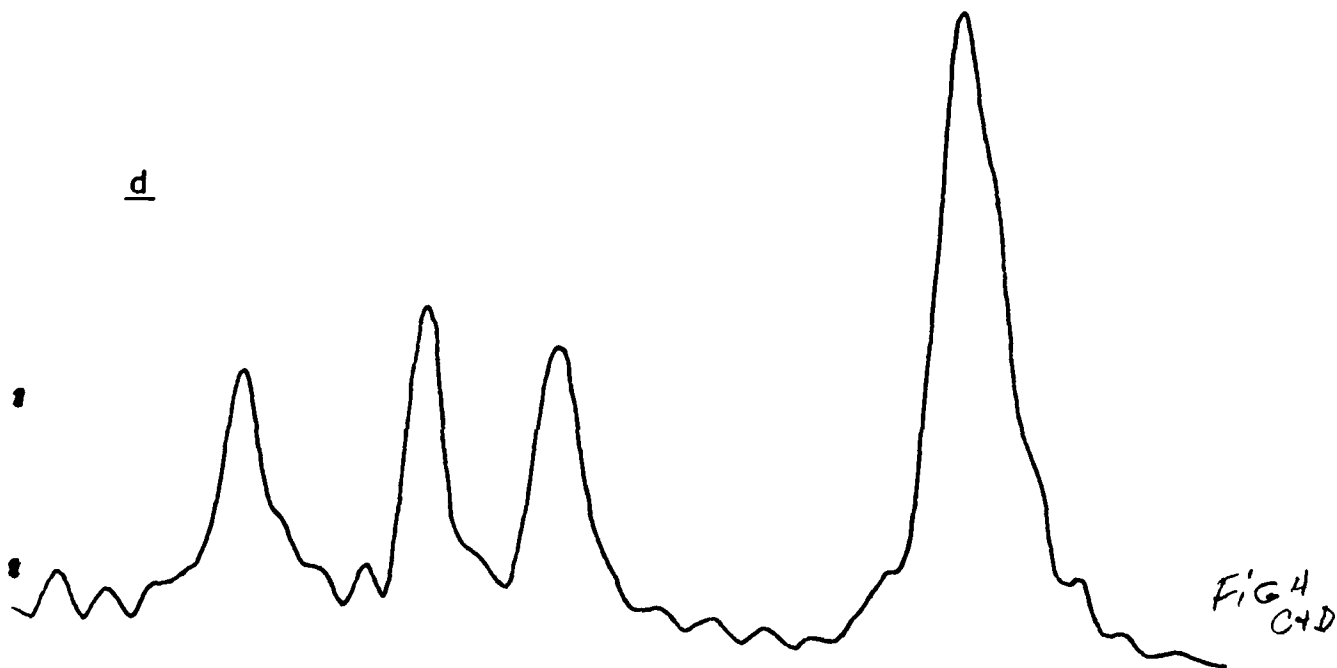


Fig 4
C+D

Fig 4 c+d

e

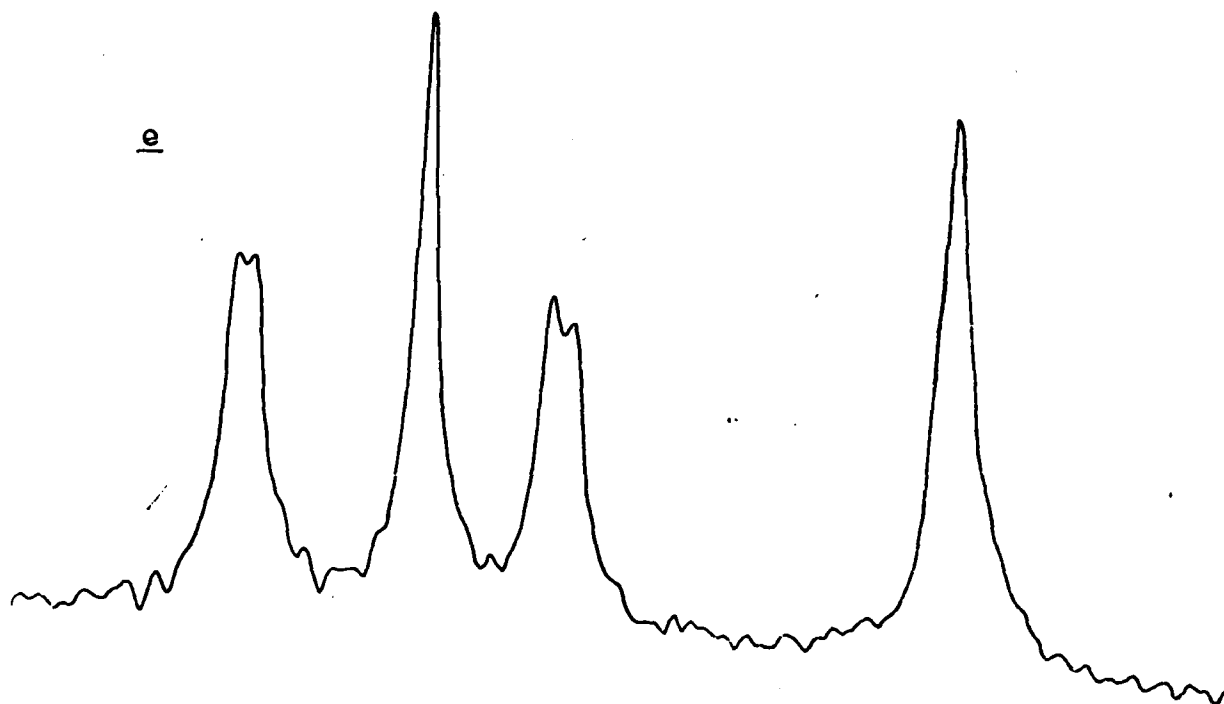


Fig. 4 e f

f

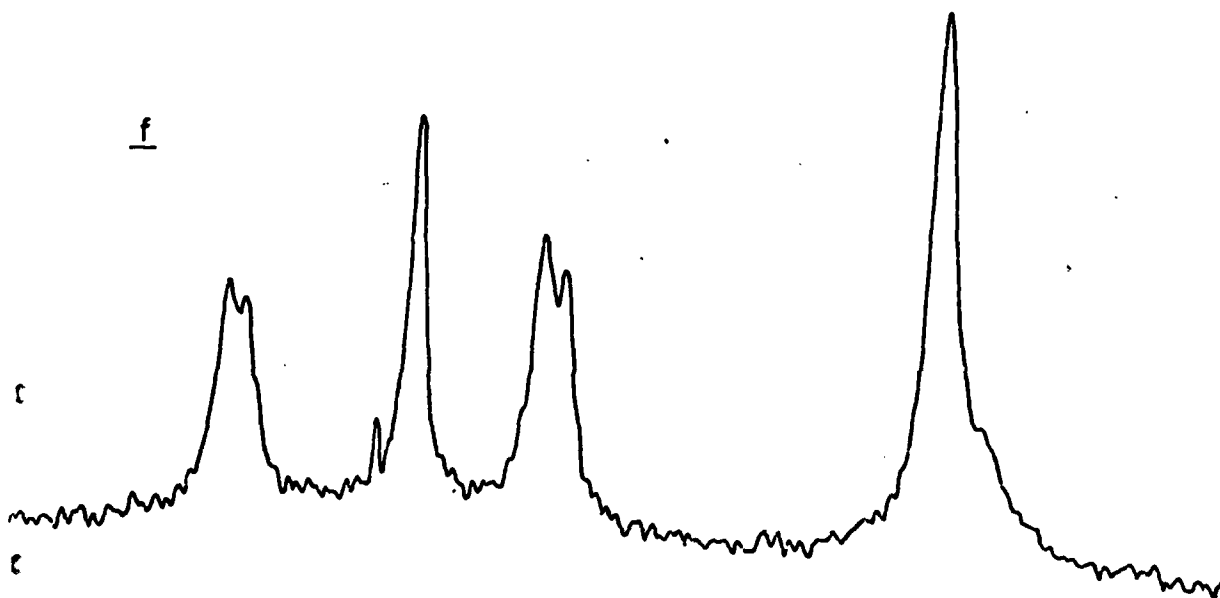


FIG. 4 e f

Fig 4 e f

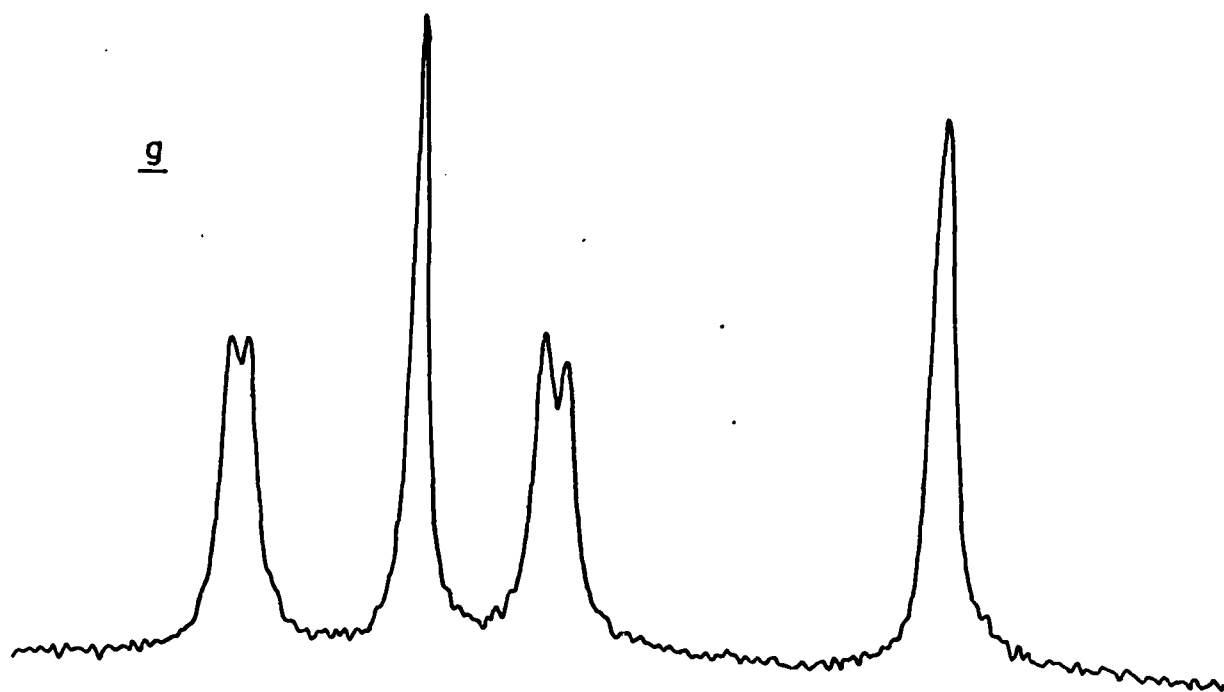


Figure 4h Cuda, Hans, Metcalfe, Parker, Smith & Bunn

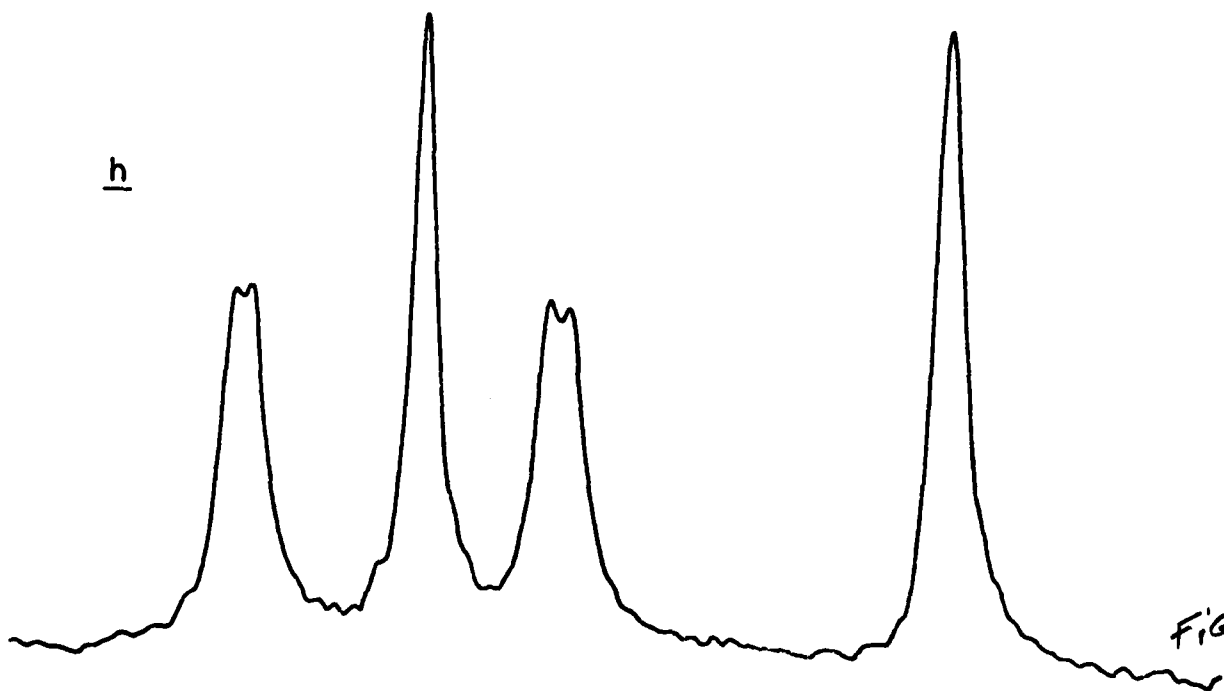
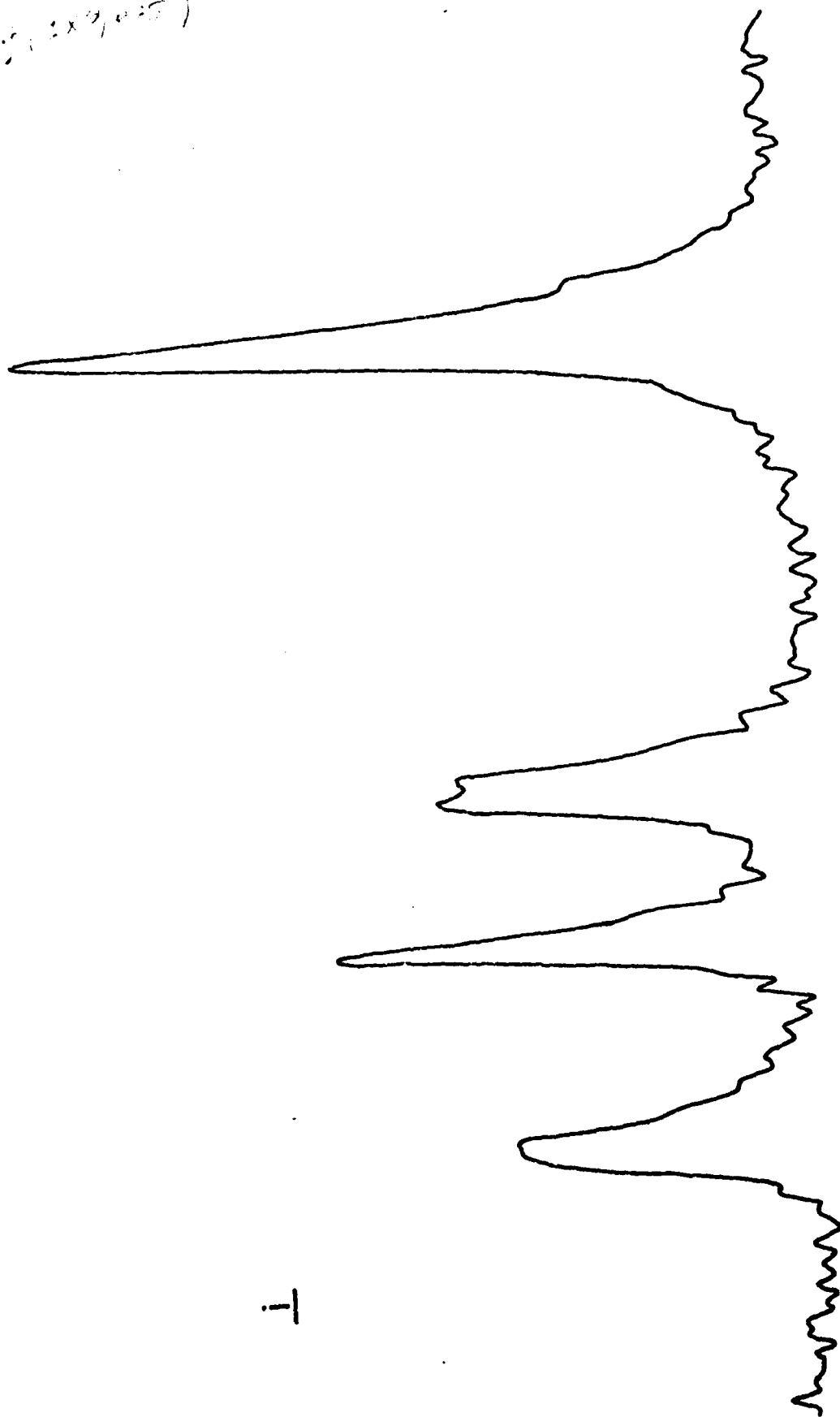


Fig 4g+h

Fig 4g+h

Fig 4 (Scale x2)

(Scale x2)



I

Figure 5a Cudby, Harris, Metcalfe,
Palmer, Smith & Quinn

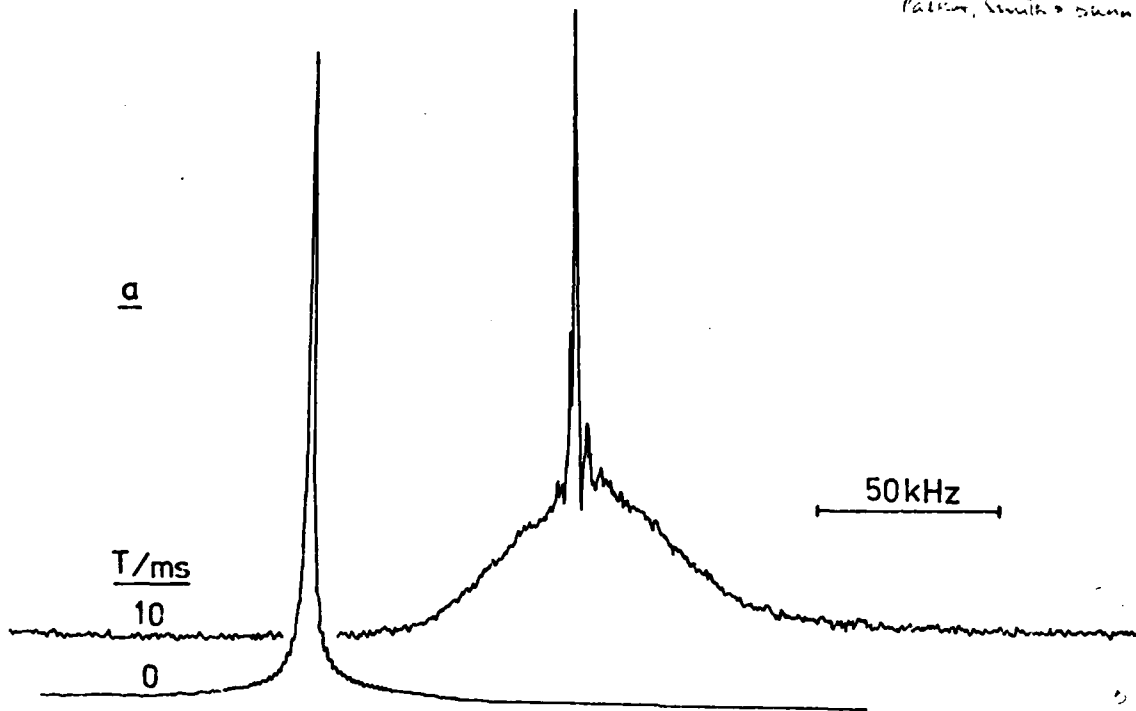


Figure 5b Cudby, Harris, Metcalfe,
Palmer, Smith & Quinn

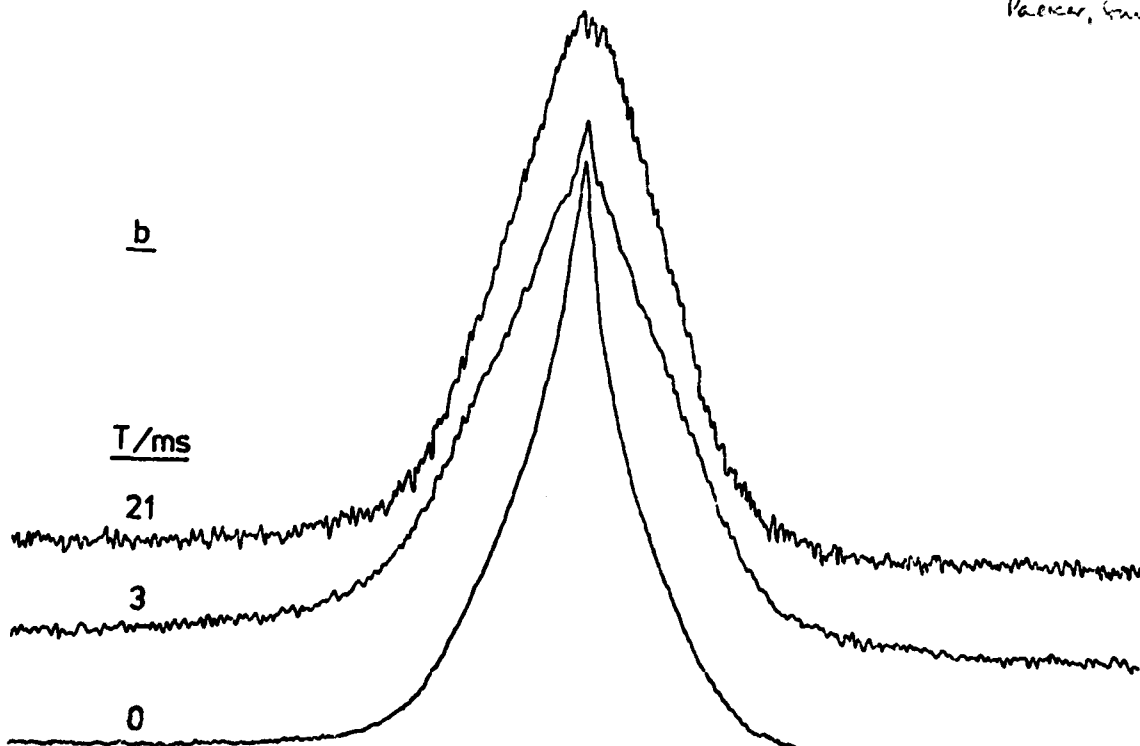


fig 5

Figure 6a

1064

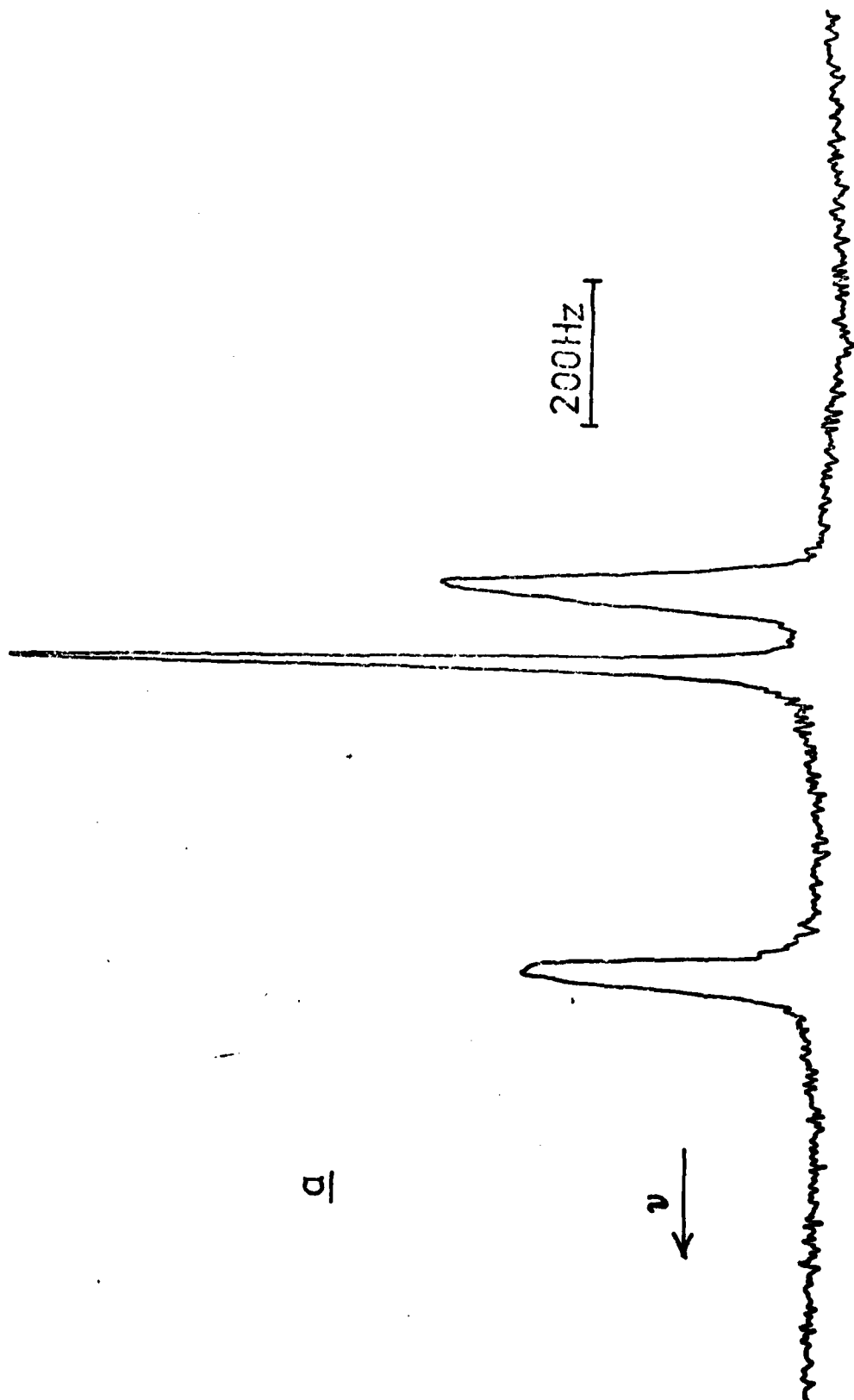
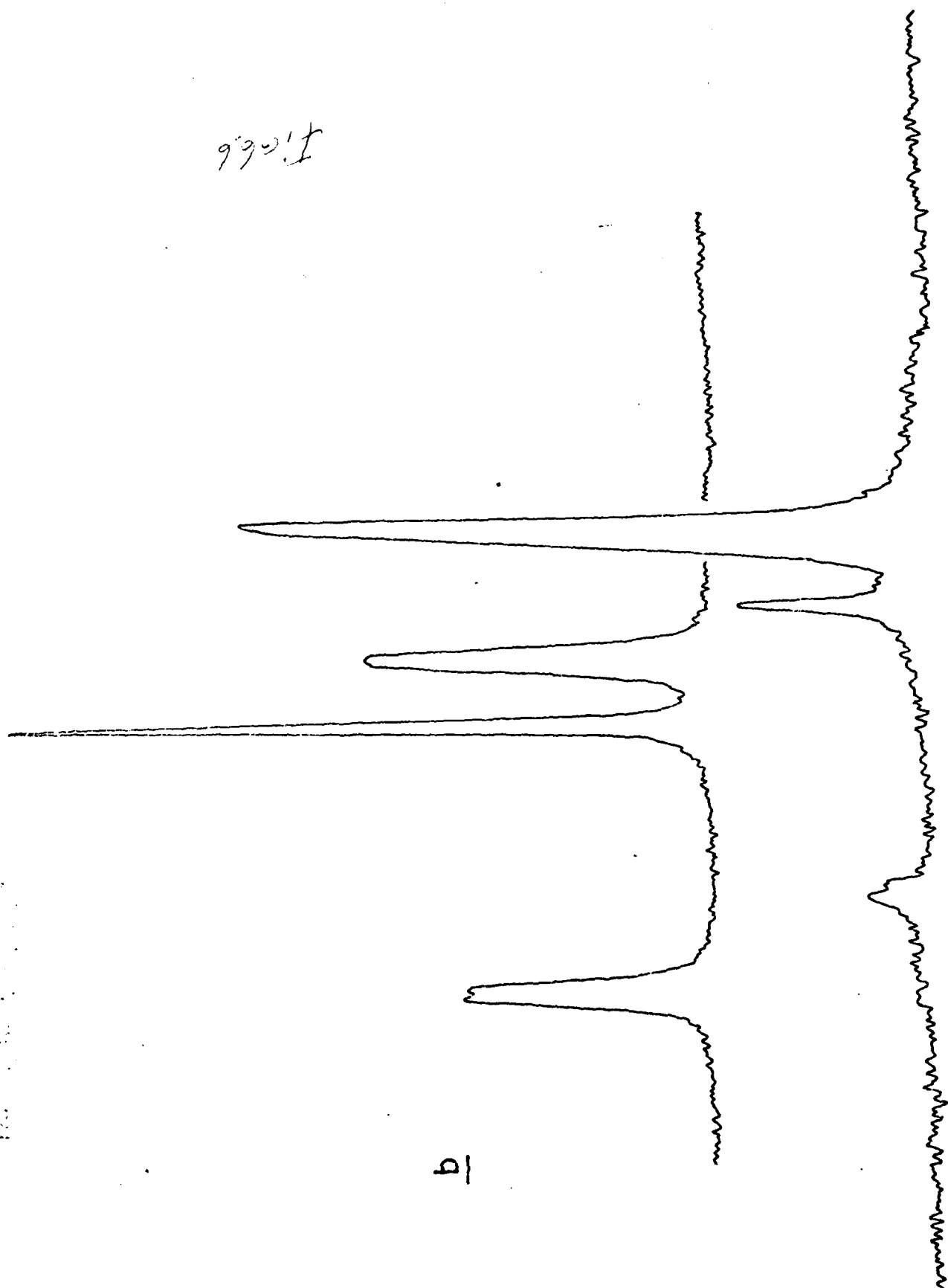


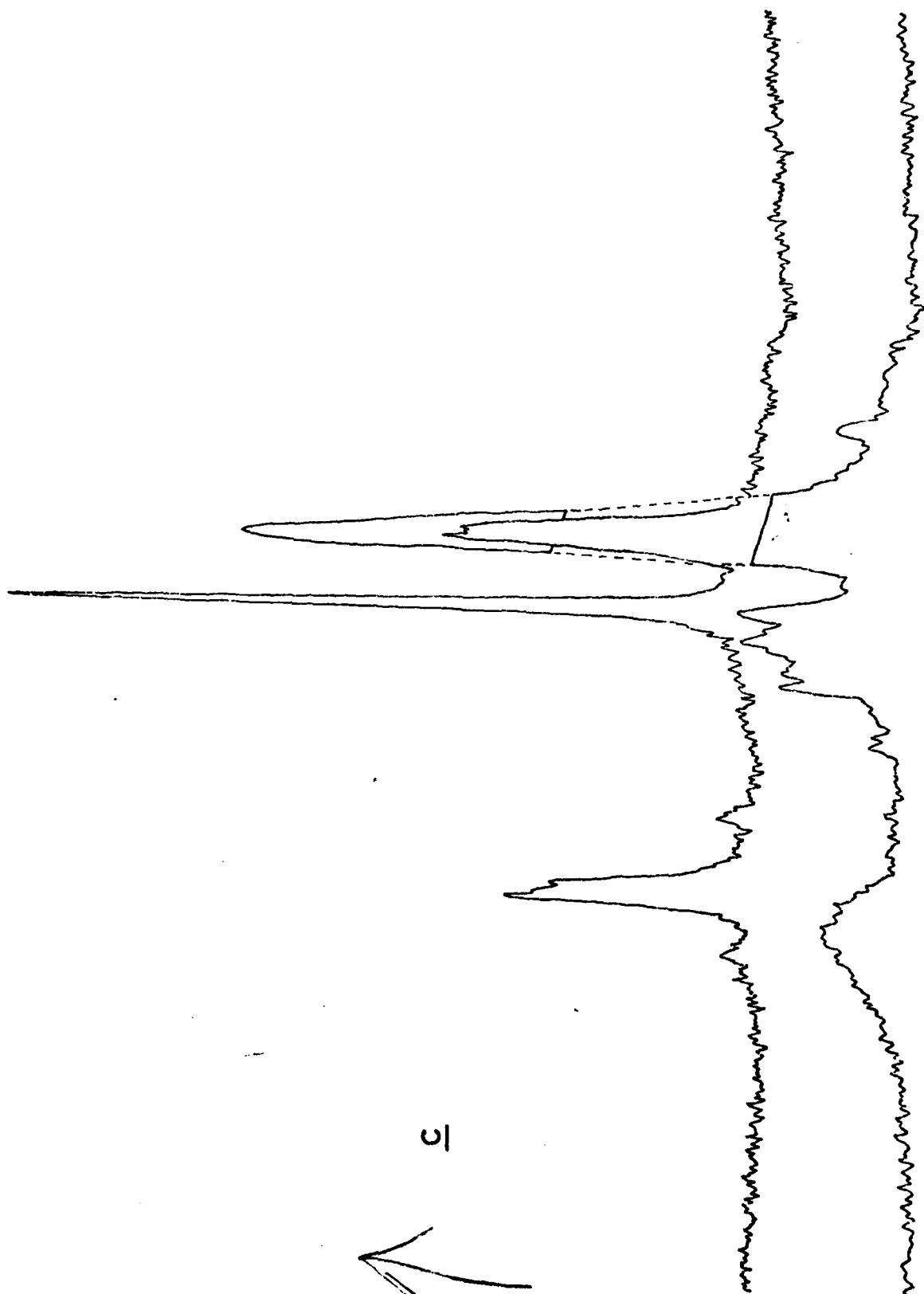
Fig. 6.6

9'90.1'



p

Fig 6c



5



AD-P003 910

Deuteron n.m.r. in relation to the glass transition in polymers.

E. Rössler, H. Sillescu, H.W. Spiess^a, and R. Wallwitz

Institut für Physikalische Chemie der Universität Mainz, Jakob-Welder-Weg 15,

D-6500 Mainz, W-Germany

→ H₂NMR

Summary

²H n.m.r. is introduced as a tool for investigating slow molecular motion in the glass transition region of amorphous polymers. In particular, we compare ²H spin alignment echo spectra of chain deuterated polystyrene with model calculations for restricted rotational Brownian motion. Molecular motion in the polystyrene-toluene system has been investigated by analysing ²H n.m.r. of partially deuterated polystyrene and toluene, respectively. The diluent mobility in the mixed glass has been decomposed into "solid" and "liquid" components where the respective average correlation times differ by more than 5 decades.

^a
Laboratorium für Makromolekulare Chemie
Universität Bayreuth
Postfach 3008
D-8580 Bayreuth

INTRODUCTION

Previous n.m.r. investigations of the glass transition in polymers¹ have provided information on relatively rapid motions with correlation times below $\sim 10^{-4}$ s at temperatures well above the static glass transition temperature T_g . Recent advances of ^2H n.m.r. have extended the dynamical range to slower motions, and in addition, they yield specific information upon the type of the molecular reorientation processes involved.²⁻⁶ In two component glasses, there is the further opportunity of investigating separately the molecular dynamics of both components by applying selective deuteration. Atactic polystyrene has for decades played the role of a "typical example" for the glass transition in amorphous polymers. Thus, we are also studying ^2H n.m.r. in polystyrene samples deuterated at the chain (PS-d_3) and at the phenyl rings (PS-d_5), respectively.⁶ PS and toluene (TOL) form a mixed glass over the whole concentration range which has already been investigated⁷ by ^1H n.m.r., dielectric relaxation, and thermal methods (DSC, DTA). It is apparent from this work that the TOL molecules are highly mobile at temperatures well below T_g of the mixture. A ^2H n.m.r. study where either toluene (TOL-d_3 , TOL-d_5) or polystyrene (PS-d_3 , PS-d_5) are deuterated should provide many details of the motion in the glass transition region.

In the following sections we first give an introduction into the relation of ^2H n.m.r. observables with molecular reorientation, for details we refer to a recent review.² Furthermore, we attempt to show the extent of new information that can be gained from ^2H n.m.r. with respect to the glass transition, taking PS as a typical example, and we give some details of the polystyrene-toluene system.^{6,8}

^2H n.m.r.

In a rigid solid, the coupling of the deuteron quadrupole moment with the axially symmetric field gradient of a C - ^2H bond gives rise to a splitting $2 \omega_Q$ of the ^2H Larmor frequency where

$$\omega_Q = \frac{3 e^2 Q q}{8 \hbar} (3 \cos^2 \theta - 1) \quad (1)$$

and θ is the angle of the C - H bond with respect to the external magnetic field. The weighted superposition of these doublets due to the random orientations in the glass yields the characteristic Pake line shape of the ^2H spectrum having a width of ~ 250 kHz for C - ^2H bonds.² Reorientation of the C - H bond can be described by a stochastic process

$$\Omega(t) = \cos \theta(t) \quad (2)$$

which can be modelled by assuming rate equations⁹

$$\frac{d}{dt} P(\Omega_i/\Omega_j, t) = \sum_k P(\Omega_i/\Omega_k, t) \pi_{kj} \quad (3)$$

where the $P(\Omega_i/\Omega_j, t)$ are conditional probabilities and the π_{ij} are rates of the transitions $\Omega_i \rightarrow \Omega_j$. The latter can be chosen in accordance with particular assumptions upon the reorientation process. It can be shown⁹ that the line shape of the n.m.r. spectrum is given by the Fourier transform of the free induction decay (FID) which can be expressed as

$$S_0(t) = \left\langle \exp i \int_0^t \omega_Q(t') dt' \right\rangle \quad (4)$$

where the average can be evaluated by solving a rate equation similar to equation (3) containing the same transition rates π_{ij} of the model for reorientation. Equation (4) applies in the whole "slow motion" region from the rigid Pake spectrum to the rapid motion limit. Detectable line shape changes of ^2H spectra occur in a correlation time range of $\sim 1 - 20$ μs . This time scale can be extended to ~ 200 μs by investigating the solid

echo spectrum which can be formulated⁴ as the Fourier transform of

$$S_1(t_1, \tau_1) = \left\langle \exp \left\{ i \int_0^{\tau_1} \omega_Q(t') dt' - i \int_0^{2\tau_1} \omega_Q(t') dt' - \int_{2\tau_1}^{t'_1} \omega_Q(t') dt' \right\} \right\rangle. \quad (5)$$

τ_1 is the distance between the two pulses of the solid echo sequence and t'_1 is the time starting from the echo maximum at $2\tau_1$ (see Fig. 1).

Equation (5) can be evaluated⁴ from the same rate equation that is used for solving equation (4). As a matter of fact, S_1 and S_0 become equal in the rigid solid limit since the contributions of the first two integrals of equation (5) cancel in this case. However, for correlation times $\tau_c \lesssim \tau_1$ no cancellation occurs, and S_1 may differ considerably⁴ from S_0 . The dynamical range of the solid echo technique is limited by the transverse relaxation time T_2 since no solid echo is detectable for $\tau_1 \gg T_2$. In most solid polymers $T_2 \sim 200 - 500 \mu s$ for 2H spectra. It should be noted that T_2 is related with the reciprocal homogeneous width that would be seen in a single crystal, c.f. equation (1). Ultra slow motions with correlation times up to $\sim 1 s$ can be investigated by application of the Jeener-Broekaert pulse sequence (Fig. 1) that yields a spin alignment echo after the 3rd pulse.³ Alignment echo spectra are obtained as the Fourier transform of^{3,5}

$$S_2(t'_2, \tau_1, \tau_2) = \left\langle \sin [\omega_Q(0)\tau_1] \sin [\omega_Q(\tau_2)(\tau_1 + t'_2)] \right\rangle \\ = \frac{1}{2} \left\langle \cos \left\{ \omega_Q(0)t'_2 + [\omega_Q(0) - \omega_Q(\tau_2)] \tau_1 \right\} \right\rangle - \langle FID \rangle. \quad (6)$$

The term⁵ $\langle FID \rangle$ is of minor importance in the context of the present paper. It is assumed that the mixing period τ_2 is much longer than the evolution and detection periods, respectively, and that Ω changes only on the time scale of τ_2 . Thus, $\tau_2 \gg \tau_1, t'_2$ and only the constant orientations $\Omega(0)$ and $\Omega(\tau_2)$ enter in equation (6) where products of the form $\omega_Q t$ have replaced the integrals $\int_0^t \omega_Q(t') dt'$ of equations (4) and (5). In the rigid solid limit, the alignment echo $S_2(t'_2, \tau_1, \tau_2)$ is a trivial superposition³ of

a solid echo and the term $\langle \text{FID} \rangle$. Molecular motion is seen through the difference

$$\Delta\omega_Q = \omega_Q(0) - \omega_Q(\tau_2) = (9 e^2 Qq / 8\hbar) (\cos^2 \theta_0 - \cos^2 \theta) \quad (7)$$

It is remarkable that reorientation by small step rotational Brownian motion causes dramatic changes in the alignment echo spectrum provided τ_2 is of the order of the time τ_s between 2 angular steps and $\Delta\omega_Q \tau_1 \sim \pi$. Since τ_s is much smaller than the rotational correlation time τ_c the alignment echo method provides an unique opportunity for distinguishing random small angular step reorientation from large angular jump motion where τ_s and τ_c are of the same order of magnitude. It should be noted that the average $\langle \dots \rangle$ of equation (6) can be evaluated from numerical solutions of equation (3) where small step rotational Brownian motion is described by a finite approximation of the diffusion equation.

BULK POLYSTYRENE

Our extensive study of partially deuterated PS- d_3 and PS- d_5 has already provided a wealth of information upon molecular motions above and below T_g part of which has been summarized in previous reviews.^{2,10} In this section, we wish to concentrate on the nature of chain motion in the glass transition region where new aspects have evolved from an analysis of alignment echo spectra. The model calculations shown in Fig. 2 confirm the large changes at times $\tau_2 \ll \tau_c$ where the C - ^2H bonds can only reorient within a small angular range of a few degrees. Furthermore, they reveal a surprising periodicity for $\tau_2 \gtrsim \tau_c$ with a peak to peak distance proportional to τ_1^{-1} . Of course, the assumption of constant $\Omega(0)$ during the evolution period τ_1 is critical for the appearance of this spectrum. On the other hand, the periodicity can be suppressed by restricting the rotational Brownian motion to a limited angular range. Thus, the alignment echo spectrum for rapid

restricted diffusion within $\pm 6^\circ$ ($\tau_2 \geq 5 \tau_c$) is similar to that of unrestricted diffusion for $\tau_2 = 0.005 \tau_c$ where the angular range is "restricted" by the time window τ_2 of the experiment. The experimental spectra of Fig. 3 show the typical behaviour of small angle reorientation where at 380 K the angular range of about $\pm 10^\circ$ is attained at $\tau_2 = 40$ ms. The absence of periodicities for longer τ_2 values rules out unrestricted rotational diffusion. Furthermore, the integral of the theoretical unrestricted diffusion spectra essentially vanishes at $\tau_2/\tau_c \geq 0.1$ since the positive and negative contributions to the spectrum almost cancel. The corresponding experimental intensities decay much slower for long τ_2 values though they do not become constant as predicted from the model of restricted rotational diffusion. The decay of the alignment echo is not yet fully clarified, however, we suggest tentatively that only a fraction of the C - H bonds can fully reorient, most likely through conformational changes, on a time scale of ~ 1 s and this fraction decreases rapidly below T_g . At higher temperatures $T \geq 400$ K, we know from the ^2H c.w. absorption spectra^{2,10} that full reorientation of the C - H bonds occurs by essentially a single process where any "distribution of correlation times" must be restricted to less than one decade. Now, it turns out that the correlation times determined from the slow motion line shapes are at least an order of magnitude larger than those obtained from spin lattice relaxation times T_1 in this temperature range.^{6,8} Apparently, the latter are determined by the fast restricted rotational diffusion discussed above. Thus, we conclude that chain motion in the glass transition region can be described by a rapid rotational diffusion process which is restricted by an angular range of approximately $\pm 10^\circ$ at T_g and decreases at lower temperatures. Full reorientation of the C - H bonds occurs by a slower process. It should be noted that ^2H n.m.r. is presently the only experimental method for detecting the reorientation of a single bond vector in the glass transition region. Photon correlation spectra as well as dielectric and mechanical relaxation are related with

fluctuations or larger volume elements where the cooperativity caused by free volume redistributions may be the reason for finding broad distributions of correlation times.¹⁰⁻¹²

THE POLYSTYRENE-TOLUENE SYSTEM

It is well known¹³ that the glass transition T_g of a polymer can be considerably reduced by adding relatively small amounts of a low molecular weight diluent. If phase separation occurs due to thermodynamical instability, no further reduction of T_g below the demixing temperature is possible. However, polystyrene and toluene remain miscible over the whole concentration range down to the glass transition of toluene.⁷ Our ^2H n.m.r. study of this system has provided information upon molecular motion that may be typical for any glassy mixture of a polymer and a small molecule diluent.

In bulk PS- d_5 , we have discovered that about 20% of the phenyl groups perform 180° jumps around their axis to the backbone even at temperatures well below T_g .² By adding toluene, the glass transition can be reduced to low temperatures. We find that the fraction of flipping phenyl groups becomes smaller and more difficult to detect for diluent concentrations where the solid glass regime is shifted to lower temperatures. There is no indication of large amplitude phenyl group libration as was concluded from ^1H wide line n.m.r. by Adachi et al.^{7,14} Thus, we could use PS- d_5 for investigating the chain motion in the PS-TOL system. In Fig. 4, we have shown the T_2 values of PS- d_5 determined by measuring the echo height as a function of the distance τ_1 between the two pulses of the solid echo sequence. The plot of $\log T_2$ versus $1/T$ is linear at temperatures above the glass transition, and it changes to an almost constant value at a temperature $T_{g,p}$ close to the static T_g as determined from other experimental methods,⁷ cf. Fig. 7. In the toluene rich region, T_2 decreases as the temperature is lowered below

$T_{g,P}$ attains a minimum, and increases again to the rigid solid value. Thus a second temperature $T'_{g,P}$ can be estimated as is shown in Fig. 4 for a solution of 35.1% PS- d_5 in TOL- d_0 . Apparently, there is a temperature range between $T_{g,P}$ and $T'_{g,P}$ where the chains are not fully immobilized due to the abundance of highly mobile solvent molecules (see below). The solid echo line shapes of PS- d_5 will be discussed in a later publication.⁶

The diluent mobility has been investigated by using TOL- d_3 or TOL- d_5 . No substantial differences between these toluenes was found for the overall TOL motion. However, the rapid methyl group rotation in TOL- d_3 persists even at the lowest temperatures of our experiments thus reducing the widths of all 2H spectra to one third of the corresponding TOL- d_5 values. On cooling a TOL- d_3 (or TOL- d_5) solution of PS below the temperature $T_{g,SE}$ shown in Figs. 6 and 7, a solid echo can be detected on top of the "liquid" FID. If this signal is Fourier transformed with respect to t'_1 starting at $t = 2 \tau_1$ (cf. Fig. 1) we obtain a spectrum as shown in Fig. 5a. The central portion originates from part of the "liquid" FID that starts at $t = 0$. It should be noted that the second 90° pulse of the solid echo sequence has no influence upon the FID of a liquid since it is shifted in phase by 90° with respect to the first pulse. In Fig. 5b, τ_1 has been increased to a value where the FID has decayed to zero ($2 \tau_1 \gg T_{2,FID}$). The solid echo spectrum of Fig. 5b has essentially the rigid limit Pake line shape. Thus, the rotational correlation time of the TOL- d_3 molecules that give rise to this spectrum must be larger than $\sim 100 \mu s$. Since we can detect a spin alignment echo after $\sim 50 ms$, the correlation times are even above this slow time scale. On the other hand, the TOL- d_3 molecules contributing to the "liquid" FID have correlation times below $\sim 1 \mu s$. Though this corresponds to re-orientation in a rather viscous liquid the correlation time difference of more than 5 decades provides sufficient evidence for qualitatively different

behaviour. We have tried to estimate the intensities of the "liquid" and "solid" contributions by extrapolating the FID to $t \rightarrow 0$ and the amplitude of the solid echo to $\tau_1 \rightarrow 0$. Since the solid echo amplitude become non-exponential at short times⁶ this estimate is admittedly crude. We should also emphasize that the decomposition implies no statement upon possible correlation time distributions within the "solid" and "liquid" components. Nevertheless, it allows for some important conclusions upon diluent motion in the mixed glass. The TOL solid echo becomes observable above $T_{g,p}$ at temperatures where PS- d_5 also gives rise to a solid echo (cf. Fig. 4). Thus, the mobility of the "rigid" TOL molecules is linked to that of the PS chains at $T \lesssim T_{g,SE}$. There are even indications that it is slower as will be discussed in ref. 6. On lowering the temperature below $T_{g,p}$, increasing amounts of TOL "freeze" towards the chains until the whole mixture becomes a solid glass at $T_{g,FID}$. It is apparent from Fig. 6 that the intensities of the "solid" and "liquid" components add to an approximately constant total intensity. The latter has been scaled in Fig. 6 by an arbitrary factor appropriate for presentation of the data in one figure, and by the Boltzmann factor determining the trivial temperature dependence of the spin populations. Thus, the intensities given in Fig. 6 are a measure of the "solid" and "liquid" fractions in the temperature region $T_{g,FID} \leq T \leq T_{g,SE}$. This region becomes very broad for large PS concentrations. Furthermore, the solid echo line shapes of the "solid" TOL fraction become motionally narrowed for PS concentrations above $\sim 80\%$ indicating the abundance of "free volume" between the rigid PS chains.⁶ It is clearly visible in Fig. 7 that the static glass transition T_g (dotted line) is close to $T_{g,p}$ in the PS rich regime indicating that the solid glass behaviour is governed by the polymer. On the other hand, the TOL glass transition takes over in the TOL rich regime with less than $\sim 50\%$ PS. Here, the

static T_g is close to $T'_{g,p}$ and $T_{g,FID}$, and some chain mobility persists in the temperature region $T_{g,p} \geq T \geq T'_{g,p}$.⁶ The temperatures $T_{g,p}$ and $T'_{g,p}$ converge at very high TOL concentrations where the TOL glass transition could be determined from T_2 measurements in TOL- d_3 having a similar temperature dependence as shown in Fig. 4 for PS- d_5 .⁶

Finally, we wish to note that different diluent mobilities in PS have also been found for the "dual mode sorption" of ammonia as investigated by 1H n.m.r.¹⁵ and for di-n-alkyl-phthalates where dielectric relaxation data were interpreted in terms of three different α processes.¹⁶

CONCLUSIONS

We conclude from a comparison of 2H spin alignment echo spectra with model calculations that chain motion in the glass transition region of PS can be described by a relatively rapid rotational diffusion process which is restricted to an angular range of approximately $\pm 10^\circ$ close to T_g . Full re-orientation by a slower process tends to become motionally heterogeneous as the glass transition is approached from above.

2H n.m.r. spectra of deuterated toluene in the PS-TOL glass can be interpreted in terms of a two component decomposition. The motion of the "solid" component is linked to that of the PS chains at temperatures below a temperature $T_{g,SE}$ where a solid echo becomes observable. On lowering the temperature, the fraction of "solid" TOL increases until the whole mixture becomes a solid glass at a temperature $T_{g,FID}$. There is a range $T_{g,FID} \leq T \leq T_{g,SE}$ where a "liquid" fraction of highly mobile TOL molecules exists at temperatures below the "static" glass transition temperature T_g as determined by dielectric relaxation or thermal methods.⁷ T_g is close to $T_{g,SE}$ in PS rich systems and close to $T_{g,FID}$ in systems with PS concen-

trations below 50% (see Fig. 7). In the TOL rich regime we can determine a temperature $T_{g,p} > T_g$ where the chain motion becomes highly restricted and a "solid" TOL fraction is observable.

References

- 1 McCall, D.W. J. of Elastomers and Plastics 1976, 8 , 60
- 2 Spiess, H.W. Colloid Polym. Sci. 1983, 261, 193
- 3 Spiess, H.W. J. Chem. Phys. 1980, 72, 6755
- 4 Spiess, H.W., Sillescu, H. J. Magnetic Resonance 1980, 42, 381
- 5 Lausch, M., Spiess, H.W. J. Magn. Resonance 1983,
- 6 Rössler, E., Sillescu, H., Spiess, H.W., Wallwitz, R. to be published
- 7 Adachi, K., Fujihara, I., Ishida, Y. J. Polym. Sci., Polym. Phys. Edn. 1975, 13, 2155
- 8 Rössler, E., Diss., Univ. Mainz, 1984
- 9 Abragam, A. The Principles of Nuclear Magnetism, Clarendon Press, Oxford 1961
- 10 Sillescu, H., in IUPAC Macromolecules, Ed. by H. Benoit and P. Rempp, Pergamon Press, Oxford - New York 1982
- 11 Lee, H., Jamieson, A.M., Simha, R. J. Macromol. Sci.-Phys. 1980, B 18, 649
- 12 Böttcher, C.J.F., Bordewijk, P. Theory of Electric Polarization, 2nd Ed., Vol. II, Elsevier Sci.Publ.Co., Amsterdam 1978
- 13 Ferry, J.D., Viscoelastic Properties of Polymers, 3rd Ed., John Wiley, New York, 1980
- 14 We believe that the central portion of the 167 K spectrum shown in Fig. 9 of ref. 7 originates from residual protons of the deuterated solvent; the large apparent intensity can be explained by overmodulation.
- 15 Hains, P.J. and Williams, G., Polymer 1975, 16, 725
- 16 Assink, R.A., J. Polym. Sci. Polym. Phys. Ed. 1975, 13, 1665

Figure Captions

Figure 1. Notation for the solid echo, and the generalized Jeener-Broekaert 3 pulse sequence. θ_y , ϕ_x , and ψ are the flip angles of the respective h.f. pulses.

Figure 2. Theoretical ^2H alignment echo spectra for the model of rotational Brownian motion.

First row: unrestricted diffusion for different ratios of the pulse distance τ_2 (Fig. 1) over the rotational correlation time τ_c .

Second row: rapid motion limit ($\tau_2/\tau_c > 5$) for diffusion restricted to the angular ranges shown in the figure.

Figure 3. Experimental ^2H alignment echo spectra of chain deuterated polystyrene above T_g .

Figure 4. Spin relaxation times T_2 of PS- d_5 in PS-TOL mixed glasses.

Numbers in the figure denote wt.% PS- d_5 . The arrows indicate glass transition temperatures $T_{g,p}$ and $T'_{g,p}$ (see text).

Figure 5. ^2H solid echo (a,b) and alignment echo (c) spectra of TOL- d_3 in a mixed glass with 28.7 % PS.

Figure 6. ^2H intensities (I in arbitrary units, see text) of TOL- d_3 (triangles) and TOL- d_5 (circles, squares) in mixed glass with PS. Numbers in the figure denote wt.% PS. Open and full symbols denote "liquid" and "solid" components, respectively (see text).

Figure 7. Glass transition temperatures in the PS-TOL system.

Abscissa: wt.% PS. Full line, open symbols: $T_{g,FID}$. Full and dashed lines, full circles: $T_{g,p}$ and $T'_{g,p}$ (see text). Full squares (PS- d_3) and triangles (PS- d_5): $T_{g,SE}$. Dotted line: T_g as determined by dielectric relaxation and thermal methods (ref. 7).

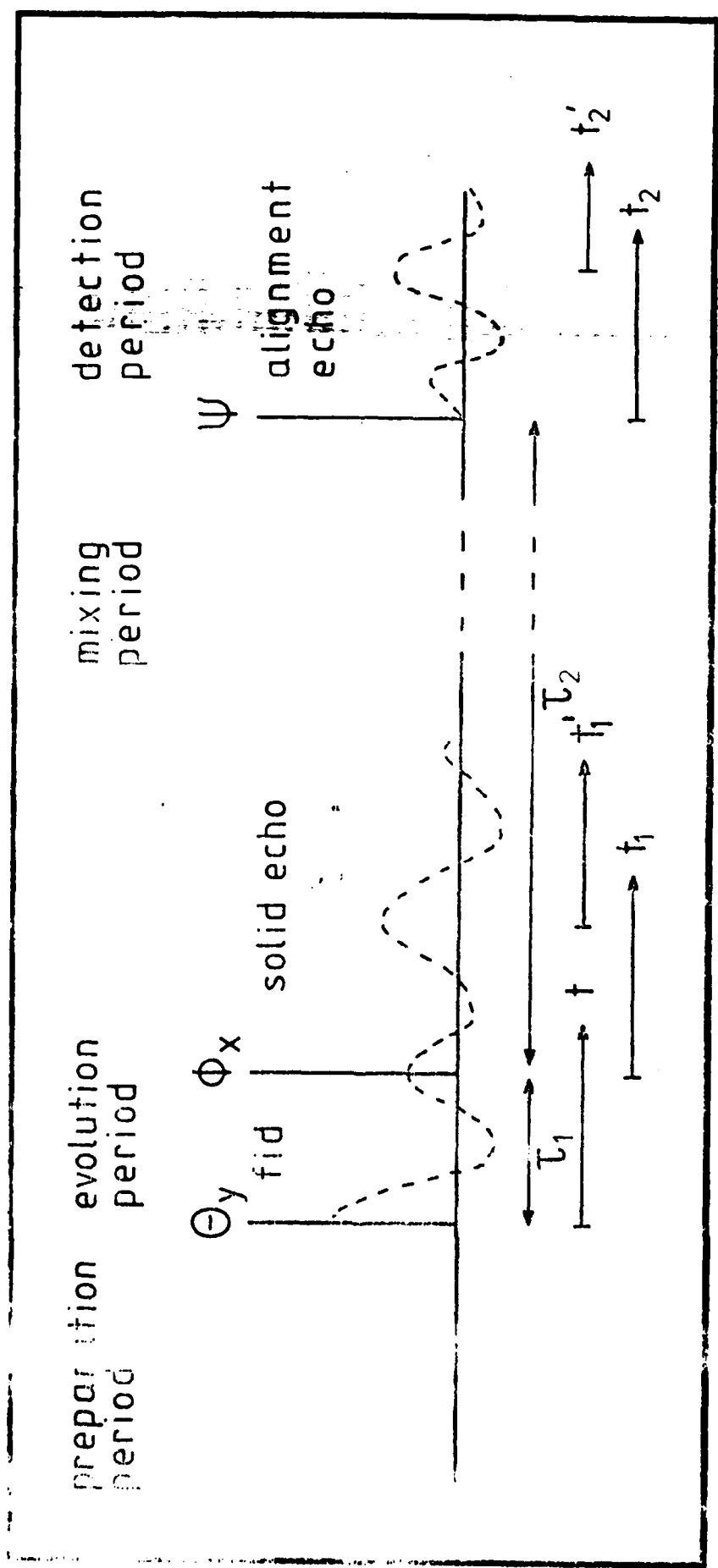
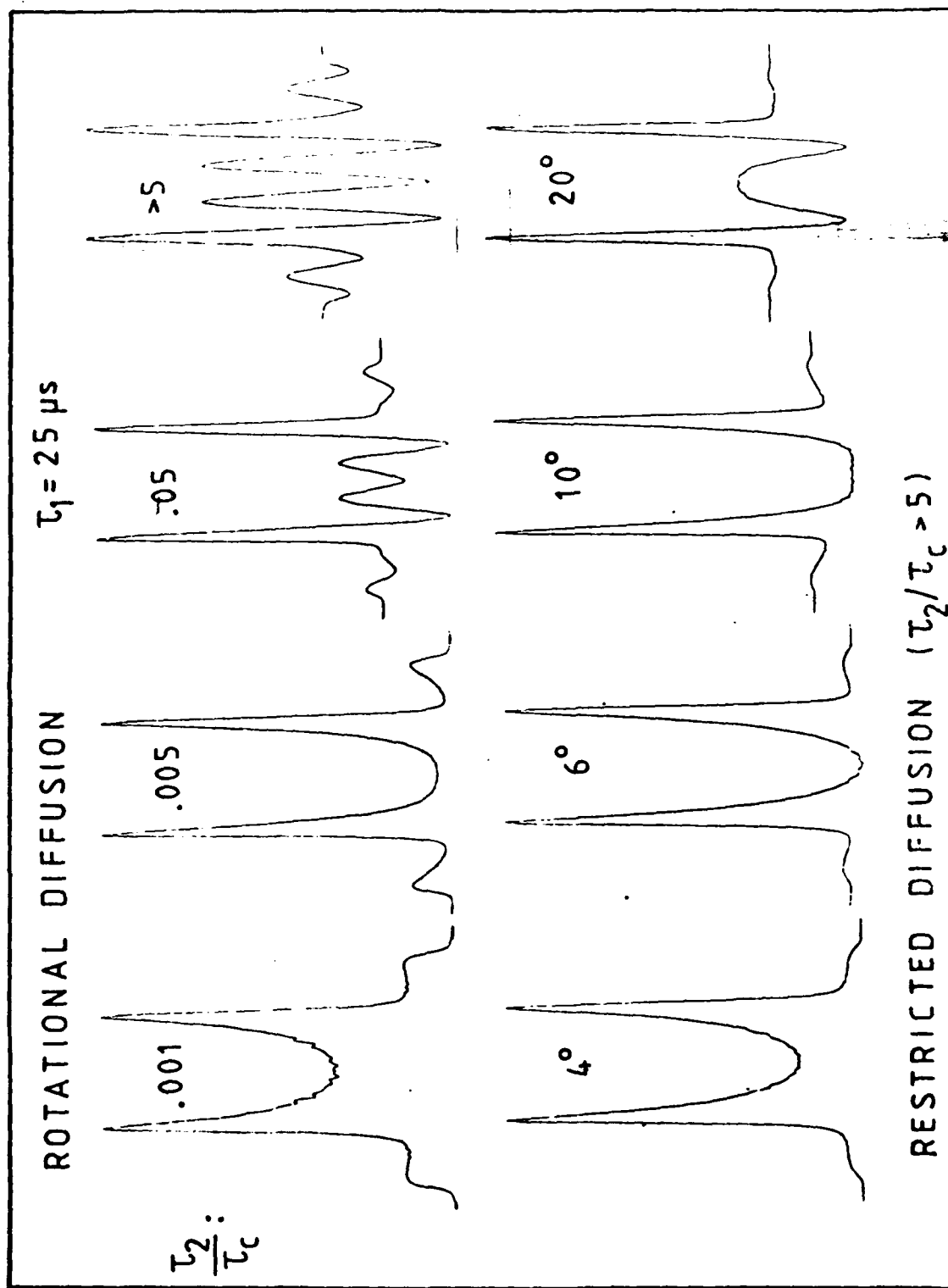


Fig 2



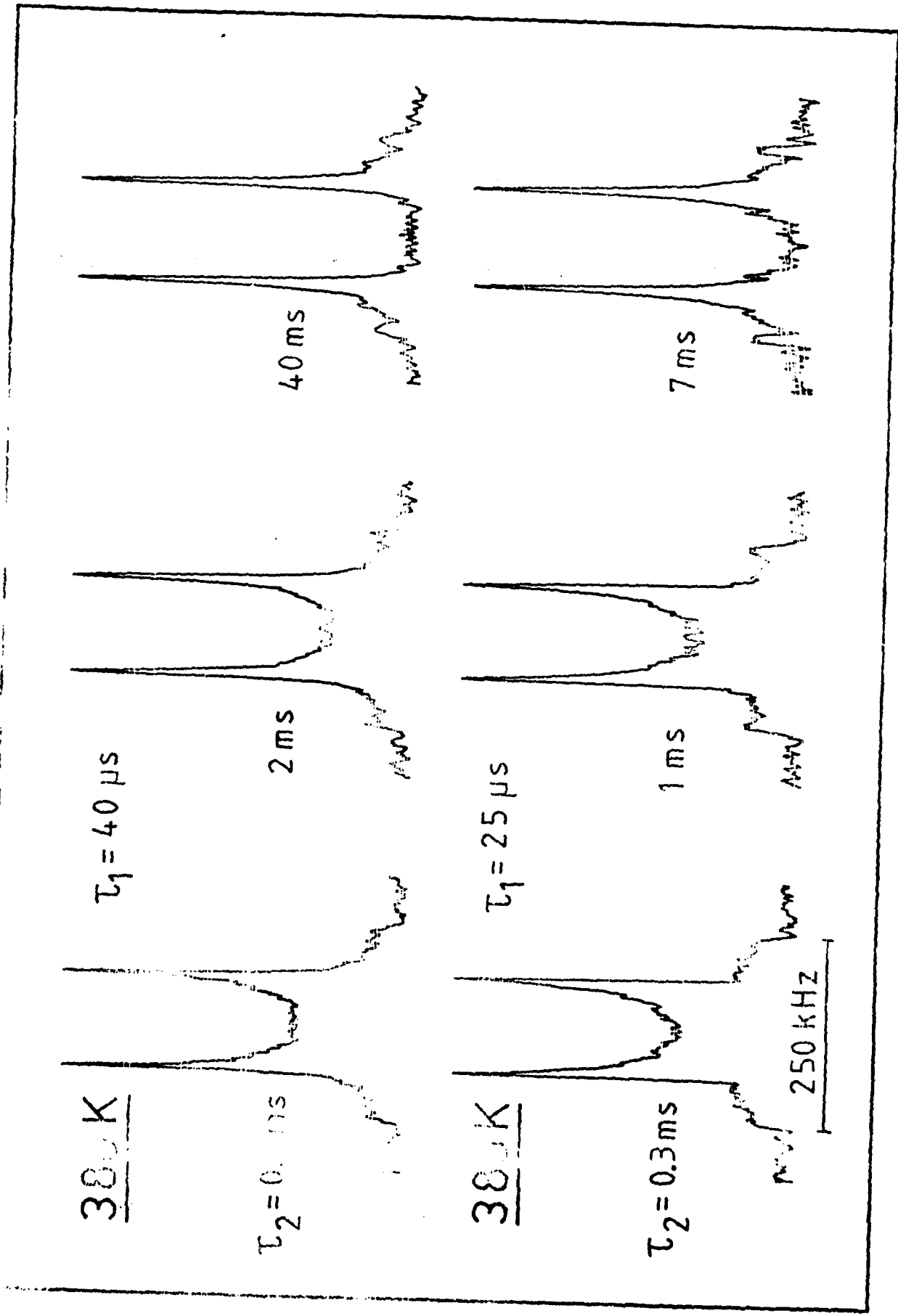


Fig 3

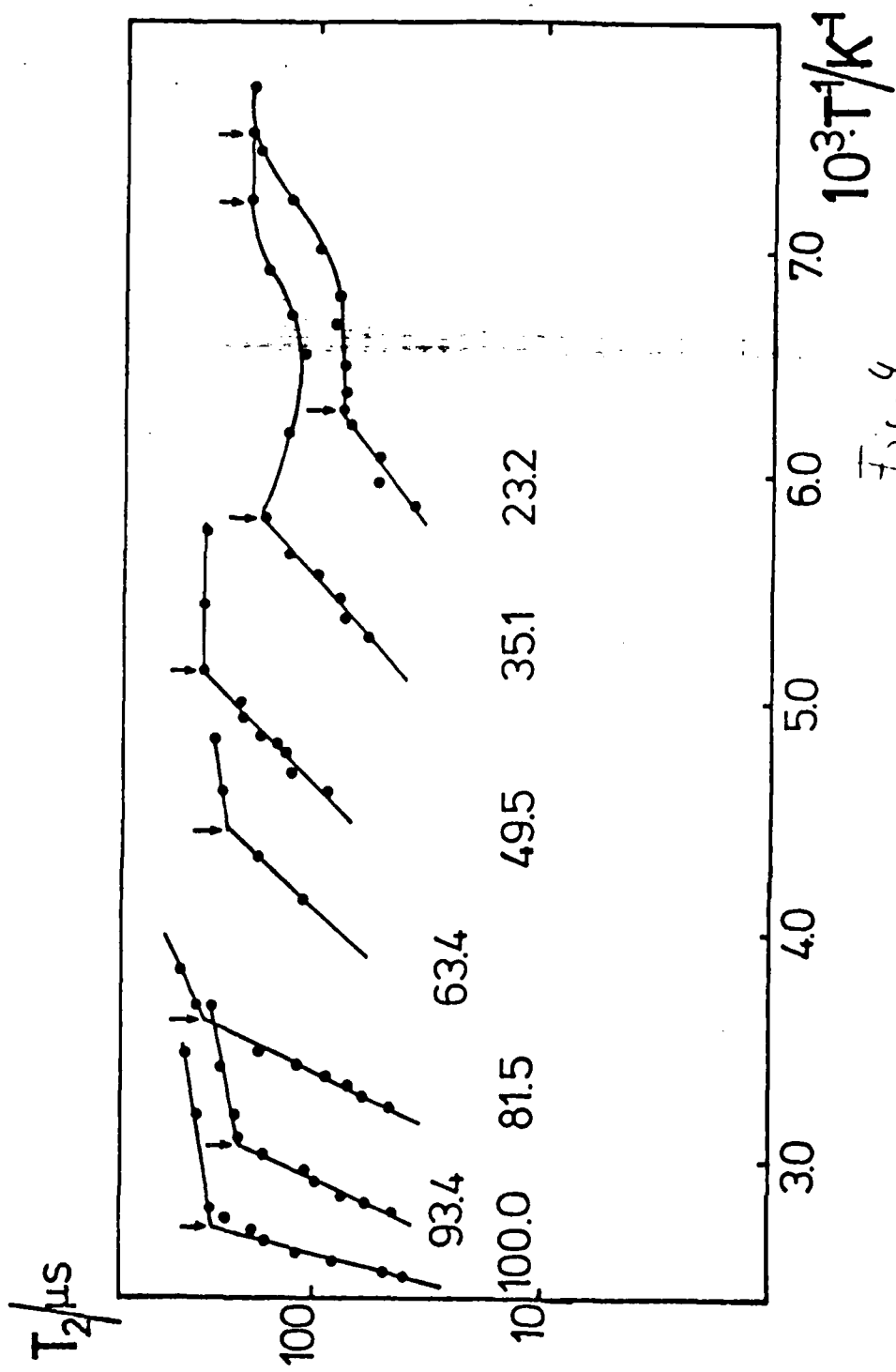


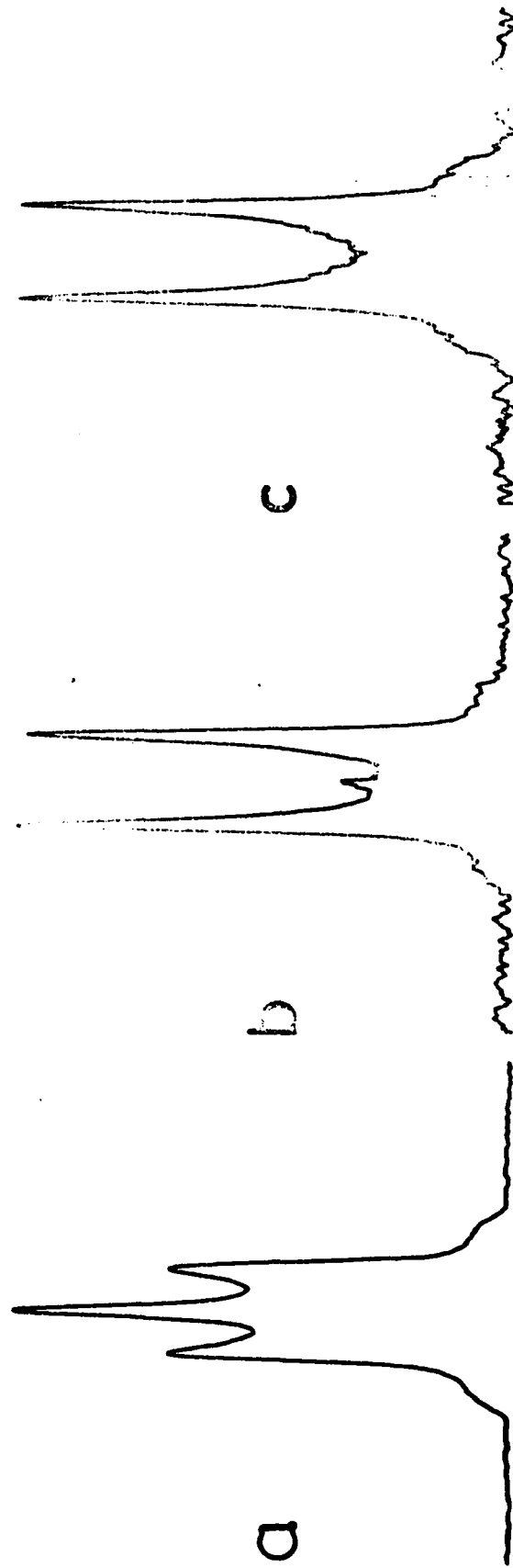
Fig. 4

$T = -118^{\circ}\text{C}$

$\tau_1 = 60\mu\text{s}$

$\tau_1 = 200\mu\text{s}$

$\tau_1 = 50\mu\text{s}$
 $\tau_2 = 50\text{ms}$



100 kHz

Fig 5

AD-A145 078

NUCLEAR MAGNETIC RESONANCE OF POLYMERIC MATERIALS:
PROCEEDINGS OF THE AUT... (U) TRINITY COLL DUBLIN
(IRELAND) 1983

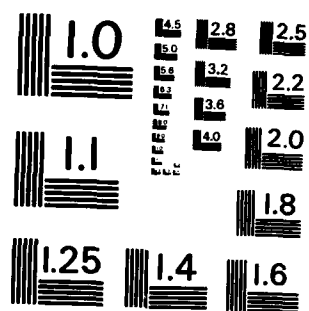
3/2

UNCLASSIFIED

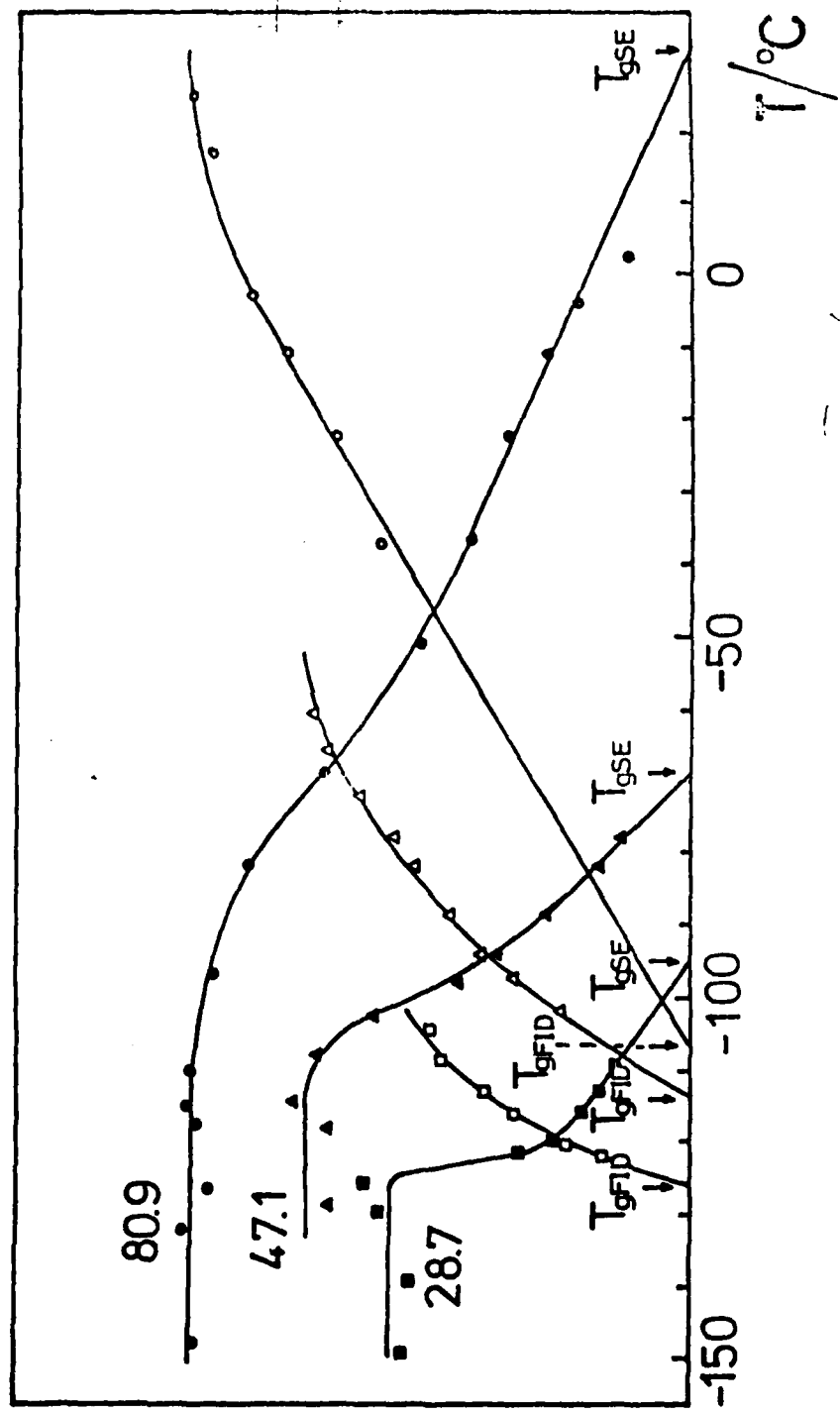
F/G 20/8

NL

END
DATE
FILMED
10 '84
DTI

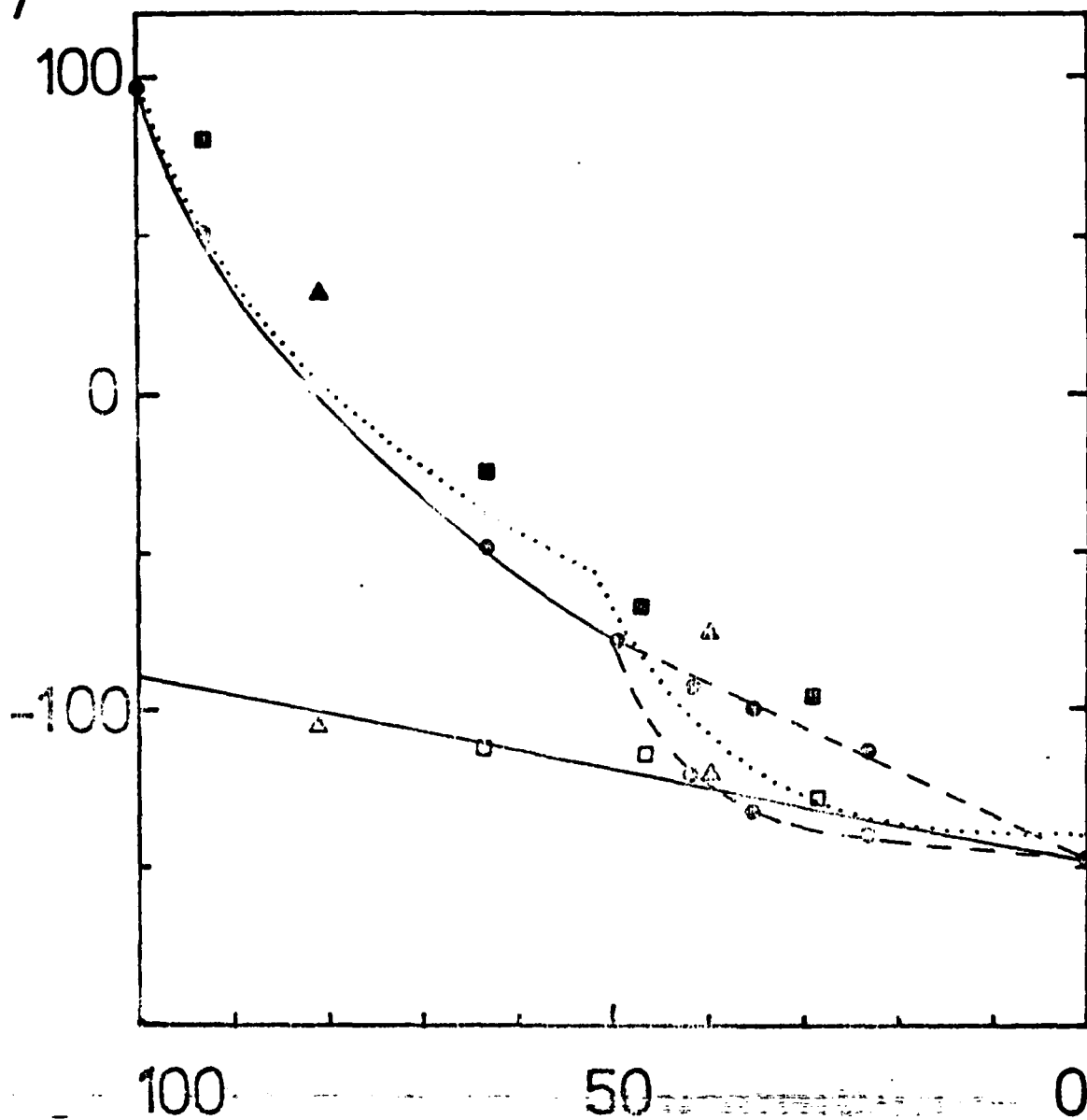


MICROCOPY RESOLUTION TEST CHART
NATIONAL BUREAU OF STANDARDS-1963-A



I

$T/^{\circ}\text{C}$



AD-P003 911

Theory of Nuclear Magnetic Relaxation

Short Abstract

A theory of nuclear magnetic interaction is based on the study of the stochastic rotation operator. The theory is applied explicitly to relaxation by anisotropic chemical shift and to spin-rotational interactions. It is applicable also to dipole-dipole and quadrupole interactions.

Keywords

PACS

02.50 + s	stochastic processes
05.40 + j	Brownian motion
33.25 - j	nuclear magnetic resonance and relaxation
33.25 Bn	N M relaxation phenomena
33.25 Dq	chemical shifts

Abbreviated Title

N M Relaxation Theory

- i -

Theory of Nuclear Magnetic Relaxation

James McConnell

Dublin Institute for Advanced Studies
Dublin 4, Ireland

A theory of nuclear magnetic relaxation centred around the rotation operator is proposed. The theory is applicable in principle to molecules of arbitrary shape, and account is taken of the effects of their inertia. Calculation of relaxation times associated with anisotropic chemical shift and spin-rotational interactions provides illustrations of how the theory may be employed.

1. INTRODUCTION

The theory of nuclear magnetic relaxation associated with random thermal motion has been presented by Abragam¹ and by Hubbard². In the present investigation a theory is proposed in which the rotation operator plays a central and explicit part. This is facilitated by employing results for the rotational Brownian motion of a rigid body of arbitrary shape, that were derived by calculations in which the effects on the inertia of the body are included³.

In the next section the stochastic rotation operator will be defined, and an outline will be given of the way in which the operator and its ensemble average are calculated. In section 3 it will be shown how relaxation times can be deduced from spectral densities associated with the rotation operator. This will be illustrated in section 4 by applications to relaxation by anisotropic chemical shift and by spin-rotational interactions.

2. THE STOCHASTIC ROTATION OPERATOR

Cap "oh"

l.c. "eff"

The concept of rotation operator may be introduced by taking a set of rectangular coordinate axes Ox, Oy, Oz and a function $f(x, y, z)$ of the coordinates (x, y, z) of a fixed point P . Let us now rotate the coordinate axes about the origin to Ox', Oy', Oz' and consider the same function f of the new coordinates (x', y', z') of P . We write

$$f(x', y', z') = R f(x, y, z) \quad (1)$$

and we say that R is the rotation operator associated with the rotation of axes and with the function f . When f has more than one component, eq. (1) is to be interpreted as

Cap gr. "sigma"

$$f_i(x', y', z') = \sum_k R_{ik} f_k(x, y, z). \quad (2)$$

Cap "piy"

It is helpful to introduce infinitesimal generators of rotation J_x, J_y, J_z by

$$J_x = -i(y \frac{\partial}{\partial z} - z \frac{\partial}{\partial y}), J_y = -i(z \frac{\partial}{\partial x} - x \frac{\partial}{\partial z}), J_z = -i(x \frac{\partial}{\partial y} - y \frac{\partial}{\partial x}).$$

gr. "chi"

l.c. "ee"

If we rotate Ox, Oy, Oz through an angle χ about an axis specified by the unit vector \underline{e} , it is easily proved⁴ that

$$R = \exp[-i\chi (\underline{J} \cdot \underline{e})]. \quad (3)$$

l.c. gr. "omega"

If a rigid body is rotating with angular velocity $\omega(t)$ about \underline{e} , it follows from (3) that

$$\frac{dR(t)}{dt} = -i(\underline{J} \cdot \underline{\omega}(t)) R(t). \quad (4)$$

l.c. gr. "gamma" prime
"delta"
"alpha"

The rotation of the coordinate axes may be achieved by rotating about the Z -axis through an angle γ' , then about the y -axis through an angle β' and lastly about the z -axis through an angle α' ⁵. We see from (3) that R is now given by

$$R = e^{-i\alpha' J_z} e^{-i\beta' J_y} e^{-i\gamma' J_z}. \quad (5)$$

Cap "wys"

l.c. gr. "theta", phi If for this rotation we apply (2) to the set of spherical harmonics $Y_{jm}(\theta, \phi)$, where

$$x = r \sin \theta \cos \phi, \quad y = r \sin \theta \sin \phi, \quad z = r \cos \theta,$$

l.c. "alpha"

then it is usual to write (2) as

$$Y_{jm}(\theta', \phi') = \sum_{m'=-j}^j D_{m'm}^j(\alpha', \beta', \gamma') Y_{jm'}(\theta, \phi), \quad (6)$$

where $D_{m'm}^j$ are Wigner functions. Equation (6) shows that $D_{m'm}^j$ is the $m'm$ -element of the matrix representative of R in the representation with basis elements $Y_{j,-j}, Y_{j,-j+1}, \dots, Y_{jj}$; that is to say,

$$D_{m'm}^j(\alpha', \beta', \gamma') = R_{m'm}^j. \quad (7)$$

l.c. gr. "omega"
(bold face)

We apply these ideas to a molecule that is undergoing steady state Brownian motion. Then the angular velocity $\underline{\omega}(t)$ in (4) is a random variable, and so also is the solution of this equation. We refer to $R(t)$ as the stochastic rotation operator. To obtain information about $\underline{\omega}$ we take axes fixed in the molecule with origin at the centre of mass and in the directions of the principal axes of inertia. We assume that the components of $\underline{\omega}$ referred to the molecular coordinate system obey the Euler-Langevin equations⁶

Cap "eye"

l.c. gr. "omega"

(not bold face)

$$I_1 \frac{d\omega_1}{dt} - (I_2 - I_3) \omega_2 \omega_3 = -I_1 B_1 \omega_1(t) + I_1 A_1(t), \text{ etc.}, \quad (8)$$

where I_1, I_2, I_3 are the principal moments of inertia, $\omega_1, \omega_2, \omega_3$ are the components of angular velocity, $I_1 A_1, I_2 A_2, I_3 A_3$ the components of the driving couple and

$I_1 B_1 \omega_1, I_2 B_2 \omega_2, I_3 B_3 \omega_3$ the components of the frictional couple resisting the motion. From (8) we may deduce the value of the time-correlation function of two components of angular velocity, which will be useful for subsequent calculations.

In order to solve (4) we employ a method of solution of nonlinear differential equations that goes back to Krylov and Bogoliubov⁷. It is assumed that the solution $R(t)$ consists of a slowly varying ensemble average $\langle R(t) \rangle$, about which there are random fluctuations, and the solution is expressed as

$$R(t) = (I + \epsilon F^{(1)}(t) + \epsilon^2 F^{(2)}(t) + \dots) \langle R(t) \rangle, \quad (9)$$

where I is the identity operator and ϵ is a small dimensionless parameter. $R(t)$ describes the rotation of the molecule from its orientation at time zero. The ensemble average $\langle R(t) \rangle$ is nonstochastic and it is supposed to satisfy some equation

$$\frac{d\langle R(t) \rangle}{dt} = (\epsilon \Omega^{(1)}(t) + \epsilon^2 \Omega^{(2)}(t) + \epsilon^3 \Omega^{(3)}(t) + \dots) \langle R(t) \rangle, \quad (10)$$

By using the knowledge that we have obtained from (8) we can often deduce from (4), (9) and (10) the values of $\epsilon F^{(1)}(t)$, $\epsilon^2 F^{(2)}(t)$, \dots , $\epsilon \Omega^{(1)}(t)$, $\epsilon^2 \Omega^{(2)}(t)$, \dots for substitution into (9) and (10). We may then be able to solve (10) for $\langle R(t) \rangle$. Analytical solutions have in fact been found for a molecule that is spherical or linear or a symmetric top or even an asymmetric top³. For most NMR problems the value of $\langle R(t) \rangle$ is all that we need. If we do need the value of $R(t)$, we can obtain it from (9).

\hbar is the Planck constant divided by 2π

3. BASIC THEORY OF NUCLEAR MAGNETIC RELAXATION

To study nuclear magnetic relaxation we take a set of cartesian axes fixed with respect to the laboratory. A constant strong magnetic field H_0 acts in the z -direction. If H_0 interacts with a nucleus of spin I and gyromagnetic ratio γ , the field produces a Hamiltonian $-\gamma \hbar H_0 I_z$, denoted also by $\hbar H_0$, with non-degenerate energy levels. We now use the normalized eigenfunctions of $\hbar H_0$ as a basis to express matrix elements of operators. A ^{relatively} small perturbing Hamiltonian $\hbar G(t)$ like that arising from dipole-dipole, quadrupole, chemical shift or spin-rotational interactions causes a relaxation process, and the results are usually expressed in terms of longitudinal and transverse relaxation times T_1 and T_2 , T_2 referring to the z -direction. For any particular interaction one has two problems:

- to express T_1 and T_2 in terms of spectral densities,
- to calculate the spectral densities.

The most direct way of handling a. is to employ a general method due to Redfield⁸. If M_r with $r=x, y, z$ is a component of magnetic moment per unit volume due to the interaction and $\rho_{\beta\beta'}$ denotes an element of the density matrix, then

$$\frac{d\langle M_r \rangle}{dt} = \sum_{\alpha\alpha'\beta\beta'} R_{\alpha\alpha'\beta\beta'} \rho_{\beta\beta'} (M_r)_{\alpha\alpha'} \quad (11)$$

where

$$R_{\alpha\alpha'\beta\beta'} = J_{\alpha\beta\alpha'\beta'}(\omega_{\alpha'} - \omega_{\beta'}) + J_{\alpha\beta\alpha'\beta'}(\omega_{\alpha} - \omega_{\beta'}) - \delta_{\alpha'\beta'} \sum_{\sigma} J_{\sigma\beta\sigma\alpha}(\omega_{\sigma} - \omega_{\beta'}) - \delta_{\alpha\beta} \sum_{\sigma} J_{\sigma\alpha'\sigma\beta'}(\omega_{\sigma} - \omega_{\beta'}) \quad (12)$$

$$J_{\alpha\alpha'\beta\beta'}(\omega) = \frac{1}{2} \int_{-\infty}^{\infty} \langle G_{\alpha\alpha'}(0) G_{\beta\beta'}^*(t) \rangle e^{-i\omega t} dt \quad (13)$$

$G(t)$ $\xrightarrow{\text{see}}$
 α, α' $\xrightarrow{\text{see}}$
 α, α' $\xrightarrow{\text{see}}$

The $J_{\alpha\alpha'}(\omega)$ is a spectral density referred to in a. and b.
 $G_{\alpha\alpha'}(t)$ is an abbreviation of $\langle \alpha | G(t) | \alpha' \rangle$, where $|\alpha\rangle, |\alpha'\rangle$
 are eigenfunctions of H_0 . The energy of the state $|\alpha\rangle$
 is $\hbar \omega_\alpha$. On substituting (12) and (13) into (11) we may
 obtain an equation

$\text{l.c. } \alpha, \alpha'$ $\xrightarrow{\text{see}}$
$$\frac{d\langle M_r \rangle}{dt} = -\lambda_r \langle M_r \rangle. \quad (14)$$

From this would follow

$\lambda_{\alpha, \alpha'} \xrightarrow{\text{see}}$
$$\frac{1}{T_1} = \lambda_z, \quad \frac{1}{T_2} = \lambda_x. \quad (15) \quad \frac{1}{T_2} \xrightarrow{\text{see}} \omega_0$$

To see how the spectral densities are to be calculated
 we shall first of all take a special form of $G(t)$, namely,

$\sum_{q=-2}^2$ $\xrightarrow{\text{see}}$
$$G(t) = \sum_{q=-2}^2 (-)^q F_{-q}(t) A_q, \quad (16)$$

where $F_{-2}(t), F_{-1}(t), F_{0, -2}^{q=-2}, F_{1}(t), F_{2}(t)$ transform under
 rotations like the spherical harmonics

Cap "my"
 $\text{l.c. } \alpha, \alpha'$ $\xrightarrow{\text{see}}$ $\theta(t), \phi(t)$
 $\text{l.c. } \alpha, \alpha'$ $\xrightarrow{\text{see}}$ $\theta(t), \phi(t)$
 $\theta(t), \phi(t)$ $\xrightarrow{\text{see}}$

$Y_{2,-2}(\theta(t), \phi(t)), Y_{2,-1}(\theta(t), \phi(t)), Y_{2,0}(\theta(t), \phi(t)), Y_{2,1}(\theta(t), \phi(t)), Y_{2,2}(\theta(t), \phi(t)).$

This will permit the application of (6) and (7) to $F_p(t)$. We
 have from (16)

Cap "my" $\text{l.c. } \alpha, \alpha'$ $\xrightarrow{\text{see}}$
$$G_{\alpha\alpha'}(t) = \sum_{q=-2}^2 (-)^q F_{-q}(t) (\alpha | A_q | \alpha')$$

$$G_{\beta\beta'}^*(t) = \sum_{q=-2}^2 (-)^q F_{-q}^*(t) (\beta | A_q | \beta')^*$$

$$= \sum_{q=-2}^2 (-)^q F_{-q}^*(t) (\beta' | A_q^+ | \beta),$$

where A_q^+ is the adjoint of the operator A_q . We deduce that

$$\langle G_{\alpha\alpha'}(t) G_{\beta\beta'}^*(t) \rangle = \sum_{q, q'=-2}^2 (-)^{q+q'} \langle F_{-q}(t) F_{-q'}^*(t) \rangle (\alpha | A_q | \alpha') (\beta' | A_{q'}^+ | \beta). \quad (17)$$

The angular brackets denote here an average over the random variables, that is to say, the angular velocity components, together with an average over the initial orientations of the molecule. A study of the transformation properties of spherical harmonics shows that ⁹

$$\langle F_{-q}(0) F_{-q'}^*(t) \rangle = \frac{1}{5} \delta_{qq'} \sum_{n, n'=-2}^2 \langle R(t) \rangle_{n'n} F_n'^* F_{n'}' ,$$

Cap "off" from
subscript l.c.
"en", "en" from

where $F_p' = F_p(0)$, a constant, and $\langle R(t) \rangle$ is the ensemble average of the rotation operator for the molecule in question. We see that we may write

$$\int_{-\infty}^{\infty} \langle F_{-q}(0) F_{-q'}^*(t) \rangle e^{-i\omega t} dt = J(\omega),$$

independent of q , and, from (13) and (17), that

$$J_{\alpha\alpha', \beta\beta'}(\omega) = \frac{1}{2} J(\omega) \sum_{q=-2}^2 (\alpha | A_q | \alpha') (\beta' | A_q^+ | \beta), \quad (18)$$

where

$$J(\omega) = \frac{1}{5} \sum_{n, n'=-2}^2 F_n'^* F_{n'}' \int_{-\infty}^{\infty} \langle R(t) \rangle_{n'n} e^{-i\omega t} dt. \quad (19)$$

We know F_q' from the nature of the perturbing Hamiltonian that gives rise to the interaction and we know $\langle R(t) \rangle$ from the investigation of the rotational Brownian motion of the molecule. Hence we can in principle calculate $J(\omega)$ from (19) and consequently the relaxation times from (11), (12), (13), (15) and (18). Moreover, since the integral in (19) is independent of the interaction Hamiltonian $\mathcal{H} G(t)$, results for relaxation times can easily be taken over from one interaction satisfying (16) to another by replacing the values of F_q' in (19).

l.c. "delta"

$F_p(0)$
↑
l.c. "lea"

4. CALCULATION OF RELAXATION TIMES

As applications of the Redfield theory we shall investigate two types of interaction that cause nuclear magnetic relaxation. The first is anisotropic chemical shift, which is an example of an interaction satisfying (16). The other is spin-rotational interaction, which does not obey (16).

For anisotropic chemical shift it may be shown that^{10,11}

$$A_0 = 2H_0 I_z, A_{\pm 1} = -\frac{\sqrt{6}}{2} H_0 I_{\pm}, A_{\pm 2} = \frac{\sqrt{6}}{2} H_0 I_{\pm}^2, A_{\pm 3} = 0, \quad (20)$$

where

$$I_{\pm} = I_x \pm i I_y,$$

and that

$$F'_0 = \frac{1}{2} \gamma \delta_z, F'_{\pm 1} = 0, F'_{\pm 2} = \frac{\gamma}{2\sqrt{6}} \delta_z, \quad (21) \quad \left(\begin{array}{l} \delta_z \\ \delta_z \end{array} \right)$$

where the non-vanishing elements of the diagonalized anisotropic chemical shift tensor are

$$-\frac{1}{2} (1 - \gamma) \delta_z, -\frac{1}{2} (1 + \gamma) \delta_z, \delta_z.$$

Hence, from (18),

$$J_{\alpha\beta\alpha'\beta'}(\omega_{\alpha'} - \omega_{\beta'}) = \frac{1}{2} J_{cs}(\omega_{\alpha'} - \omega_{\beta'}) \sum_{q=-1}^1 (\alpha | A_q | \beta) (\beta' | A_q^\dagger | \alpha')$$

and $J_{cs}(\omega)$ is given by (19) with the values of F'_q taken from (21). Since

$$\langle M_x \rangle = \gamma \hbar N \langle I_x \rangle,$$

where N is the number per unit volume of nuclei taking part in the relaxation process, we may obtain the relaxation times by applying (11), (14) and (15) to I_x . Employing (20) we find after an elementary calculation that¹⁰

$$\frac{1}{T_1} = 3 H_0^2 J_{cs}(\omega_0)$$

$$\frac{1}{T_2} = \frac{1}{2} H_0^2 [4 J_{cs}(0) + 3 J_{cs}(\omega_0)]. \quad (22)$$

To complete the calculations we must obtain an expression for $J_{cs}(\omega)$ from (19) and (21). What was equivalently the same thing was done by Abragam but only for a spherical molecule and with inertial effects neglected¹². The explicit use of the rotation operator has allowed us to include the inertial effects and to extend the discussion to a linear molecule and to a symmetric top molecule¹⁰. We shall put down the result only for the latter case taking the nucleus to be at the centre and the axis of symmetry as the third coordinate axis in (8), so that $I_2 = I_1$, $B_2 = B_1$:

$$J_{cs}(\omega) = \frac{1}{5} \gamma^2 \delta_z^2 \left\{ \frac{3D_1(1 + \frac{6D_1}{B_1})}{36D_1^2 + \omega^2} + \frac{1}{3} \frac{(D_1 + 2D_3)(1 + \frac{2D_1}{B_1} + \frac{4D_3}{B_3})}{(2D_1 + 4D_3)^2 + \omega^2} + \dots \right\}$$

where

$$D_1 = \frac{kT}{I_1 B_1}, \quad D_3 = \frac{kT}{I_3 B_3}. \quad (23)$$

The relaxation times follow from (22).

We see from (16), (18) and (19) that, when the interaction Hamiltonian can be expanded as a linear combination of elements of a five-dimensional spherical tensor, we require only $\langle R(t) \rangle$ for the molecule in order to calculate the spectral density $J(\omega)$ and consequently the relaxation times. This procedure fails in the study of nuclear magnetic relaxation by spin-rotational interactions.

Then

$$\hbar G = \hbar (\underline{I} \cdot \underline{C} \cdot \underline{J}), \quad (24)$$

where \underline{I} is the spin operator of the nucleus that interests us, \underline{C} is the three-dimensional spin-rotational tensor and $\hbar \underline{J}$ is the angular momentum operator of the molecule that contains the

"bold face Cap" eye
"see"
"jag"

nucleus. Since the number of independent elements of \underline{C} is not five, the \underline{G} of (24) cannot be expanded as in (16).

A general theory of nuclear magnetic relaxation by spin-rotational interactions has been based on the stochastic rotation operator ¹³. The angular momentum \underline{J} is replaced by its classical value $(I_1 \omega_1, I_2 \omega_2, I_3 \omega_3)$. We have found that the Redfield method yields relaxation times T_1^{sr}, T_2^{sr} given by

$$\frac{1}{T_1^{sr}} = 2 J_{sr}(\omega_0) \quad , \quad \frac{1}{T_2^{sr}} = J_{sr}(0) + J_{sr}(\omega_0) \quad (25)$$

where

$$J_{sr}(\omega) = \frac{1}{2} \{ C(i\omega) + C(-i\omega) \} \quad (26)$$

$$C(s) = \frac{1}{3\hbar^2} \sum_{\mu, \nu=1}^3 \sum_{m, n=-1}^1 (-1)^m b_{\mu\mu} b_{\nu\nu} I_\mu I_\nu \left(\int_0^\infty e^{-st} \langle R(t) \omega_\mu(t) \omega_\nu(0) \rangle dt \right) \quad (27)$$

$$b_{0\nu} = C_{3\nu} \quad , \quad b_{\pm 1, \nu} = \mp \frac{C_{1\nu} \mp i C_{2\nu}}{\sqrt{2}}$$

and $\pi_{s,-m}$ denotes matrix representation with respect to the basis $Y_{1,-1}, Y_{10}, Y_{11}$.

We see from (25), (26), (27) that a knowledge of $\langle R(t) \rangle$ is no longer adequate for the calculation of spectral densities and relaxation times. We must now use our knowledge of the values of $\varepsilon F^{(1)}(t), \varepsilon^2 F^{(2)}(t), \dots$ and of $\langle R(t) \rangle$ to calculate $R(t)$ from (9). Then we must obtain $\langle R(t) \omega_\mu(t) \omega_\nu(0) \rangle$, calculate its Laplace transform and the matrix elements of this, evaluate $C(s)$ from (27) and employ (25) and (26) to deduce the relaxation times. This has been done in principle for an asymmetric molecule and with the inclusion of inertial effects. Explicit results can be given for molecules that are linear, axially symmetric or spherical.

For simplicity we shall report these results only in the extreme narrowing approximation of $\omega_0 \ll \hbar T / (IB)$, where I and B stand generically for the moments of inertia and the friction constants in (8). Then T_1^{sr} and T_2^{sr} are equal, and we shall denote their common value by T_{sr} . In the case of

↓ Cap "see"

$C_{||}$ ← these are parallel lines, not "one-one"

12

a spherical molecule ¹³

$$\frac{1}{T_{sr}} = \frac{21kT}{3\hbar^2 B} \left\{ (C_{||}^2 + 2C_{\perp}^2) - K(C_{\perp} - C_{||})^2 + \frac{13}{6} K^2 (C_{\perp} - C_{||})^2 + \dots \right\} \quad (28)$$

i.e. α "halpha"

where $K = kT/(IB^2)$, the spin-rotational tensor component $C_{||}$ refers to the direction of the radius through the nucleus and C_{\perp} refers to a perpendicular direction. In the case of a molecule which has a principal axis of inertia through the centre of mass that passes through the nucleus and which is such that this principal axis is an axis of symmetry C_n for the molecule with $n \geq 3$ ¹⁴

$$\frac{1}{T_{sr}} = \frac{2kT}{3\hbar^2} \left\{ \frac{2I_{\perp} C_{\perp}^2}{B_1 + D_1 + D_3} + \frac{I_3 C_{||}^2}{B_3 + 2D_1} + kT \left[\left(\frac{2}{B_1^3} + \frac{2I_{\perp}}{I_3 B_1^2 B_3} - \frac{2I_3}{I_3 B_1^2 (B_1 + B_3)} \right) C_{\perp}^2 + \frac{2I_3 (C_{||}^2 + 2C_{\perp} C_{||})}{I_1 B_1 B_3 (B_1 + B_3)} \right] \right\} \quad (29)$$

In this equation $C_{||}, I_3, B_3$ refer to the axis of symmetry, C_{\perp}, I_1, B_1 refer to a perpendicular axis and D_1, D_3 are defined in (23). In the case of a linear molecule ¹⁵

$$\frac{1}{T_{sr}} = \frac{4kTI C_{\perp}^2}{3\hbar^2 B} \quad (30)$$

Calculations have been performed for the above molecular models, when inertial effects are ignored ¹⁶. It has been found that (28) is altered to

$$\frac{1}{T_{sr}} = \frac{21kT(C_{||}^2 + 2C_{\perp}^2)}{3\hbar^2 B},$$

that (29) is altered to

$$\frac{1}{T_{sr}} = \frac{2kT}{3\hbar^2} \left\{ \frac{2I_{\perp} C_{\perp}^2}{B_1} + \frac{I_3 C_{||}^2}{B_3} \right\},$$

and that (30) is unaltered. The inclusion of inertial effects

produces for the sphere and for the symmetric rotator corrections of order K , which is at most a few per cent. There is zero correction for the linear molecule, even though the calculations have been performed to an accuracy of K^2 .

5. CONCLUSION

An analytical theory of nuclear magnetic relaxation has been based on the stochastic rotation operator and on the Redfield method of establishing a differential equation for the ensemble average of the magnetic moment produced by a specified interaction mechanism. The theory has been applied to examples of two different classes of interaction, namely, anisotropic chemical shift and spin-rotational. The present theory is confined to the study of the behaviour of a single molecule.

REFERENCES

- 1 Abragam, A. 'The Principles of Nuclear Magnetism', Clarendon Press, Oxford, 1961
- 2 Hubbard, P.S. Rev. Mod. Phys. 1961, 33, 249
- 3 McConnell, J. 'Rotational Brownian Motion and Dielectric Theory', Academic Press, London, New York, Toronto, Sydney, San Francisco, 1980
- 4 McConnell, J. Dublin Institute for Advanced Studies preprint, DIAS-STP-83-30
- 5 Rose, M.E. 'Elementary Theory of Angular Momentum', John Wiley and Sons, New York, 1957, pp. 50, 51
- 6 Ford, G.W., Lewis, J.T. and McConnell, J. Phys. Rev. A 1979, 19, 907
- 7 Krylov, N.M. and Bogoliubov, N.N. 'Introduction to Nonlinear Mechanics', Princeton Univ. Press, Princeton, 1947
- 8 Redfield, A.G., I.B.M. J. Research Develop. 1957, 1, 19
- 9 Ref. 6, Appendix
- 10 McConnell, J. Dublin Institute for Advanced Studies preprint, DIAS-STP-83-34
- 11 Ref. 1, p. 316
- 12 Ref. 1, pp. 313, 316
- 13 McConnell, J. Physica A 1982, 111, 85
- 14 McConnell, J. Physica A 1982, 112, 479

- 15 McConnell, J. Physica A 1982, 112, 488
- 16 McConnell, J. Dublin Institute for Advanced Studies preprint,
DIAS-STP-83-33



NMR of Solid Biopolymers

E. R. Andrew

Departments of Physics, Radiology and Nuclear Engineering Sciences,
University of Florida, Gainesville, Florida 32611, USA

From the very earliest days of NMR it has been possible to study the motion of molecules in the solid state, first from the narrowing of the proton dipolar-broadened spectrum, and in more detail from the measurements of the proton spin-lattice relaxation time T_1 . So we wondered how much we could learn about the dynamical behavior of larger molecules such as proteins from NMR in the solid state. This has the interest that we are examining the molecules in the same environment as that in which their X-ray structures were determined and it would also complement NMR studies on these molecules in solution.

One advantage of working in the solid state is the very wide temperature range which is accessible from room temperature down to quite low temperatures and this gives the chance to characterize the motions well with activation parameters. In solution often only a small temperature range is accessible before denaturing and degradation occur.

A second advantage of working in the solid state is that the large protein molecule is essentially fixed in the crystal lattice so that we examine directly the intramolecular motions. In solution on the other hand the intramolecular motions are superposed on tumbling of the whole molecule, which complicates the analysis, and of course it can only be applied to those groups whose spectral lines are separately resolved and assigned.

In the present work we are looking at the relaxation of the whole collective assembly of dipolar-coupled protons. So we cannot be specific about the details of particular individual groups, but as we shall see we can determine the types of motion which contribute most and we can characterize them. A protein contains several hundred protons, maybe a thousand or more, each with its own molecular environment, which makes it a complicated system to investigate. So the philosophy of our work was to start with simpler

precursors and having established some types of behavior and understood them quantitatively we could then move on to protein molecules themselves with more confidence.

So we began by looking at the proton relaxation time T_1 of all the classical 20 amino acids of which proteins are composed, in the solid state from 100 to 500K. This work has been reported in a series of three papers (1,2,3). Analysis using the well-known Kubo-Tomita theory of dipolar relaxation (4) developed from the original relaxation theory of Bloembergen, Purcell and Pound (5), quantitatively identified reorientation of methyl and NH_3 groups and motions of other side groups. At each temperature a single correlation time τ_c characterized each motion and its temperature-variation followed a simple Arrhenius activation law, from which an activation energy E_A and pre-exponential factor τ_0 was determined. The whole relaxation-temperature curve was fitted by computer, not just the asymptotes. Measurements were made at two frequencies and the same parameters were used in fitting the results from both. A comparison of the measured and calculated dipolar coupling constants provided a strong test of the correct identification of the motions. This work on the solid amino acids is a subject in itself and some of the amino acids exhibited most interesting side chain motions, particularly arginine, cysteine, methionine, phenylalanine and valine.

These measurements were extended to polycrystalline dipeptides and tripeptides (6), for example alanylglycine and glycylalanine and the series glycine, diglycine, triglycine, polyglycine. We usually found the features of the monomeric amino acids carried over with minor modifications into the peptides. Next we examined a series of homopolypeptides (7) and by then felt we had enough experience to help us tackle some solid proteins.

The four proteins examined in polycrystalline form were α -chymotrypsin, insulin, lysozyme and ribonuclease A, selected because they are well-characterized, their X-ray structures have been determined, they are readily available in pure form and are not too expensive. We used about 0.5g for each specimen, and pumped them for 24 hours at room temperature to remove oxygen and most of the water. Measurements were made at 18, 30 and 60 MHz on each protein from 300K down to 10K. Results for ribonuclease A are shown in Fig. 1.

The results (8-11) exhibited altogether broader shallower curves than

those found for the monomeric amino acids and the simple peptides, and could only be accounted for assuming a distribution of correlation times τ_c . This is really not surprising. In the pure amino acids we sometimes resolved two or even three correlation times from two or three independent molecular group motions at each temperature. In a biopolymer such as these protein molecules, with very many different proton sites and degrees of freedom, many correlation times are needed. We should note that we could fit any one of the relaxation curves measured at a single measuring frequency with a single thermally-activated correlation time, but not all three curves for the three measuring frequencies simultaneously. This illustrates how important it is to work at several measuring frequencies.

Four well-known distribution functions were tried: Gaussian (log-normal), Cole-Cole, Cole-Davidson, Fuoss-Kirkwood. It was found that the Gaussian distribution provided the best characterization of the data for all four polycrystalline proteins over the range 70-250K.

We can go a long way towards identifying the motions responsible. The earlier work on precursors leads us to expect methyl groups and their reorientation to be important in the side chains of six amino acids, namely alanine, isoleucine, leucine, methionine, threonine and valine. The relaxation minima of the proteins occur in approximately the same temperature range as in most precursors. The activation energies are very similar to those of the amino acids; we do not expect them to be exactly the same, but it is satisfactory that they are similar and it suggests that most of the restrictions to reorientation are intramolecular. Moreover we can calculate the expected relaxation constant, assuming that rapid spin diffusion maintains a common spin temperature and that the methyl proteins have to relax all protons in the protein molecules. This analysis shows that methyl reorientation in the side chains accounts for about 70% of the measured relaxation constants, leaving some 30% to be accounted for by side chain motions, segmental motion, reptation and whole-body motions.

Since we are dealing with an inhomogeneous system with methyl and other groups in a wide variety of environments, the assumption of a distribution of values of τ_c , each characterizing an exponential correlation function, seems physically more appropriate than use of a single suitably-chosen non-exponential correlation function such as that of Williams and Watts (12).

Above 250K and below 60K the experimental values of T_1 fall below the calculated curves for all four proteins and evidently other processes become important here. At low temperatures there seems to be a weaker but less-hindered process. To cast light on this we examined two homopolypeptides devoid of methyl groups, namely polyproline and polyglycine.

Polyproline showed a surprisingly strong proton relaxation (13). Analysis of the relaxation constant showed that this could be attributed to conformational motion of the proline rings. There are a number of proline residues in proteins, for example there are nine in α -chymotrypsin. This motion can therefore be expected to contribute significantly to proton relaxation over the whole temperature range.

By contrast the proton relaxation in polyglycine is much weaker (13), arising from segmental motions of the chains which modulate the dipolar interactions of the methylene and imino groups. Below 60K the relaxation of solid proteins and polyglycine tend to become equal; this supports the view that segmental motions of the protein chain make important contributions to relaxation in solid proteins at low temperatures.

Above 250K the deviation of T_1 below the computed curves is attributed to additional relaxation contributions of water molecules in the structure. We have investigated this with measurements on polycrystalline lysozyme and α -chymotrypsin progressively hydrated with H_2O and D_2O up to 60% by weight (14). The amount of water added was measured by increase of weight and by Karl-Fischer titration. The Karl-Fischer titration showed that our normal specimens pumped at room temperature retained about 2% water, strongly bound.
see fig. 2.

Two main features were noticed (14). Above 180K increase of hydration progressively decreased T_1 exhibiting a characteristic minimum which shifted to progressively lower temperatures. Below 180K increase of hydration progressively increased T_1 . The increased relaxation rate above 180K is due to reorientation of the water molecules. Additional water is bound less strongly causing the T_1 minimum to shift to lower temperatures. Analysis shows (14) that the activation energy for this motion decreases from 30kJ/mole for the first increments of water to 20kJ/mole for the last increments. It is noteworthy that the last increments of water contribute to relaxation even down to 180K. The relaxation constant for the water reorientation turns out to be about 56% of that for isotropic intramolecular dipolar relaxation of

pure water. This reduced value can be attributed to three causes: (1) anisotropy of the reorientation of the water molecules on their sites, (2) a distribution of activation parameters on the various sites of attachment, (3) a lengthening of the interproton distance due to hydrogen bonding of the water molecules on their sites.

Below 160K T_1 increased monotonically and approximately linearly with successive additions of water. At these lower temperatures the water molecules are frozen in the structure and contribute nothing to relaxation, but they do add to the load of protons needing to be relaxed by other protein motions.

When D_2O is added instead of H_2O we have similar effects, but very much weaker because of the relative inefficiency of deuterons in relaxing the load of protons; indeed calculations shows that it is 4.2% smaller which approximately accounts for what is observed.

This study confirms that the presence of water in proteins causes extra relaxation at higher temperatures due to motions of the water molecules themselves, but there is no evidence of any change in the protein molecules induced by the presence of the water.

All the work described so far is based on measurements of T_1 which are particularly responsive to dynamic behavior in the frequency range $10^5 - 10^{10}$ Hz. Recently we have extended our studies to measurements of the dipolar relaxation time T_{1D} using the Jeneer-Broekaert pulse sequence (15), since this is responsive to dynamical behavior in the spectral region 1 to 10^5 Hz, enabling a wide spectral range 1 to 10^{10} Hz to be investigated overall.

Extending the expression for T_{1D} for a distribution of correlation times in the same manner as we did previously for T_1 and using the activation parameters previously obtained from measurements of T_1 , we predict that a minimum in T_{1D} should be found at about 85K, about 100K lower than for T_1 . Experiment bore this prediction out closely for both α -chymotrypsin and lysozyme (16). This extrapolation was a severe test of the parameters obtained from T_1 measurements and gave some confidence to the description and characterization of the motions obtained through T_1 . The shift of the T_{1D} minimum 100K lower, where the motions are some 10^4 times slower gives the opportunity to examine new motions at higher temperatures. The minimum value

of T_{1D} is 210 times shorter than that of T_1 at 60MHz for lysozyme, but theory predicts a ratio of 3000. A similar discrepancy was found for α -chymotrypsin, and is attributed to a spin-diffusion bottleneck.

In some cases the use of T_{1D} enables relaxation mechanisms and motions to be resolved which are not resolved in T_1 . An example was provided by solid polyvaline. In addition to a deep minimum in T_{1D} attributed to methyl group reorientation in the monomer side chains, there is a weaker minimum at about 200K which is attributed to a more hindered reorientation of the whole side chain which modulates a much smaller fraction of the overall dipolar second moment.

So summarizing, it has been possible through the study of proton relaxation in solid proteins and related molecules to identify and characterize the following molecular motions which contribute to relaxation:

- (1) methyl group reorientation;
- (2) segmental motion;
- (3) side chain motion;
- (4) proline ring puckering; and
- (5) water molecule reorientation.

Finally it is a pleasure to express my great indebtedness to my colleagues at Nottingham without whom these studies could not have been undertaken, especially D. J. Bryant, E. M. Cashell, Q. A. Meng, R. Gaspar, D. N. Bone and T. Z. Rizvi.

References

1. Andrew, E. R., Hinshaw, W. S., Hutchins, M. G. and Sjoblom, R.O.I., Molec. Phys. 31, 1479 (1976).
2. Andrew, E. R., Hinshaw, W. S., Hutchins, M. G., Sjoblom, R.O.I. and Canepa, P. C., Molec. Phys. 32, 795 (1976).
3. Andrew, E. R., Hinshaw, W. S., Hutchins, M. G. and Sjoblom, R.O.I., Molec. Phys. 34, 1695 (1977).
4. Kubo, R. and Tomita, K., J. Phys. Soc. Japan 9, 888 (1954).
5. Bloembergen, N., Purcell, E. M. and Pound, R. V., Phys. Rev. 73, 679 (1948).
6. Andrew, E. R., Green, T. J. and Hoch, M. J. R., J. Mag. Res. 29, 33 (1978).
7. Andrew, E. R., Gaspar, R. and Vennart, W., Biopolymers 17, 1913 (1978).
8. Andrew, E. R., Bryant, D. J. and Cashell, E. M., Chem. Phys. Letters 69, 551 (1980).
9. Andrew, E. R., Bryant, D. J., Cashell, E. M. and Meng, Q. A., FEBS Letters, 126, 208 (1981).
10. Andrew, E. R., Bryant, D. J., Cashell, E. M. and Meng, Q. A., Phys. Letters 88A, 487 (1982).
11. Andrew, E. R., Bone, D. N., Bryant, D. J., Cashell, E. M., Gaspar, R., and Meng, Q. A., Pure and Appl. Chem. 54, 585 (1982).
12. Williams, G. and Watts, D. C., Trans. Farad. Soc. 66, 80 (1970).
13. Andrew, E. R., Bryant, D. J., Cashell, E. M., Gaspar, R. and Meng, Q. A., Polymer 22, 715 (1981).
14. Andrew, E. R., Bryant, D. J. and Rizvi, T. Z., Chem. Phys. Letters 95, 403 (1983).
15. Jeneer, J. and Broekaert, P., Phys. Rev. 157, 232 (1967).
16. Gaspar, R., Andrew, E. R., Bryant, D. J. and Cashell, E. M., Chem. Phys. Letters 86, 327 (1982).

Figure Captions

Fig. 1. The temperature dependence of the proton spin-lattice relaxation time T_1 in solid ribonuclease A between 10 and 300K. The full lines are theoretical curves calculated as described in the text.

Fig. 2. The variation with temperature of the proton spin-lattice relaxation time T_1 at 60 MHz is polycrystalline lysozyme with various degrees of hydration. Full circles and full lines refer to hydration with H_2O ; open circles and dashed lines refer to hydration with D_2O .

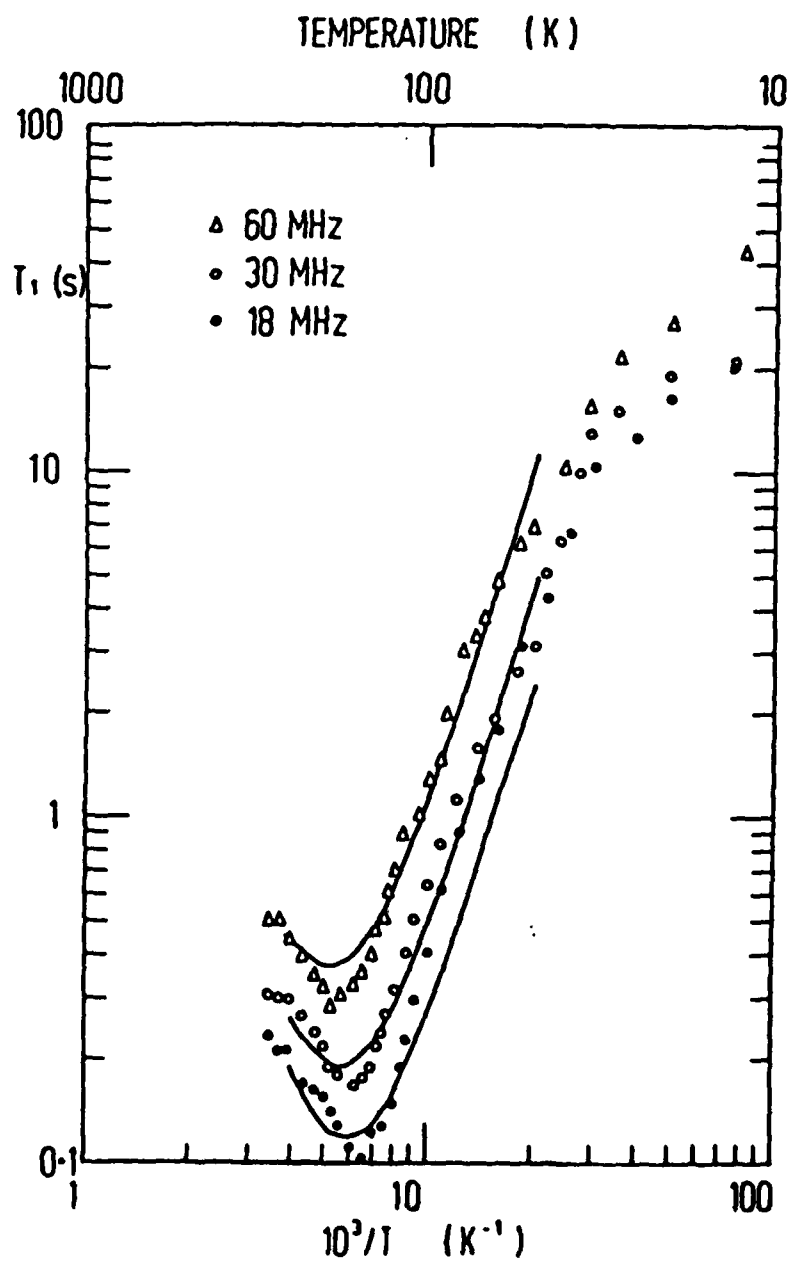


Figure 1

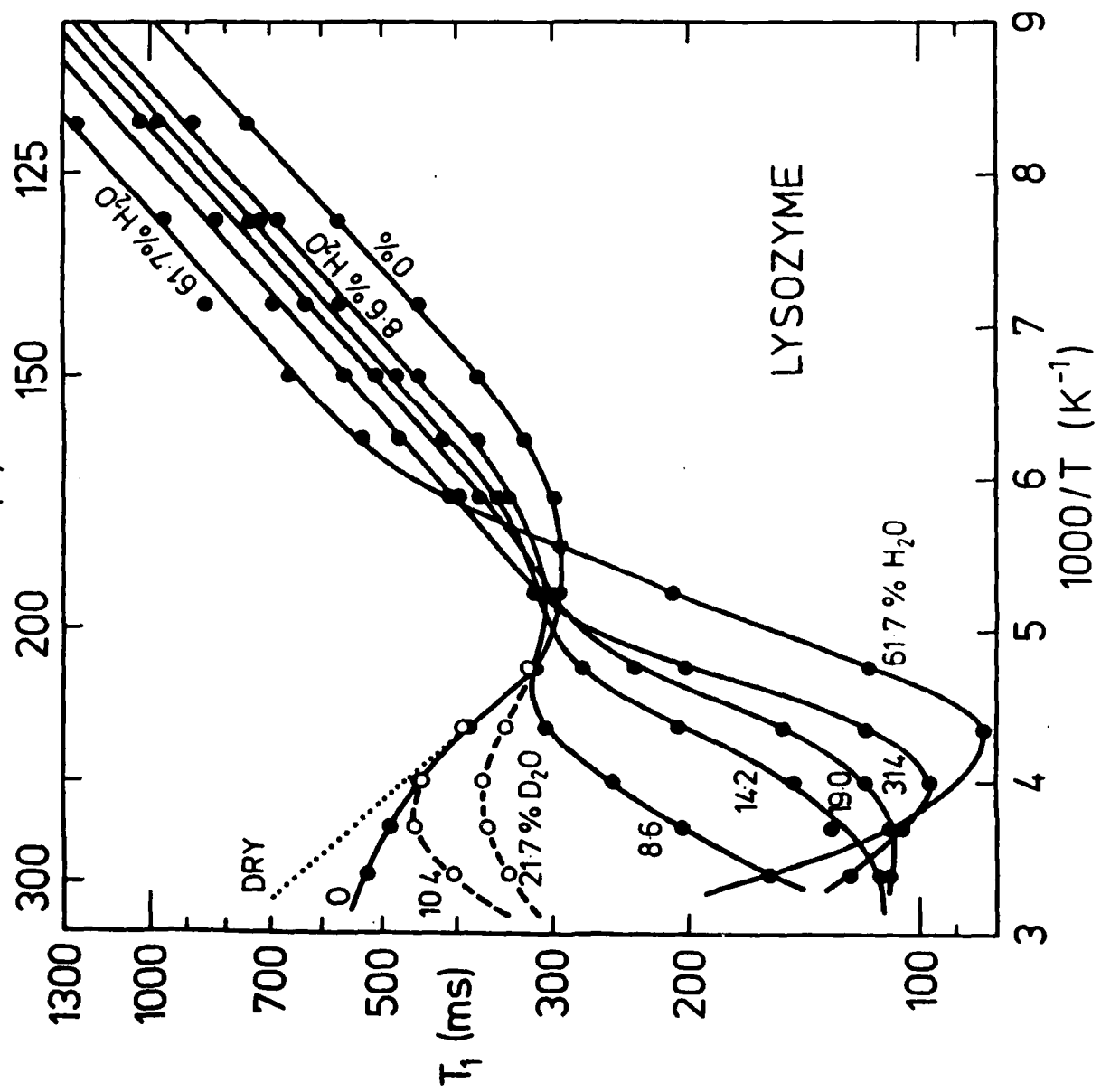


Figure 2